



756
2021

Berichte

zur Polar- und Meeresforschung

Reports on Polar and Marine Research

Russian-German Cooperation: Expeditions to Siberia in 2020

Edited by

Boris K. Biskaborn, Dmitry Yu. Bolshiyarov,
Mikhail N. Grigoriev, Anne Morgenstern,
Luidmila A. Pestryakova, Leonid V. Tsibizov,
and Antonia Dill

Die Berichte zur Polar- und Meeresforschung werden vom Alfred-Wegener-Institut, Helmholtz-Zentrum für Polar- und Meeresforschung (AWI) in Bremerhaven, Deutschland, in Fortsetzung der vormaligen Berichte zur Polarforschung herausgegeben. Sie erscheinen in unregelmäßiger Abfolge.

Die Berichte zur Polar- und Meeresforschung enthalten Darstellungen und Ergebnisse der vom AWI selbst oder mit seiner Unterstützung durchgeführten Forschungsarbeiten in den Polargebieten und in den Meeren.

Die Publikationen umfassen Expeditionsberichte der vom AWI betriebenen Schiffe, Flugzeuge und Stationen, Forschungsergebnisse (inkl. Dissertationen) des Instituts und des Archivs für deutsche Polarforschung, sowie Abstracts und Proceedings von nationalen und internationalen Tagungen und Workshops des AWI.

Die Beiträge geben nicht notwendigerweise die Auffassung des AWI wider.

Herausgeber

Dr. Horst Bornemann

Redaktionelle Bearbeitung und Layout

Susan Amir Sawadkuhi

Alfred-Wegener-Institut
Helmholtz-Zentrum für Polar- und Meeresforschung
Am Handelshafen 12
27570 Bremerhaven
Germany

www.awi.de
www.awi.de/reports

Der Erstautor bzw. herausgebende Autor eines Bandes der Berichte zur Polar- und Meeresforschung versichert, dass er über alle Rechte am Werk verfügt und überträgt sämtliche Rechte auch im Namen seiner Koautoren an das AWI. Ein einfaches Nutzungsrecht verbleibt, wenn nicht anders angegeben, beim Autor (bei den Autoren). Das AWI beansprucht die Publikation der eingereichten Manuskripte über sein Repositorium ePIC (electronic Publication Information Center, s. Innenseite am Rückdeckel) mit optionalem print-on-demand.

The Reports on Polar and Marine Research are issued by the Alfred Wegener Institute, Helmholtz Centre for Polar and Marine Research (AWI) in Bremerhaven, Germany, succeeding the former Reports on Polar Research. They are published at irregular intervals.

The Reports on Polar and Marine Research contain presentations and results of research activities in polar regions and in the seas either carried out by the AWI or with its support.

Publications comprise expedition reports of the ships, aircrafts, and stations operated by the AWI, research results (incl. dissertations) of the Institute and the Archiv für deutsche Polarforschung, as well as abstracts and proceedings of national and international conferences and workshops of the AWI.

The papers contained in the Reports do not necessarily reflect the opinion of the AWI.

Editor

Dr. Horst Bornemann

Editorial editing and layout

Susan Amir Sawadkuhi

Alfred-Wegener-Institut
Helmholtz-Zentrum für Polar- und Meeresforschung
Am Handelshafen 12
27570 Bremerhaven
Germany

www.awi.de
www.awi.de/en/reports

The first or editing author of an issue of Reports on Polar and Marine Research ensures that he possesses all rights of the opus, and transfers all rights to the AWI, including those associated with the co-authors. The non-exclusive right of use (einfaches Nutzungsrecht) remains with the author unless stated otherwise. The AWI reserves the right to publish the submitted articles in its repository ePIC (electronic Publication Information Center, see inside page of verso) with the option to "print-on-demand".

*Titel: Sedimentkerngewinnung durch ein Eisloch am Khamra-See (Central Yakutia) im März 2020
(Foto: Stefano Meucci & Boris Biskaborn, AWI)*

*Cover: Sediment coring through an ice hole on Lake Khamra (Central Yakutia) in March 2020
(Photo: Stefano Meucci & Boris Biskaborn, AWI)*

Russian-German Cooperation: Expeditions to Siberia in 2020

Edited by

**Boris K. Biskaborn, Dmitry Yu. Bolshiyarov,
Mikhail N. Grigoriev, Anne Morgenstern, Luidmila A. Pestryakova,
Leonid V. Tsibizov, and Antonia Dill**

Please cite or link this publication using the identifiers

hdl:10013/epic.c6e37417-71ec-43f9-88ea-246e38a2582c

https://doi.org/10.48433/BzPM_0756_2021

ISSN 1866-3192

Expeditions to Siberia in 2020

Expedition LENA to Research Station Samoylov Island and Lena Delta 22.07. - 15.09.2020

Expedition Khamra 01.03. - 20.03.2020

Chief scientists

Boris K. Biskaborn (AWI), Julia Boike (AWI), Dmitry Yu. Bolshiyarov (AARI), Wolfram H. Geissler (AWI), Mikhail N. Grigoriev (MPI, IPGG), Andrei A. Kartozia (IPGG), Stefan Kruse (AWI), Anna A. Kut (MPI), Luidmila A. Pestryakova (NEFU), Anna M. Tarbeeva (MSU)

Contents

1	Introduction	2
2	Expedition Lena 2020 (RU-Land_2020_Lena)	7
2.1	Samoylov Long-Term Observatory	8
2.2	Lena River Water Monitoring at Research Station Samoylov Island	10
2.3	Coastal dynamics studies in the Buor-Khaya Bay	14
2.4	Distribution and structure of subaqueous permafrost in the Lena River Delta	18
2.5	Micromorphology structure of sediments and ice wedges on Kurungnakh Island	21
2.6	Thermal erosion in the small basins of the Arctic coast in the vicinity of the Khabarovo Polar Station	27
2.7	New studies of the deep geophysical structure in the southern part of the Lena Delta	35
2.8	Seismicity of the Laptev Sea Rift	37
3	Expeditions to Central Siberia	47
3.1	Lake sediment core retrieval and vegetation analysis at Lake Khamra, Central Siberia: Expedition Khamra 2020	48
3.2	Monitoring a full year-cycle of land surface and snow depth within an alas and close forests close to Churapcha (Yakutia)	55
4	Appendix	62
A.1	List of participants	63
A.2	Supplementary material - Expedition Lena 2020	65

Chapter 1

Introduction

*Boris K. Biskaborn*¹, *Dmitry Yu. Bolshiyarov*², *Mikhail N. Grigoriev*^{3,4}, *Anne Morgenstern*¹, *Luidmila A. Pestryakova*⁵, and *Leonid V. Tsibizov*⁴

¹ Alfred Wegener Institute Helmholtz Centre for Polar and Marine Research, Potsdam, Germany

² Arctic and Antarctic Research Institute, St. Petersburg, Russian Federation

³ Melnikov Permafrost Institute, Siberian Branch, Russian Academy of Sciences, Yakutsk, Russian Federation

⁴ Trofimuk Institute for Petroleum Geology and Geophysics, Siberian Branch, Russian Academy of Sciences, Russian Federation

⁵ M.K. Ammosov North-Eastern Federal University, Yakutsk, Russian Federation

Overview

This report provides an overview of the study locations, scientific objectives and field activities of the joint Russian-German expeditions to Siberia conducted in 2020. The expeditions cover investigations on the biology, geology, geomorphology, coastal dynamics, ecology and reconstructions of the paleoenvironment. Focus regions of this year's expedition were the Lena River Delta and Samoylov Island, and locations in Central Yakutia west and east of Yakutsk close to the Lena River (Figure 1.0.1).

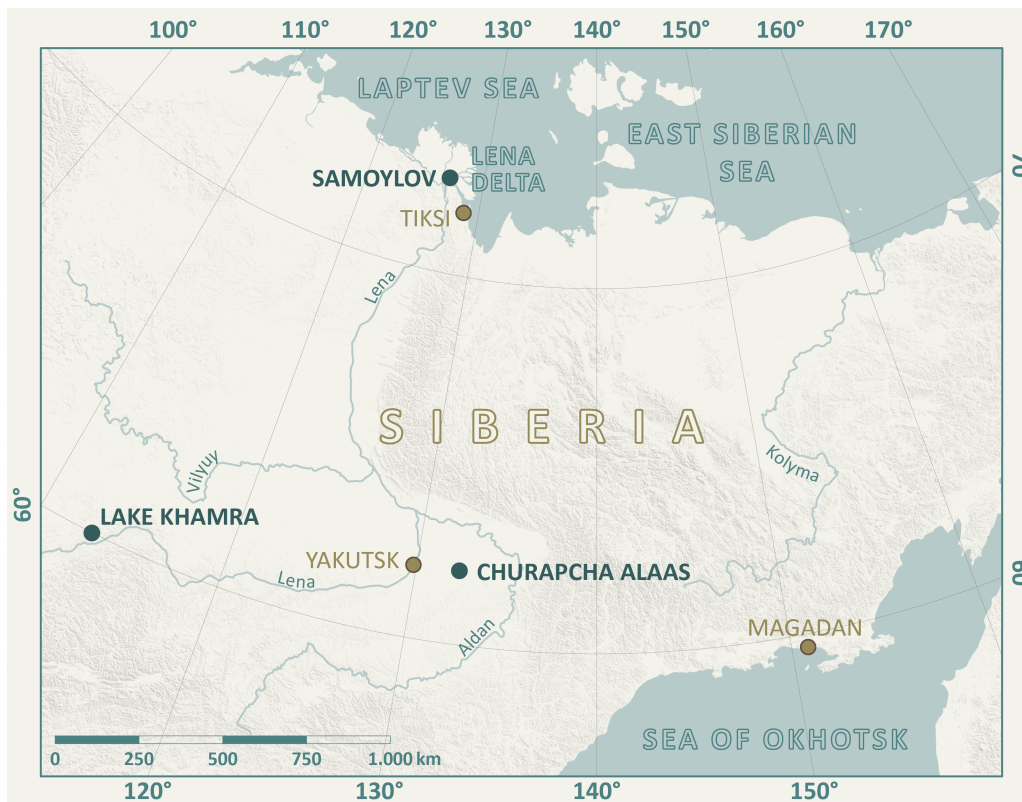


Figure 1.0.1: Field sites of Russian-German expeditions to Siberia in 2020

Co-operative Russian-German geoscientific research in Siberia included annual expeditions to Yakutia and the Siberian Arctic since 1993. An expedition to the Lena River Delta in 1998 within the framework of the Russian-German Cooperation SYSTEM LAPTEV SEA, supported by the research ministries of both countries was the first in the series of the annual joint Russian-German “LENA Expeditions”. This first expedition laid the foundation for the establishment of a permafrost observatory on Samoylov Island in the central Lena Delta and the operation of a research station, which has been serving as a scientific and logistical base for the LENA expeditions ever since. Permafrost conditions, micrometeorology, trace gas exchange, biology, and many other parameters are monitored at long-term measurement sites on the island. The new Research Station Samoylov Island (Figure 1.0.2) has been operated by the Trofimuk Institute for Petroleum Geology and Geophysics, Siberian Branch, Russian Academy of Sciences (IPGG SB RAS) since 2013, and provides a logistics-staging base, laboratories for field work and accommodation for the scientists, technicians and students. The LENA expeditions are jointly organized by the Arctic and Antarctic Research Institute (AARI), the Alfred Wegener Institute Helmholtz Centre for Polar and Marine Research (AWI) and the Melnikov Permafrost Institute, Siberian Branch, Russian Academy of Sciences (MPI SB RAS).

For many years, the Northeastern Federal University Yakutsk (NEFU) collaborates with the AWI to investigate lake systems and vegetation dynamics in Siberia. Expeditions based on field camps in remote areas of Siberia and the Russian Far East aim at better understanding processes and environmental trajectories in this vast permafrost regions. Given the fast warming of the Arctic but the very sparse coverage of paleolimnological data in eastern Siberia the Russian-German scientific team aims to gain sample material data from remote lakes, i.e. sediment cores, field measurements, e.g. sub-bottom profiling and aerial imagery, and vegetation material, e.g. tree-rings and material for DNA analyses.

Expedition Lena 2020 - Participants and itinerary

In 2020, the LENA expedition was severely affected by the COVID-19 pandemic. Initially planned for the period from March to September, large parts of the expedition program had to be cancelled. Only few groups of Russian researchers (15 participants in total), but no German or foreign participants were able to travel to Samoylov Island and the Lena Delta. Thanks to the great support of station staff and Russian colleagues, long-term measurements and sampling programs could still be maintained.

The LENA 2020 expedition was coordinated by Prof. Dr. Guido Grosse (Alfred Wegener Institute Helmholtz Centre for Polar and Marine Research - AWI, Potsdam), Prof. Dr. Dmitry Yu. Bolshiyakov (Arctic and Antarctic Research Institute - AARI, St. Petersburg), Dr. Mikhail N. Grigoriev (Melnikov Permafrost Institute, Siberian Branch, Russian Academy of Sciences – MPI SB RAS, Yakutsk) and Prof. Dr. Igor Yeltsov (Trofimuk Institute of Petroleum-Gas Geology and Geophysics - IPPG, Novosibirsk) and led by Sergei A. Pravkin (AARI) and Julia Boike (AWI).

In addition to research on Samoylov Island, field sites included other locations within the Lena River Delta and adjacent to it, e.g. Kurungnakh and Sardakh islands, to Khabarova meteo station, as well as the Tiksi and Buor-Khaya Bay in July and August.



Figure 1.0.2: Logos of the Expedition LENA 2020 and Research Station Samoylov Island



Figure 1.0.3: Group photo of the Lena 2020 geophysics team



Figure 1.0.4: *Group photo of the Lena 2020 participants in August*

Expedition Khamra 2020 – Participants and itinerary

The expedition Khamra 2020 led by Boris K. Biskaborn (AWI) started early enough in March to reach the remote Lake Khamra before the COVID-19 pandemic spread to an extent that would affect the participants. Luidmila A. Pestryakova (NEFU) and Ulrike Herzsuh (AWI) were coordinating the Russian-German collaboration and safe return of all participants shortly before closing of the borders. Gennadiy V. Nesterov (HUS) led the field work in Churapcha in close (remote) collaboration with Stefan Kruse (AWI). In total 9 persons actively participated in expeditions to Central Yakutia of which 4 persons came from Germany (Khamra 2020 expedition) and 5 from Russia (Khamra 2020 and Churapcha fieldwork).



Figure 1.0.5: *Logo of the Expedition Khamra 2020*



Figure 1.0.6: Group photo of the Expedition Khamra 2020 team

Participants of all expeditions and their affiliations are listed in the appendix (Table A.1.1 - Table A.1.5). In addition, the appendix lists collected samples and measurements made in 2020. This report consists of contributions from the expedition participants. The authors of the contributions are responsible for content and correctness.

Data management

The data collected within the framework *Expeditions to Siberia 2020* are stored on the PANGAEA data repository (www.pangaea.de). Data from chapter 2 are archived under the campaign label **RU-Land_2020_Lena**. Data from chapter 3 are archived under the campaign label **RU-Land_2020_Khamra**.

The AWI in cooperation with the research station on Samoylov Island has been an important hub for permafrost temperature measurements and the integration of data into international data base repositories, such as the Global Terrestrial Network for Permafrost (GTN-P; <http://gtnp.arcticportal.org/>).

Acknowledgements

The expeditions to Siberia in 2020 depended on essential support of the Russian and German organizing institutions, funding agencies, authorities and individuals. In particular, we would like to express our appreciation to the staff of the Research Station Samoylov Island, the Lena Delta Reserve, the Tiksi Hydrobase, the Arctica GeoCenter, and the North-Eastern Federal University Yakutsk (NEFU).

Chapter 2

Expedition Lena 2020 (RU-Land_2020_Lena)

Edited by Anne Morgenstern

2.1 Samoylov Long-Term Observatory

Christian Wille ^{1,*,@}, Niko Bornemann ^{2,*}, Torsten Sachs ^{1,*}, Lars Kutzbach ^{3,*}, Julia Boike ^{2,*}

¹ Helmholtz-Zentrum Potsdam - GFZ German Research Center for Geosciences, Potsdam, Germany

² Alfred Wegener Institute Helmholtz Centre for Polar and Marine Research, Potsdam, Germany

³ Institute of Soil Science, Universität Hamburg, Hamburg, Germany

* not in field

@ Corresponding author: christian.wille@gfz-potsdam.de

Fieldwork period and location

No fieldwork in 2020 by the German team.

Objectives

The Samoylov Long-Term Observatory (SALTO) aims to continue the existing long-term observation of vertical carbon and energy fluxes as well as meteorological, hydrological, and permafrost conditions on Samoylov Island. This continuous time series provides unique insights into the change of the permafrost landscape on Samoylov Island. Especially long time series of the vertical fluxes of carbon (CO₂ and CH₄) are required to detect inter-annual variability and long-term changes in the carbon balance.

Methods (or) Fieldwork summary

In 2020, all fieldwork of German expedition teams was canceled due to the COVID-19 pandemic. Thus, the maintenance work planned for the various measurement systems of the long-term observatory could not be carried out. However, with the help of Russian colleagues from the Research Station Samoylov Island and the Trofimuk Institute of Petroleum Geology and Geophysics (IPGG), Novosibirsk, it was possible to solve several technical problems so that the systems could be kept in operation. The tasks taken over by the Russian colleagues were e.g. the recommissioning of the field laboratory's air conditioning system, the change of air filters of the eddy covariance trace gas analyzers, and the reset of several measurement systems after their failure. Also, the remote 100 m permafrost borehole on Sardakh Island was visited by Andrey Kartoziia (IPGG) on 17.08.2020 to read out the data and to change the battery (Figure 2.1.1). The manual long-term observation of active layer thickness started in 2002 (Boike et al. 2019) and ground subsidence from 2013 (Antonova et al. 2018) were continued. The 31 subsidence sites on Kurungnakh were visited on 29.06.2020 and 17/21.09.2020 and the 7 sites on Samoylov were visited 7 times from 18.06.200 to 20.09.2020.



Figure 2.1.1: Casing and logger box of the Sardakh 100 m temperature borehole (N 72.57150, E 127.24160), picture by Andrey Kartoziia

Preliminary results

Trace gas flux measurements with open-path (CO₂, H₂O) and closed-path (CO₂, H₂O, CH₄) gas analyzers were conducted automatically continuously from September 2019 to September 2020. Several data gaps exist due to technical problems. A full assessment of the data availability and quality will be possible after the data has become available. In 2020 the Samoylov active layer thickness CALM grid R51 of 150 nodes was measured 6 times from 18.06.2020 to 20.09.2020 (Figure 2.1.2). The mean active layer thickness at the end of season was 59 cm with a minimum of 42 cm and a maximum of 81 cm within the grid. The data are available at the webpage of the Global Terrestrial Network on Permafrost (GTN-P: <http://gtnpdatabase.org/activelayers/view/245/>) and the Circumpolar Active Layer Monitoring Network (CALM: <https://www2.gwu.edu/~calm/data/north.htm>).

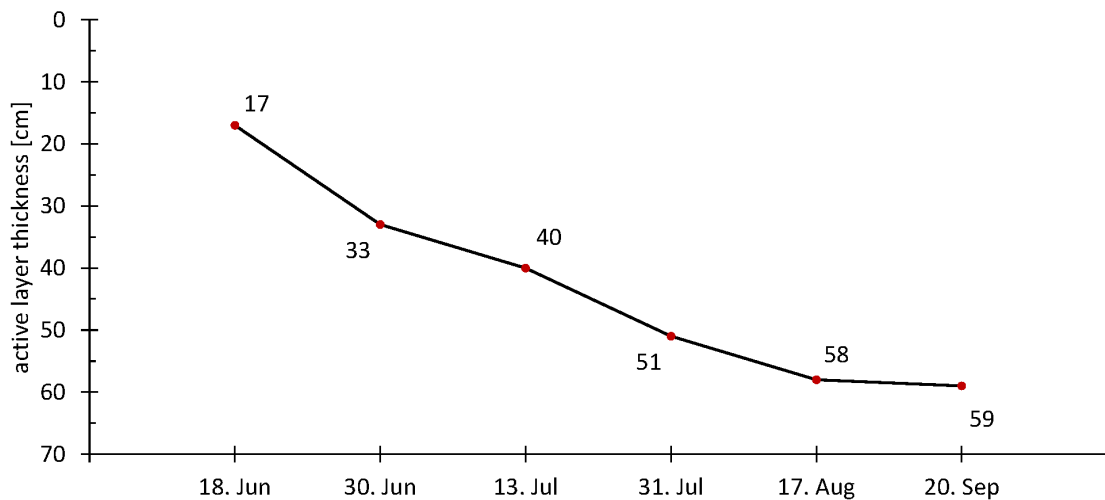


Figure 2.1.2: Mean active layer thickness measured at Samoylov CALM site R51 in 2020

Acknowledgment

Many thanks to the Russian partner and colleagues, particularly to Andrey Kartoziia, Fyodor Sellyakhov, and Viktor Zykov for their effort and work.

2.2 Lena River Water Monitoring at Research Station Samoylov Island

Bennet Juhls ^{1,2,*,@}, Antje Eulenburg ^{2,*}, Anne Morgenstern ^{2,*}, Olga Ogneva ^{3,*}, Paul Overduin ^{2,*}, Sergey Volkov ⁴, Ekaterina N. Abramova ⁵

¹ Institute for Space Science, Free University Berlin, Berlin, Germany

² Alfred Wegener Institute Helmholtz Center for Polar and Marine Research, Potsdam, Germany

³ Alfred Wegener Institute Helmholtz Center for Polar and Marine Research, Bremerhaven, Germany

⁴ Research Station Samoylov Island, Trofimuk Institute for Petroleum Geology and Geophysics, Siberian Branch, Russian Academy of Sciences, Novosibirsk, Russian Federation

⁵ Lena Delta Nature Reserve, Tiksi, Sakha Republic, Russian Federation

* not in field

@ Corresponding author: bennet.juhls@awi.de

Fieldwork period and location

From January 1st to December 31st, 2020 at Research Station Samoylov Island.

Objectives

A number of studies expect an increase of carbon export by rivers to the Arctic Ocean due to rapidly changing climate in the Arctic (Camill 2005; Freeman et al. 2001; Frey 2005). One possible reason for the increase of carbon export is thawing permafrost, which can lead to a mobilization of previously frozen dissolved organic matter (DOM). The Lena River delivers about one fifth of all river water to the Arctic Ocean (Holmes et al. 2011) and is the main source of DOM in the Laptev Sea shelf (Thibodeau et al. 2014). The discharge of the Lena River and the DOM concentration shows an extreme seasonality. Scarce measurements of DOC and the coloured fraction of DOM (CDOM) (< 8 samples/year) were previously used to estimate fluxes to the Arctic Ocean for the whole year based on a proportional connection between DOM and discharge (Stedmon et al. 2011). Such estimations can potentially result in large errors. Longer-term sampling and higher sampling frequency would help to establish a baseline and understand the future impact of climate, landscape and hydrological change on land-to-ocean transfer, as well as the causes of seasonal and shorter timescale variability. With this study, we seek to improve our understanding of seasonal variations of fluxes transported by the Lena River. The sampling program regularly collects samples for measurements of several water parameters, such as temperature, conductivity, dissolved organic carbon (DOC), spectral CDOM absorption ($a_{CDOM}(\lambda)$), dissolved and total nutrients and stable isotopes. The sampling interval has been variable, between 1 and 11 days, with an average 2.7 days. After successful sampling from spring 2018 until spring 2019 (data: Juhls et al. 2020a: Lena River surface water monitoring near the Samoylov Island Research Station) resulted in an initial partition of Lena River sources with an end-member model (Juhls et al. 2020b), the sampling program continued into 2020 and is ongoing, with slight changes to the sampling protocols and further sample series for additional parameters.

Fieldwork summary

Sampling originally began on 20.04.2018, carried out by staff from the Research Station Samoylov Island following sampling instructions that included a description of the sampling procedure, a protocol for recording each sampling event and a manual for sample filtration, preservation and storage.

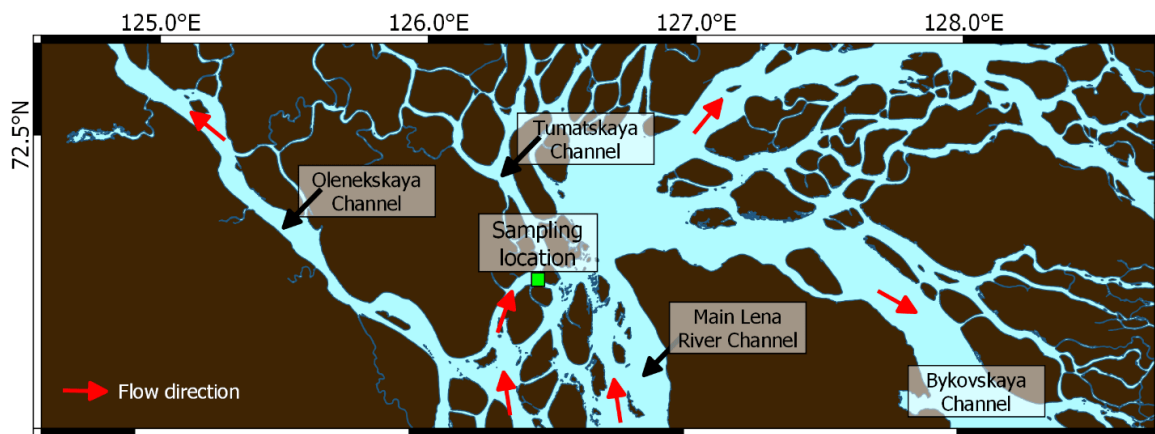


Figure 2.2.1: Overview map of the part of the Lena River Delta displaying the sampling location, different Lena River channels, and flow directions

If weather or ice conditions allow, samples are usually taken from the center of the Olenekskaya Channel (Figure 2.2.1) from a boat or from the river ice. Otherwise, samples are taken from the shoreline.

Samples for a core set of parameters (Table 2.2-1) have been collected throughout the monitoring program. Additional parameters have been added to the regular sampling program (Table 2.2-1). Changes in sampling interval varied depending on variability in discharge, on the availability of sampling materials and on station staffing.

- EC WTW COND 3401 was recalibrated on 03.07.2019 by E. Abramova
- EC (lab) (0079-0202) was measured in AWI Potsdam 14.09.2020 on subsets of unfiltered rest sample. EC (lab) (0202-0287) was measured in AWI Potsdam 14.09.2020 on subsets of filtered CDOM sample (P. Overduin)
- CDOM (0079-0202) was measured in OSL, St. Petersburg on 21.01.2020 (B. Juhls).
- CDOM (0202-0287) was measured in GFZ, Potsdam on 5.11.2020
- DOC (0202-0287) was measured in AWI, Potsdam on 19.11.2020 (P. Overduin)
- FDOM (0079-0201) was measured on subsets of rest samples in Copenhagen (Danish Technical University); FDOM (0202-0287) was measured on subsets of CDOM samples on DTU, Aqua (C. Stedmon)
- Cations and anions (0078-0201) were measured in Nov. 2020 and Feb. 2021, respectively, on subsets of rest samples that had been stored unfrozen (cooled and unfiltered). Cations and anions (0202-0287) were measured in Nov. 2020 and Feb. 2021, respectively, on subsets of cooled (unfrozen), filtered CDOM samples. (P. Overduin)
- Stable isotopes of water (0079-0201) were measured at AWI, Potsdam on 27.04.2020 (H. Meyer)

Table 2.2-1: Core set of parameters

Parameter	Details	Sample Volume [ml]	Preservation	Storage
Core parameters (always ampled & measured)				
Temperature (in field)	measured at sampling (WTW COND 340I)	-	-	-
Electrical conductivity (in field)	measured at sampling (WTW COND 340I)	-	-	-
Electrical conductivity (in lab)	measured on WTW Multilab 540	variable	-	variable
Dissolved organic carbon (DOC)	filtered, 0.45 μ M cellulose acetate (CA)	-	acidified to pH<2 with HCl	cool, dark, glass vial
Colored dissolved organic material (CDOM)	filtered, 0.45 μ M cellulose acetate (CA)	-	-	cool,dark, brown glass
Stable isotopes of water	unfiltered	-	-	cool, polyethylene bottle
Rest sample	unfiltered (for EC (lab), additional parameter or reanalysis if needed)	-	-	frozen, polyethylene bottle
Nutrients, total	unfiltered	-	-	frozen, polyethylene bottle
Nutrients, dissolved	filtered, 0.45 μ M cellulose acetate (CA)	-	-	frozen, polyethylene bottle
Additional parameters (not always ampled & measured)				
Major cations	filtered, 0.45 μ M cellulose acetate (CA)	on rest sample	-	-
Major anions	filtered, 0.45 μ M cellulose acetate (CA)	on rest sample	-	-
FDOM	filtered, 0.45 μ M cellulose acetate (CA)	on CDOM rest	-	-
D ¹⁴ C-DOC	filtered, 0.45 μ M cellulose acetate (CA), beginning on 06.04.2019; sample frequency irregular	250 / 60	acidified to pH<2 with HCl	acid-washed HDPE bottle, frozen
Si & Sr isotopes	for time period 20.04.2018 - 30.03.2019; measured on	-	-	-

Preliminary results

A list of samples collected to date is given in Table A.2.1.

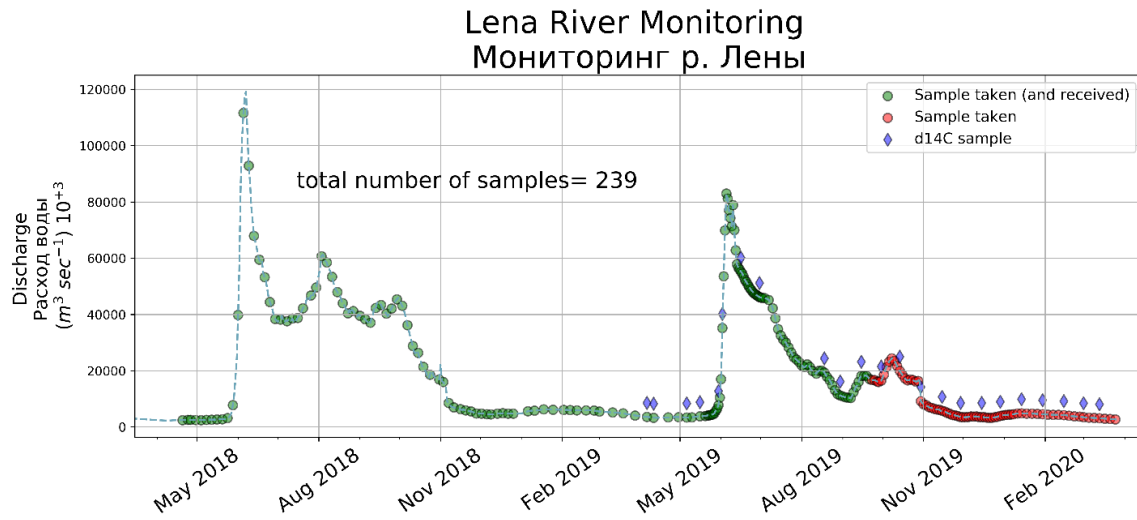


Figure 2.2.2: Sample dates and discharge (Shiklomanov et al., 2018) (as of August 2020). Note that $D^{14}C$ samples were taken at lower frequency.

2.3 Coastal dynamics studies in the Buor-Khaya Bay

Mikhail N. Grigoriev ^{1,2,@}, Georgii T. Maksimov ^{1,2}

¹ Melnikov Permafrost Institute, Siberian Branch of Russian Academy of Sciences, Yakutsk, Russian Federation

² Trofimuk Institute of Petroleum Geology and Geophysics, Siberian Branch of Russian Academy of Sciences, Novosibirsk, Russian Federation

@ Corresponding author: grigoriev@mpi.ysn.ru

Fieldwork period and location

From August 29th to September 2nd, 2020 on Muostakh Island and Bykovsky Peninsula.

Objectives

In August 2020, studies of coastal cryogenic geomorphological processes dynamics were carried out at long-term monitoring sites in the central coastal sector of the Laptev Sea, which include Muostakh Island and Bykovsky Peninsula (Figure 2.3.1, 2.3.2). The rates of thermal abrasion and thermal denudation of icy shores in key areas were studied. The main task was to assess the rate of coastal erosion at key sites where such observations have been carried out annually since 1982. Studied key sites were provided by detailed tacheometric surveys, benchmarks and navigation geographic networks.



Figure 2.3.1: Thermal abrasion of ice-rich coast. Monitoring site on Muostakh Island (August, 2020)



Figure 2.3.2: *Thermodenudation processes on the key site. Monitoring profile on the Bykovsky Peninsula (August, 2020)*

Preliminary results

The base long-term observational profiles are located on the northern cape and the northeastern coast of Muostakh Island, where the rates of development of coastal thermal abrasion were studied, and on the northeastern coast of the Bykovsky Peninsula, where processes of thermal denudation of coastal slopes in combination with thermal abrasion phenomena were observed (Figure 2.3.3).

Average long-term rates of coastal retreat on the Muostakh Island (northeastern coast and northern cape) amounted to about 10 - 13 m per year (with the maximum recorded, respectively, 14 and 25 m per year), and on the northeast coast of the Bykovsky Peninsula - 1.5 - 2, 5 m per year (maximum speed - 11 m per year). At long-term monitoring sites, observations carried out in August 2013-16 showed that the rates of thermal denudation and thermal abrasion of ice coast in the region over the past four years decreased significantly, approached the average long-term and became much lower than the coastal retreat rates on these shores in 2000-2011.

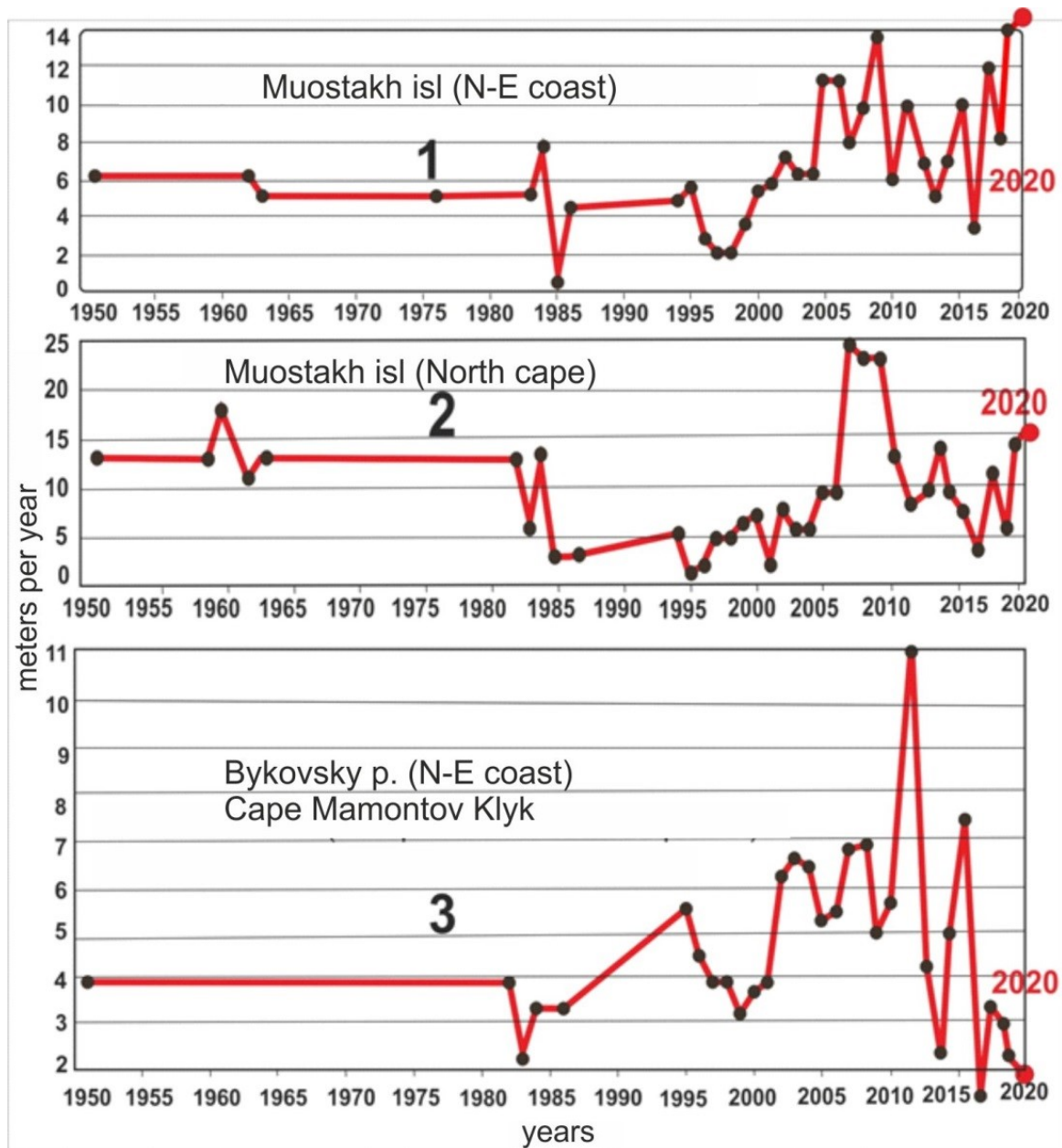


Figure 2.3.3: The coastal retreat rate on the long-term monitoring sites (rates of thermal abrasion – profiles 1, 2 and thermal denudation - profile 3)

It should be noted that in the studied site on the Bykovsky Peninsula, the upper thermodenudation slope has flattened down and in this area has become almost stable (Figure 2.3.4). At the same time, the retreat rate of the lower thermal abrasion cliff in this complicated slope system has significantly intensified over the past 5-7 years (up to 8-14 m per year). Accelerating the retreat of the lower thermal abrasion cliff over the next few years will inevitably lead to the further destruction of the thermal denudation slope and the emergence of a new thermal denudation cliff at the top of the thermal terrace.

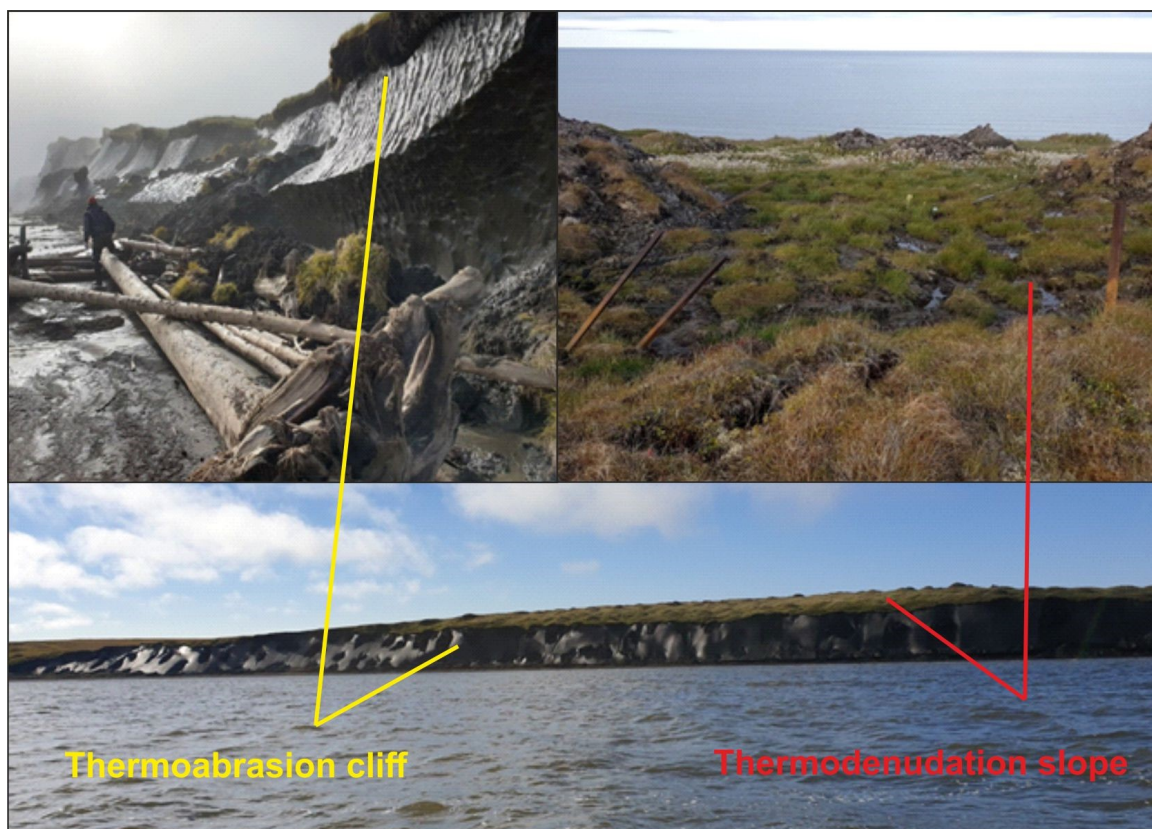


Figure 2.3.4: Development of a complicated slope coastal system, represented by the lower thermal abrasion cliff, thermal terrace and the upper, almost flattened, thermodenudation slope. North-eastern coast of the Bykovsky Peninsula, August, 2020

Conclusion

In general, the rates of coastal retreat approximately correspond to changes in the seasonal climatic situation in the region, in particular, the dynamics of the area of summer solid ice, which affects the development of storm activity in the Laptev Sea. It should be noted that in 2018-2020, the erosion rate in key section 1 approximately corresponds to the average over the last 15 years, while in section 2 it is the minimum over this period, and the rate of coastal destruction in section 3 shows an absolute minimum (almost 0 m per year) for the entire observation period (37 years).

2.4 Distribution and structure of subaqueous permafrost in the Lena River Delta

Georgii T. Maksimov ^{1,2}, Mikhail N. Grigoriev ^{1,2,@}

¹ Melnikov Permafrost Institute, Siberian Branch of Russian Academy of Sciences, Yakutsk, Russian Federation

² Trofimuk Institute of Petroleum Geology and Geophysics, Siberian Branch of Russian Academy of Sciences, Novosibirsk, Russian Federation

@ Corresponding author: grigoriev@mpi.ysn.ru

Fieldwork period and location

From August 10th to August 27th, 2020 on small channels, near Samoylov station.

Objectives

The deltas of the Arctic rivers are areas of active growth of subaquatic permafrost and at the same time, the place of formation of talik zones. However, the nature of permafrost distribution and the features of development of talik zones under the channels in the Arctic deltas are practically not studied.

Field works in the frame of the expedition Lena 2020 were carried out from 10.08.2020 to 27.08.2020. The main base of the team was the Samoilovsky station. The work was conducted in several channels at the Lena Delta apex (Figure 2.4.1).

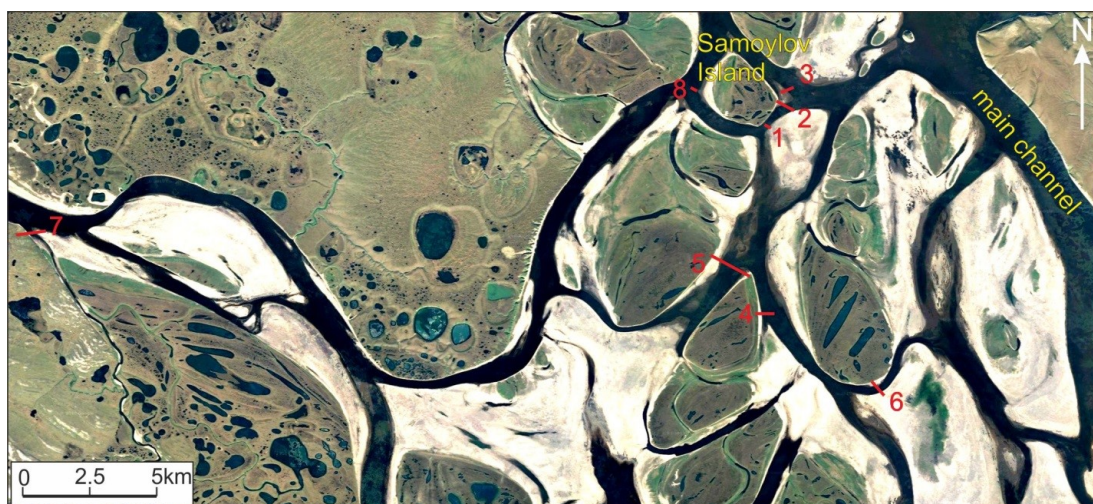


Figure 2.4.1: Work site diagram

The main goal of our field work was to study the features of subaqueous permafrost and talik zones formation under the channels of the Lena Delta. One of the main task was to determine the position of the permafrost table under the channels of the largest Arctic delta along the selected profiles.

A motorboat was used for route studies. A standard ground bottom-grab and special bottom sampler of 10 meter length was used to determine a bottom sediment structure and position of the permafrost table on selected typical profiles.

Preliminary results

The results obtained on the location of the aquatic permafrost table is presented on 8 profiles. In shallow water conditions (depth up to 2.5 m), permafrost was found almost everywhere. The thawed layer of under-channel sediments under the permafrost varies from 0.5 to 2-3 m. In a number of channels, where there is a strong erosion of coastal and bottom sediments, thawed deposits could be washed away, down to the permafrost table (Figure 2.4.3).



Figure 2.4.2: *Determining the subaquatic permafrost table in the Lena Delta (August, 2020)*



Figure 2.4.3: *Actively eroded shore (Siesti-Ars-Uesia Channel, August, 2020)*

A bathymetric channel survey conducted in the apex of delta shows a rather variegated alternation of deep and shallow sections of the channels. Depths on the fairway of large channels vary from 7 to 10 m, and on the largest channels can reach up to 30 m.

The lithological composition of bottom sediments is represented mainly by alternating sands of various grain sizes and silts, with partial inclusions of wood detritus. Sands usually have horizontal, sometimes oblique bedding with inclusions of organic residues in the form of filamentous roots, wood fragments, and dark spots of organic matter. Frozen sands usually have a massive cryostructure. New obtained data on the position of the permafrost table and the thickness of the thawed sediments under river channels allow us to find out the peculiarities of the formation of permafrost and talik zones under the channels of the largest Arctic delta. (Figure 2.4.4; Table A.2.2). It was found that at water depths of 0.5-1.0 m, the thickness of the seasonally thawed layer varies 1.0-2.0 m; with a water depth of 1.5-3 m, and the permafrost table lies 1.0-2.5 m below the bottom. At a water depth of more than 3 m, the permafrost table is also recorded to a depth of 1.5 m below the bottom. Most often this takes place in the marginal zone of subaquatic permafrost. However, on profile 5, in the middle of the channel, within the small underwater elevation, a frozen table was recorded at a depth of 4.7 m with a water thickness of 3 m. In relatively deep areas of channels (up to 3 meters deep), permafrost occurs in the bottom sediment quite often, as in spring the thickness of river ice can exceed 2 m, and water level, as a rule, by the end of spring can go down by 1-2 m. The massive ice can sink to the bottom in this period and bottom deposits can freeze to a considerable depth.

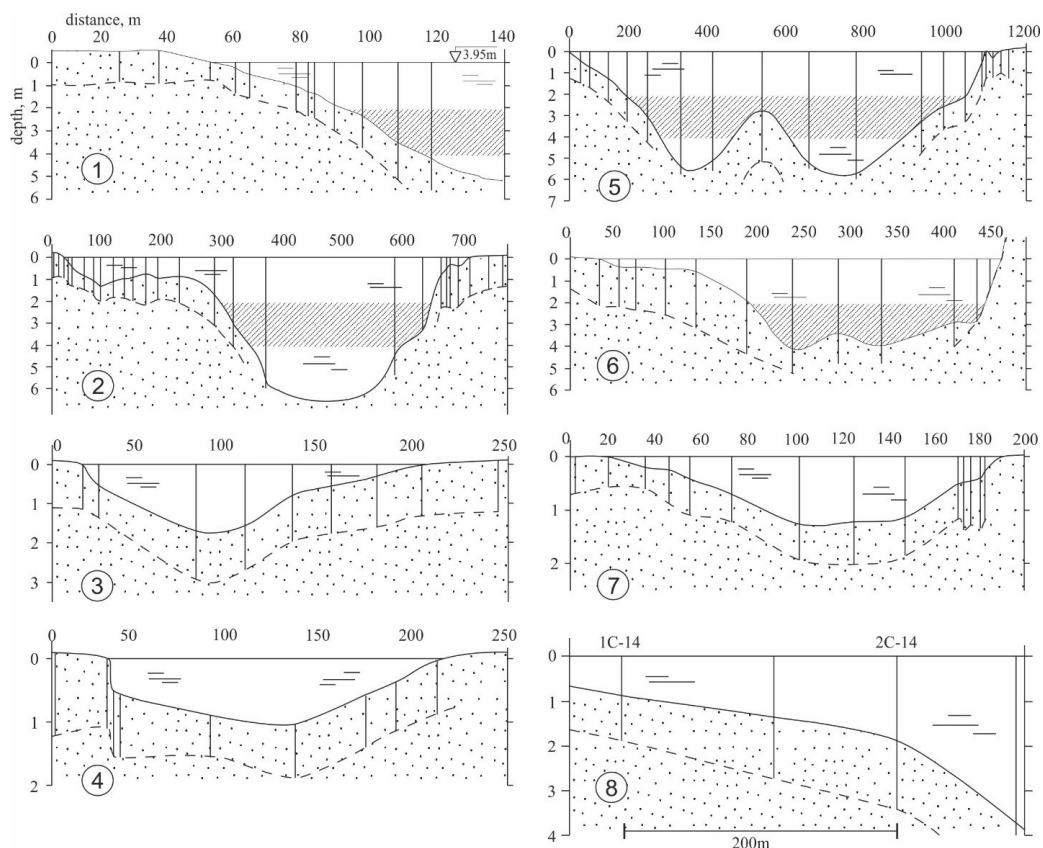


Figure 2.4.4: Results of subchannel permafrost probing. 1- South-East shore of Samoylov Island; 2- East cape of Samoylov Island; across Olenekskaya channel; 3- From Samoylov Island till Ebe-Kumaga sands; 4- Sistyakh-Ary-Uesya channel; 5- Between islands Sasyk-Ary and Sordokh-Ary; 6- On unnamed channel which pour in Sistyakh-Ary-Uesya channel; 7- Chai-Tumus site, small channel which pour in Olenekskaya channel; 8- on drilling profile between Bh 1c-14 and 2c-14.

Conclusion

The results of sub-channel permafrost evolution studies show that the bottom permafrost under the channels of the Arctic deltas is extremely widespread, occupying all shallow parts of largest channels and almost complete area on small channels.

The all-season under-channel talik is formed only within a relatively deep part of channels and has a complex lateral boundary connected with peculiarities of the dynamics of the channel displacement.

2.5 Micromorphology structure of sediments and ice wedges on Kurungnakh Island

Yana V. Tikhonravova ¹, Anna A. Kut ^{1,@}, Alexey V. Lupachev ²

¹ Melnikov Permafrost Institute SB RAS, Yakutsk, Russian Federation

² Institute of Physico-Chemical and Biological Problems in Soil Science RAS, Pushchino, Russian Federation

@ Corresponding author: ann.urban@mail.ru

Fieldwork period and location

From August 10th to August 27th, 2020 on Tiksi and Kurungnakh Island.

Objectives

The research aimed to study the composition and structure of Quaternary frozen sediments and ice wedges in the Lena Delta for a better understanding of the regional history of depositional and post-depositional processes.

Methods and Fieldwork summary

The study of permafrost and ground ices included a comprehensive approach of both – conventional facies analysis and microstructural analysis of sediments, recent and buried soils, and ground ice. The description of the key permafrost exposures, along with a sampling of the deposits, ground ice, botanic and hydrologic sampling was done during fieldwork. Laboratory studies will include:

Particle size composition of sediment using laser diffraction analyzer the Mastersizer 3000 (Kurchatova et al. 2014) in the Earth's cryosphere institute, Tyumen, Russia. Particle size distribution is determined using an expanded method of laser granulometry. The analyzer conducts the calculation of the coefficient automatically like mode of particle size (Mo) and Trask sorting coefficient (So) (Trask 1932), etc. The grain size classification was based on Wentworth 1922.

Micromorphological analysis of mineral surface for characteristic texture elements distinguishing corresponding to different sedimentation environments. The method based on grains of terrigenous material gets texture elements of environments of transfer and accumulation Calculation of roundness and frosting coefficients to show environment changing dynamic. Cryogenic weathering as a physics and chemical process leaves specific elements on the grain surface.

Micromorphological analysis of ice by petrography method in Melnikov Permafrost Institute SB RAS, Yakutsk, Russia. This petrographic analysis, the definition of the ratio of different natural ice types within an object, will establish the primary and secondary processes of formation. To determine ground ice structure features, the monoliths were first trimmed to examine bubble patterns, sizes and shapes, and the ice structure under plain light. Thin sections (~0.8 mm) were then made horizontally and vertically across the samples. To quantify ice crystals and shapes, the thin sections were photographed under crossed polarisation. The structure and texture of wedge ice were determined: the size and morphology of ice crystals, distribution of air bubbles, and mineral-to-organic inclusions. To quantify ice crystals and shapes, the thin sections were photographed under crossed polarisation.

Measurements of the stable isotope ratios of oxygen and hydrogen in types of ground ice have carried out on a Picarro L-2140i in Melnikov Permafrost Institute SB RAS, Yakutsk, Russia. Analysis of the device is based on the unique Wavelength Scanned Ring Down Spectroscopy (WS-CRDS) method.

Hydrochemical analysis of natural waters, water extract of deposits, and ice melts using standard methods in the laboratory of groundwater and permafrost geochemistry in Melnikov Permafrost Institute SB RAS.

Preliminary results

The result of the fieldwork was described 5 cross sections on Kurungnakh Island and sampled materials for particle size composition of sediment (38 samples), peat and organic (8 samples), ice monoliths (6 samples), isotope samples (48 samples) and samples for micromorphological analysis (24 samples).

Kurungnakh island is located in the central part of the Lena River delta, washed by the Olenekskaya channel. The island is composed mainly of Late Quaternary sediments (Schwamborn et al. 2002), and belongs to the third terrace of the Lena River (Grigoriev 1993). In the structure of the ~40-meter thickness, sand deposits in the lower part (up to 22 m) are identified, overlain by silt deposits of the ice complex and peat Holocene deposits (Wetterich et al. 2008; Bolshiyarov et al. 2013). The island is riddled with wide ice wedges. Syngenetic ice wedges are characterized by an elevation of 15-20 m (Schirmermeister et al. 2011), the tails of the veins were recorded at the level of 13-14 m from the surface (Wetterich et al. 2008).

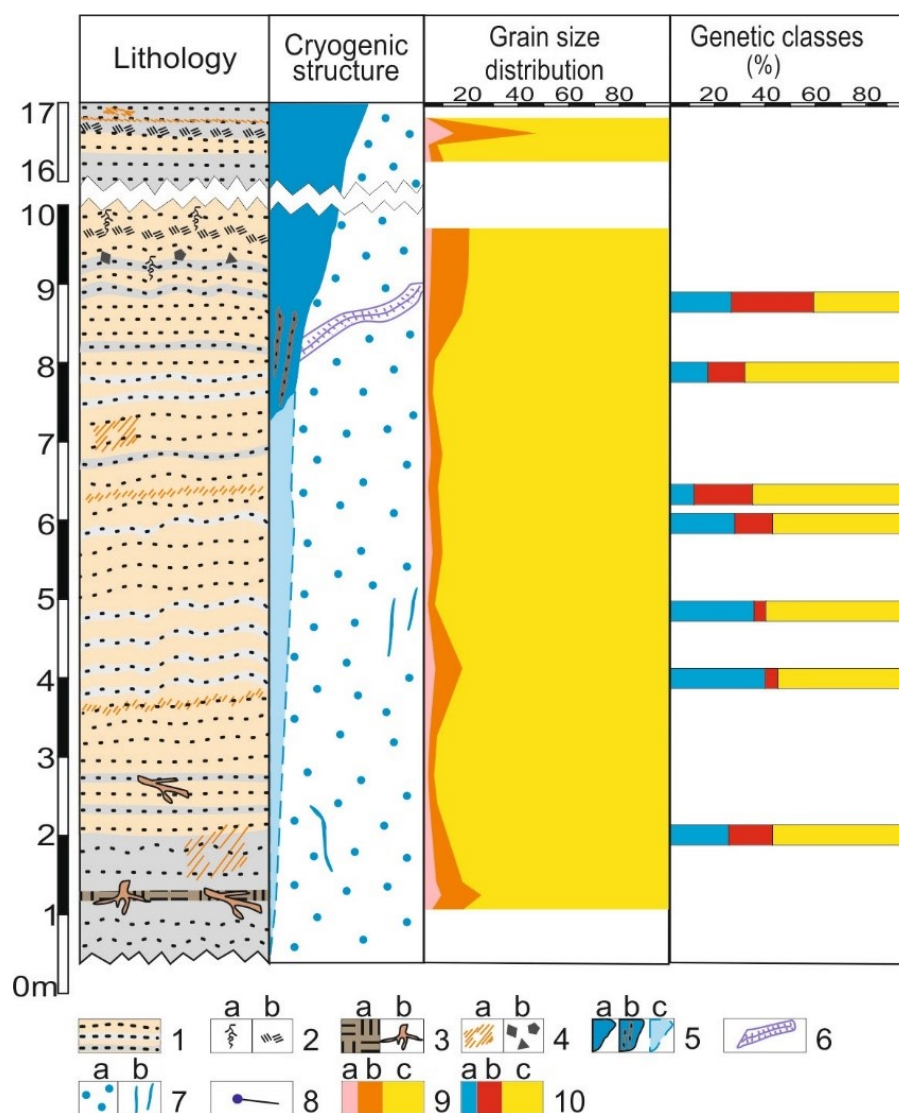


Figure 2.5.1: 1 - sand, 2 - plant remains autochthonous (a), allochthonous (b), 3 - peat interbed (a), wood remains (b), 4 - ferruginous spots and streaks (a), gravel (b), 5 - ice wedge (a), composite part of ice wedge (b), supposed ice wedge (c), 6 - crack ice, 7 - porous invisible cryostructure (a), vertical thin ice lenses, 8 - total water content [%], 9 - granulometric composition: clay (a), silt (b), sand (c), 10 - genetic classes of grains: NU (a), EL (b), EM/EL (c)

Cryolithological structure

The island sediments were studied based on five cross sections during fieldwork 2020. Cross sections Kur-01, Kur-03 and Kur-04 are ripped up in the Ice Complex overlapped. Cross section Kur-02 and Kur-06 are underlying layers.

The deposits of the lower part of Kurungnakh cross section, underlay of the Ice Complex, consist of interbedded yellow and gray fine-grained and medium-grained sands ($M_o = 0.1-0.27$ mm), well and moderately sorted ($S_o = 1.2-2.7$) (Figure 2.5.1).

The Ice Complex sediments are characterized with high ice content and moisture. The deposits of the lower part of the Ice Complex consist of interbedded silty sand ($M_o = 0.05-0.2$ mm), loam ($M_o = 0.047$ mm) and silt loam ($M_o = 0.03$ mm), mostly moderately sorted ($S_o = 1.9-3.0$). Interbeds silty sand are 3 cm, interbeds of the loam are 2 cm, interbeds of the silt loam are 0.1-0.5 mm. The deposits include lenses of sand (5 cm) and peat (4 cm across). There are lenticular cryostructure (0.1-0.2 mm), paralleled to lamination of the loam and porous invisible cryostructure of the silty sand. To the top part of the Ice Complex, deposits change to a more fine fraction: interbedded loam ($M_o = 0.09-0.04$ mm) and silt loam ($M_o = 0.02-0.037$ mm), moderately sorted ($S_o = 2.5-2.98$). Cryostructure is reticulated. The deposit includes a lot of peat inclusions (3-5 cm diameter).

Vegetation cover of Kurungnakh Island includes *Betula nana*, *Salix sp.*, mosses. Holoceny peat is a low degree of decomposition upper the Ice Complex sediments.

The results of Cailleux 1942 analysis, later modified by Mycielska-Dowgiallo and Woronko (Mycielska-Dowgiallo et al. 1998) show that the deposits along the profile are dominated by EM/EL grains representing a fluvial environment. Their content varies from 51,6 to 68,4 %. In the lower part of the profile (8,7-8,9 m) its content decreases to 41,1 %. For this interval content of EL grains being characterized by a high degree of roundness and smooth, glossy surface is increasing up to 33,9 %. NU Grains with sharp edges and glossy surface were found. Its content varies from 12,5 to 39,1 %. Other classes grains were not found. The profile represents a fluvial environment with a different hydrodynamic regimen of water stream. Ncreasing of NU grains along profile indicates water flow and erosion processes intensification.

Ice wedge structure and composition

Syngenetic ice wedges are 11-13 m wide and more. It stretches to the Lena Delta level, that was fixed in the fieldwork 2020. Ice wedges are ice milky in appearance with vertical bands in the cross section of Kurungnakh Island. The ice wedge tail was observed close to Lena river level. Also, a composed part (ice and soil) was observed in the bottom part of the ice wedge.

Ice wedge part within sand deposits has a clear appearance with vertically distributed spherical air bubbles and a few mineral inclusions. Ice crystals are euhedral to subhedral and a little bit anhedral. Ice texture pattern includes ice veins that are composed of elongate crystals horizontally oriented to vertical axial seam. The $\delta^{18}O$ values from ice wedge top sampled on Kur-04 are varied between -32 and -19 ‰, whereas the δD values ranged from -252 to -135 ‰. Where the heavy isotopes are belonged to ice wedge's shoulders (Figure 2.5.2).

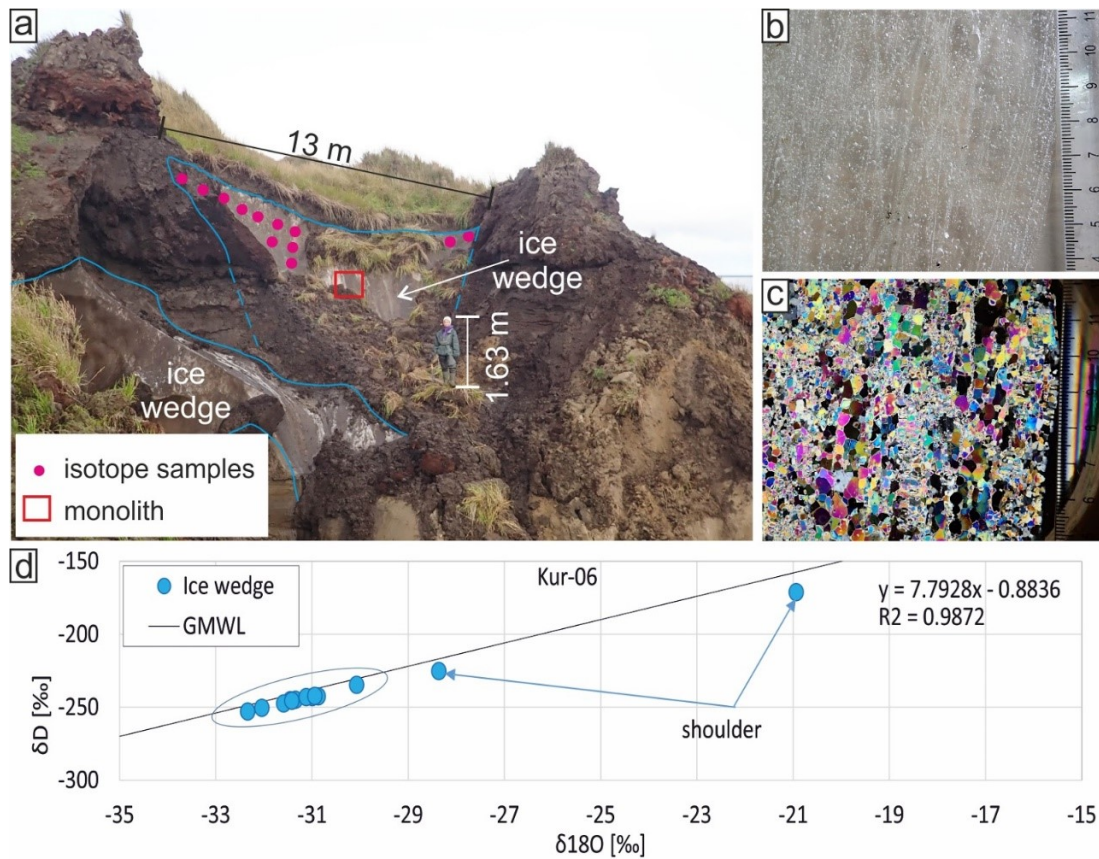


Figure 2.5.2: Ice wedge within sand deposits on Kurungnakh Island: sampling places (a), ice structure (b) and ice texture in vertical thin section (c), $\delta^{18}O - \delta D$ plot of the ice wedge for Kur-06 as with respect to the Global Meteoric Water Line (GMWL), which correlates fresh surface waters on a global scale (Craig 1961) (d)

Ice wedge within the Ice Complex deposits was studied in Kur-01. Lateral part of the ice wedge has a crack filled other ice types (Figure 2.5.3). The ice wedge structure is clear appearance with vertical bands formed by spherical air bubbles and mineral inclusions. Ice crystals of ice wedge are euhedral to subhedral and clear vertical axial seams. The ice crystals are enlarged close ice crack (Figure 2.5.3). The ice crack structure is clear appearance without air bubbles, it includes subvertical organic particles. Ice crystals of crack ice are subhedral to anhedral. Horizontally elongate ice crack crystals oriented from fissure walls to center. Many the smallest ice crystals composed ice milky appearance near the crack ice (Figure 2.5.3). The $\delta^{18}O$ values from ice wedge are varied between -32 and -28 ‰, whereas the δD values ranged from -249 to -222 ‰. The $\delta^{18}O$ values from crack ice are varied between -19 and -18 ‰, whereas the δD values ranged from -141 to -139 ‰. The $\delta^{18}O$ values from ice milky appearance are varied between -24 and -22 ‰, whereas the δD values ranged from -178 to -164 ‰. The $\delta^{18}O$ values from icy soil are varied between -23 and -22 ‰, whereas the δD values ranged from -172 to -171 ‰.

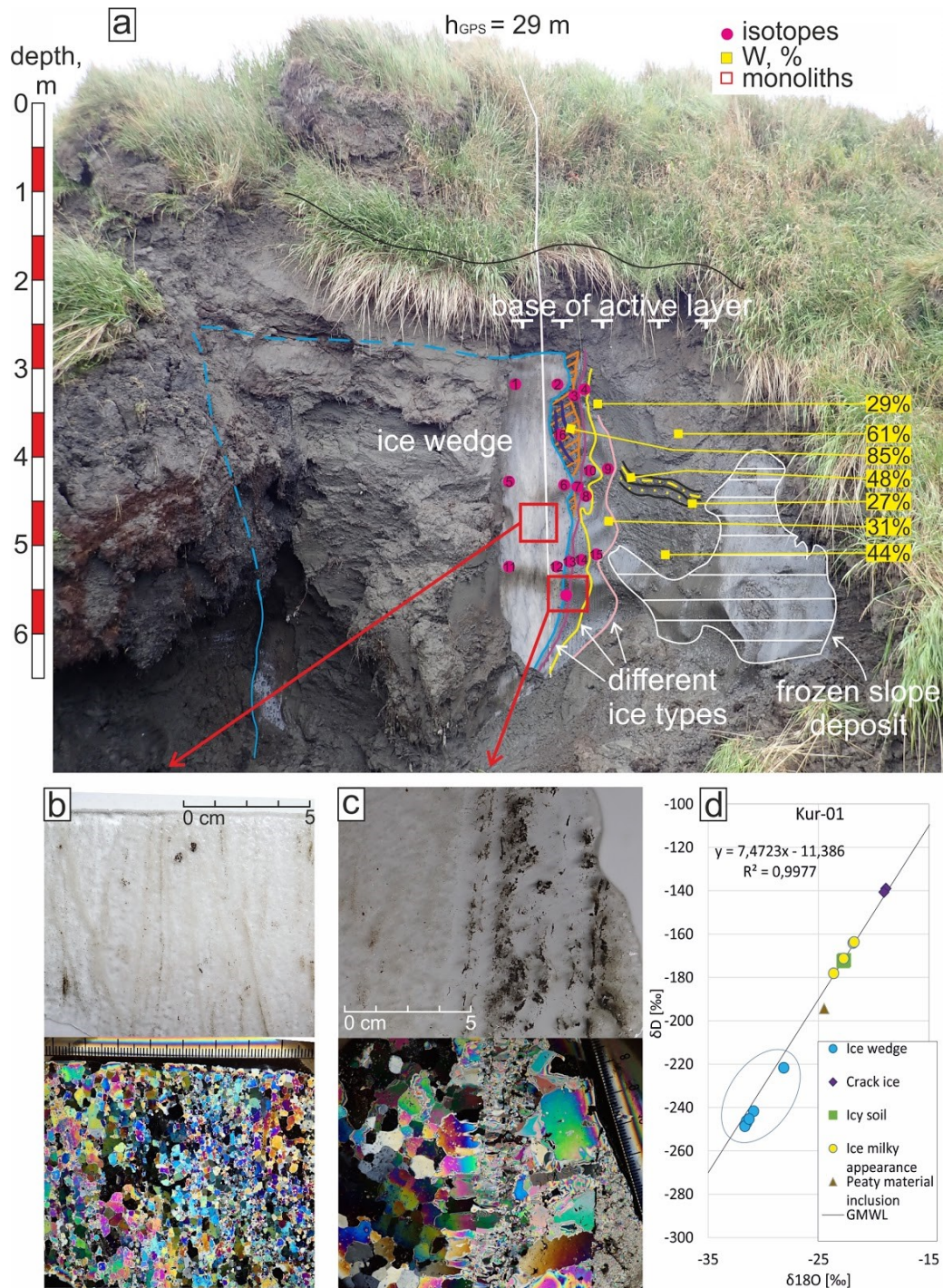


Figure 2.5.3: Ice wedge with other ice types on Kurungnakh Island: sampling places (a), structure and texture of ice wedge in vertical thin section (b), structure and texture for a contact of the ice wedge and crack ice in vertical thin section (c), $\delta^{18}O - \delta D$ plot of the different ice types for Kur-01 as with respect to the Global Meteoric Water Line (GMWL), which correlates fresh surface waters on a global scale (Craig 1961) (d)

In the ice wedge top, the ice structure is vertical bands, formed by spherical air bubbles and mineral particles. Ice crystals are euhedral to subhedral with vertical axial seams (Figure 2.5.4). The $\delta^{18}O$ values from ice wedge top sampled on Kur-04 are varied between -30 and -25 ‰, whereas the dD values ranged from -237 to -189 ‰.

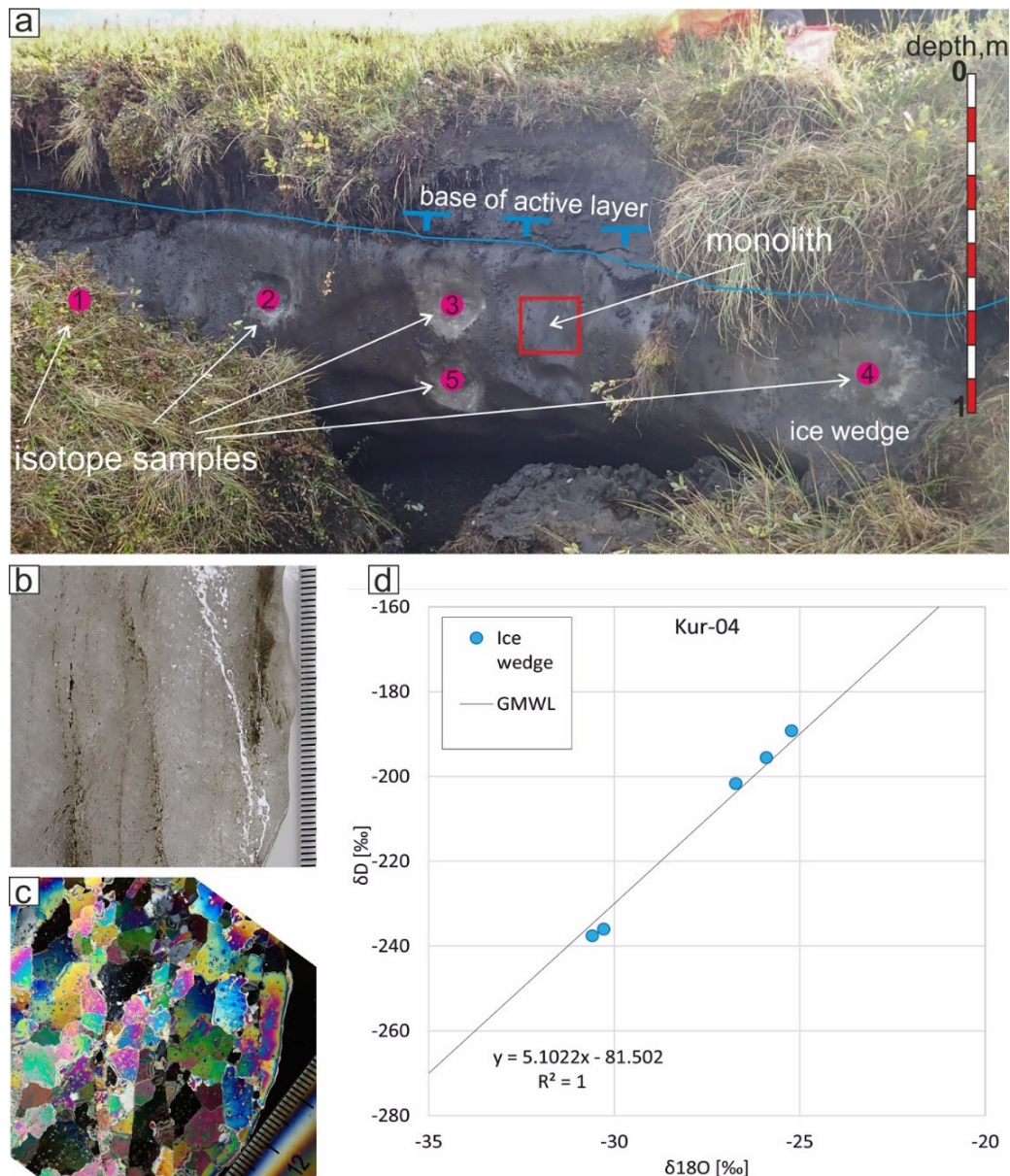


Figure 2.5.4: Ice wedge top on Kurungnakh Island: sampling places (a), ice structure (b) and ice texture in vertical thin section (c), $\delta^{18}O - \delta D$ plot of the ice wedge as with respect to the Global Meteoric Water Line (GMWL), which correlates fresh surface waters on a global scale (Craig 1961) (d)

Conclusion

As a preliminary, for the profile on the Kurungnakh island it was proposed transportation and accumulation of sand underlying the Ice Complex was in fluvial environment in suspended state in dynamic water flow. Ice and ice-ground tails of ice wedge at an altitude of up to 1 m from the level of the Lena River were recorded on Kurungnakh Island. The ice wedges stretch to 30-35 m high. The lower narrow part of the ice wedges is probably epigenetic in relation to the enclosing sands. The processes of thermal contraction and the ice wedge formation probably began at the end of the first half – the middle of the Karginsky age. The ice wedges have mainly light isotopic values similar to the data about the Sartan ice wedge in the works of colleagues. Heavy isotopic values are most likely associated with fractionation processes.

2.6 Thermal erosion in the small basins of the Arctic coast in the vicinity of the Khabarovo Polar Station

Anna M. Tarbeeva ¹, Luidmila S. Lebedeva ^{2,@}, Vladimir S. Efremov ²

¹ Lomonosov Moscow State University, Moscow, Russian Federation

² Melnikov Permafrost Institute, Yakutsk, Russian Federation

@ Corresponding author: lyudmilaslebedeva@gmail.com

Fieldwork period and location:

From August 25th to September 5th, 2020 on Khabarovo (Stolb) meteorological station and around.

Objectives

Headwaters are sensitive to environmental changes, that is reflected in the alternation of erosion dissection, infilling, and stabilization of fluvial forms (Panin et al. 2015b, Panin et al. 2015a). Arctic regions are no exception, although the erosion in frozen sediments has certain specifics. A thermal effect is added to the mechanical action of moving water, so the process is called thermal erosion (Ershov 1982; Everdingen 1998 (revised 2005)). The activation of thermal erosion processes in the Arctic in recent decades, synchronous with the global warming, is noted by many researchers (Fortier et al. 2007; Bowden et al. 2008; Godin et al. 2010; Perreault et al. 2017). Meanwhile, thermo-erosional relief in the permafrost zone is still poorly studied (Morgenstern et al. 2020).

The main regularities of the distribution and geometry of thermo-erosional forms in ice-rich lowlands in the Lena Delta were recently investigated (Morgenstern et al. 2020). The relationships between thermo-erosion, thermokarst, regional slope gradient and neotectonics have been established. The purpose of our work is a detailed assessment of the current state and modern dynamics of thermal erosion on the spurs of the Kharaulakh Ridge - the mainland part adjacent to the Lena Delta, as well as reconstruction of the history of the thermo-erosion development.

Fieldwork summary

In 2020, field descriptions of thermal erosion landforms of different ranks were conducted in the small basins of Meteorologicheskyy and the Crest-Yuryakh creeks. Aerial photography of various forms of thermal erosion was carried out in order to clarify their morphometric characteristics using a DJI Mavic mini quadcopter (Figure 2.6.1). Orthophotomaps, DEMs and transverse profiles through the characteristic section of the forms based on the aerial images were constructed in Agisoft Metashape Professional Version 1.5.2 (Figure 2.6.2). Tacheometric surveys of three headwater gullies were carried out using a Sokkia CX-106 device with reference to ground benchmarks to determine the dynamics of forms (Figure 2.6.3). To estimate rates of bank retreat the tacheometric surveys were compared with similar surveys carried out in 2019 (Figure 2.6.4).

A repetition of combined aerial and tacheometry surveys is planned in the future to assess the future dynamics of gullies and small thermo-erosional features. To observe the dynamics of slope processes, Pendant Hobo Onset loggers - tilt angle sensors - were placed in the solifluction slope, on the slope of the gully, and on the washed-out slope of the valley. The descriptions and C14-sampling of the outcrops of the river terrace and valley slopes were also carried out to assess the long term accumulation and erosion rates. The results of monitoring of slope processes, as well as radiocarbon dating of deposits are planned to be obtained in 2021.

It is also planned to compare the data on the dynamics of thermal erosional forms with the characteristics of water streamflow and sediment load. To assess the dynamics of the water level, dissolved and suspended solids, three loggers were installed in the streams. At the selected sections, water samples were taken to assess changes in its chemical composition. Also, basic water chemistry (water temperature, specific conductivity and pH) was measured along the length of streams. It is planned to continue these works in different phases of the water regime, which will reveal the role of gullies in the formation of water composition.

Preliminary results

The gentle relief of the study area has a heterogeneous lithological structure: the uplands are composed of mudstones overlain by a thin eluvial cover. The gentle slopes and foothills are overlain by ice-rich silt, presumably the remains of yedoma Ice-Complex (Grosse et al. 2007) (Figure 2.6.5). A terrace 2-4 m high above the channel in the valleys is composed of layered deposits overlain the yedoma silt (Figure 2.6.6). The terrace deposits are less ice-rich than the yedoma slopes. The variety of lithological and permafrost structures determines the nature and intensity of thermal erosion processes.

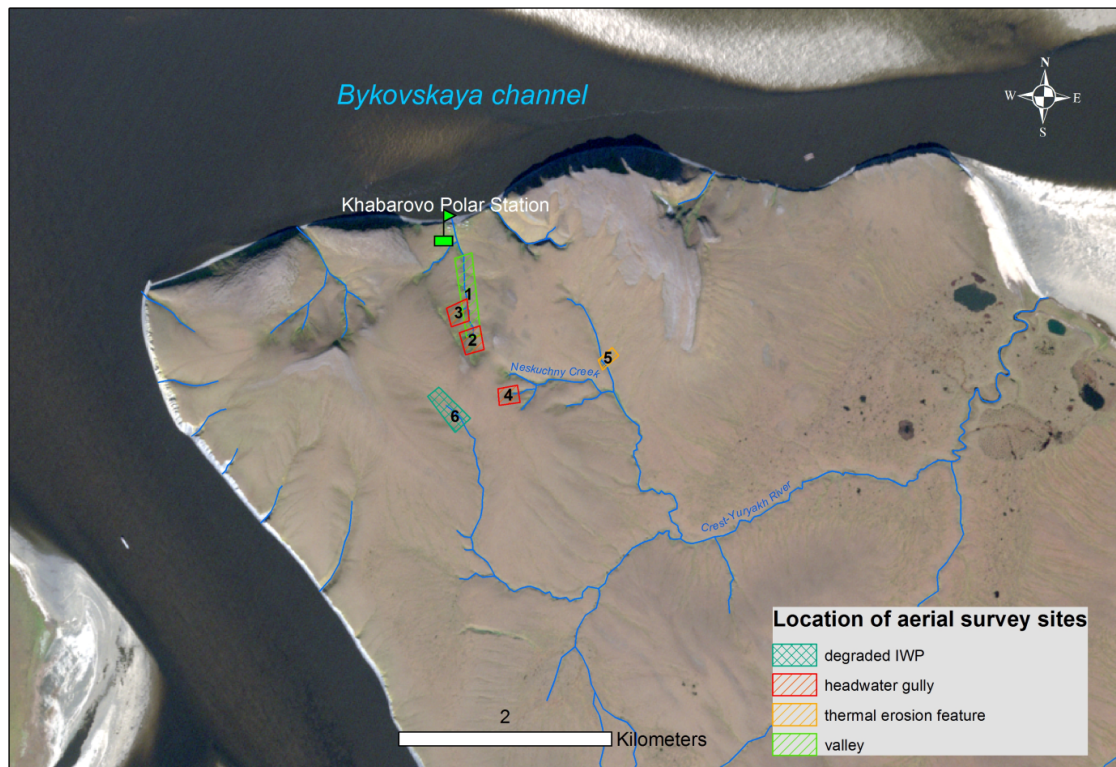


Figure 2.6.1: Location of aerial survey sites: 1 - Meteorologichesky Creek Valley; 2 - headwater gully of the Meteorologichesky Creek; 3 - headwater gully of the left tributary of the Meteorologichesky Creek; 4 - headwater gully of the Neskuchny Creek; 5 - fresh thermo-erosional feature (ephemeral gully) on the Ananasny valley slope; 6 - degrading polygonal ice wedges in headwaters of the Crest-Yuryakh River.

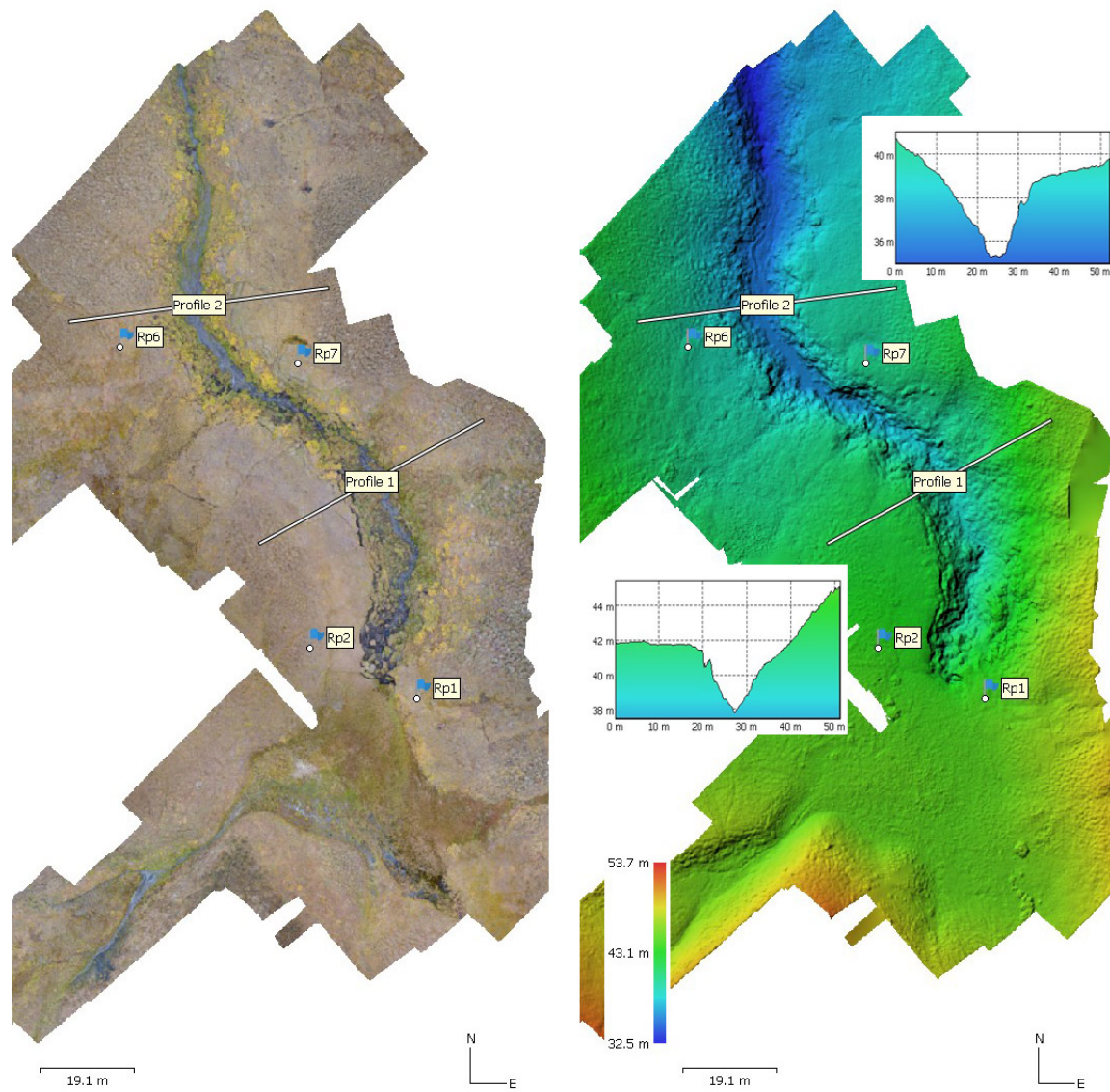


Figure 2.6.2: Gully in the head of the Meteorologicheskyy Creek, Orthomosaic 1 cm/pix (left), DEM 4.5 cm/pix (right) and transverse profiles, showing the terrace on the left (Profile 1) and right (Profile 2) sides of the valley. Blue flags show the location of the benchmarks.

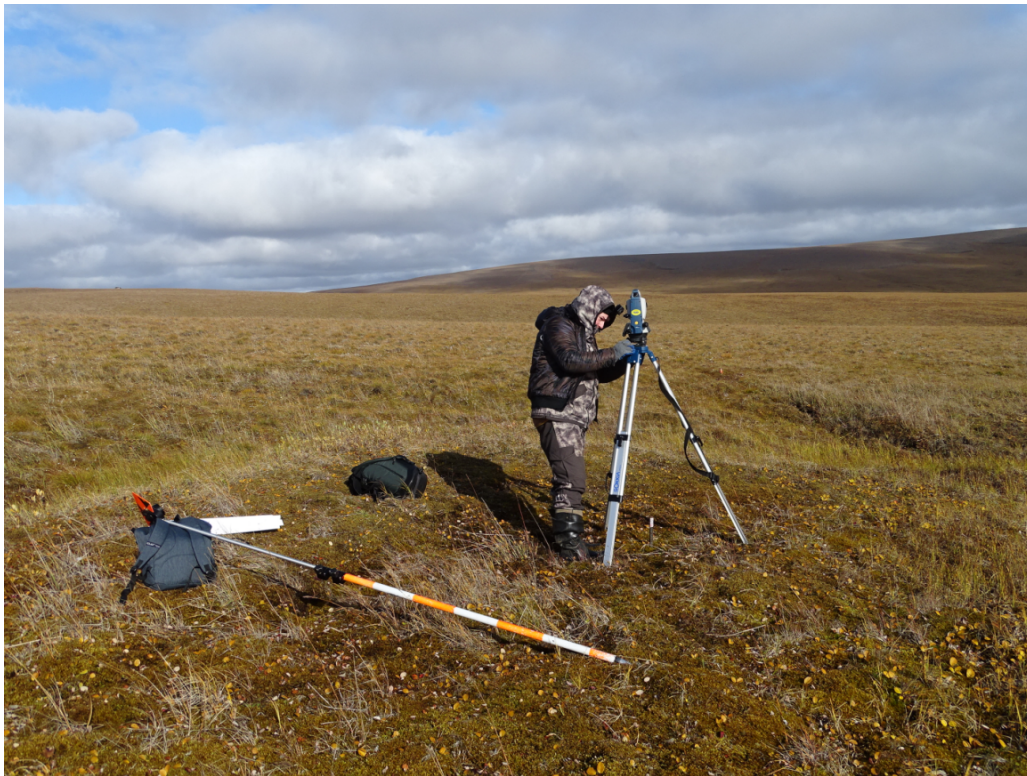


Figure 2.6.3: Vladimir S. Efremov is doing tacheometry survey in the Neskuchny Basin.

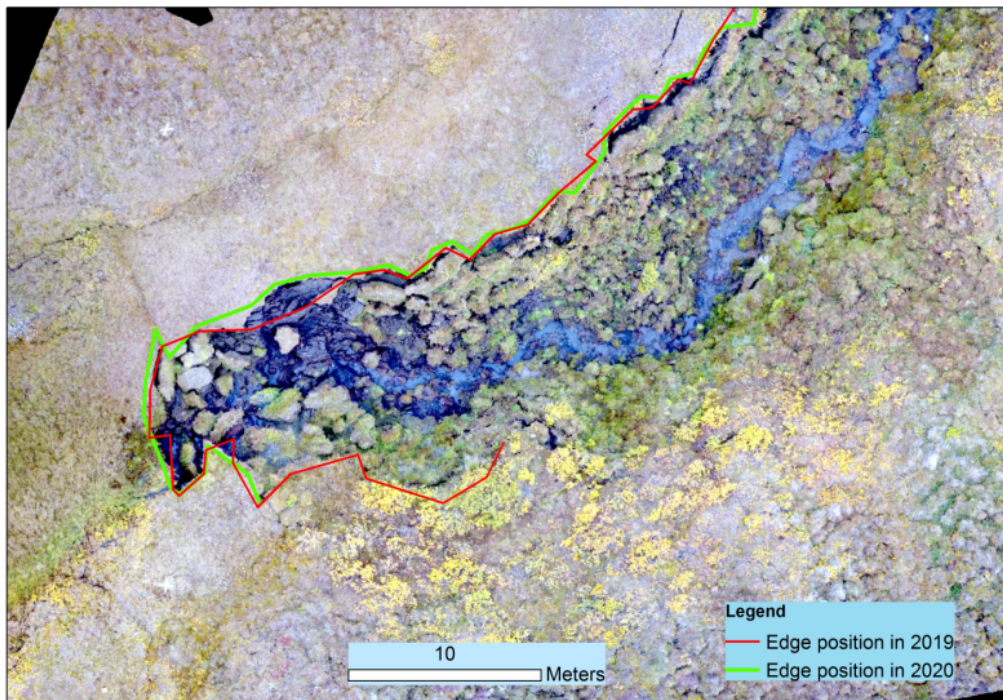


Figure 2.6.4: Displacement of the edge of the gully in the head of the Meteorologicheskyy Creek for 2019-2020 according to tacheometry data (on the aerial photograph of 2020).



Figure 2.6.5: *Section of ice-rich sediments in the cellar at the Khabarovo Polar Station. Luidmila L. Lebedeva for scale.*



Figure 2.6.6: *Outcrop in the upper part of the layered valley infill in the head of Meteorologichesky.*

The fluvial relief of the study area is represented by forms of various ranks.

The smallest are hollows on slopes (named also “dells” or “water tracks”) (Figure 2.6.7 a). They are common on all gentle (2-5 degrees) slopes composed of ice-rich silt. They are shallow, completely vegetated, have no pronounced thalweg and do not bear any traces of erosion and accumulation. Surface runoff in them is formed only during floods and after heavy precipitation (Tarbeeva et al. 2020).

The second level consists of headwater gullies and small ephemeral gullies (or thermal erosion features, after Bowden et al. 2008 - the most dynamic landforms. The investigated thermal erosion feature was formed in 2020 on the slope of the Ananasny valley, composed of ice-rich sandy loam. This ephemeral gully was formed as a result of the melting of veined ice along a large water track that concentrates water (Figure 2.6.7 a). A similar confinement of a thermo-erosional form to a water track is described in Bowden et al. 2008. Under the hollows, the ice-wedges probably are already thawed, while on the surrounding slopes they are still persisting. The depth of the thermo-erosional feature formed in 2020 reaches 1-1.5 m, width 1-1.5 m, length 60 m. In the upper part of the ephemeral gully, there is an alternation of surface and underground runoff due to the formation of sinkholes in the ice with the subsequent collapse of the roof. Ephemeral gullies appeared within the study area in 2018 and 2020. It is likely that they are then filled with sediment, leading to an increase in the width of the adjacent water track.

The depth of the headwater gullies reaches 4-5 m, the width is 15-30 m. The maximum measured rates of retreat of the edge was estimate at 1.6 m per year (Figure 2.6.4). Headwater gullies, as a rule, cut into the ancient valley sedimentary infill (Figure 2.6.7 b), which have a lower ice content compared to the yedoma slopes. Thermo-erosional gullies that are formed in the ice-rich sediments of the Canadian Bylot island grow at rates from 30 to 390 m per year (Godin et al. 2010). Non-vegetated deep headwater gullies are characteristic of the valleys with steep slopes in the headwater. In valleys with gentle headwater gradients, such gullies are not formed. Headwater there are represented by polygonal peat bogs, along which thermokarst is developed (Figure 2.6.7 c).

The small valleys are the largest of the studied forms, they are distinguished by a widespread floodplain and a terrace, the height of which decreases downstream from 4-5 to 2 m above the stream water level (Figure 2.6.7 d). In the headwaters, the terrace joins with the valley sediment infill, into which a gully is cut (Figure 2.6.7 b). In the upper part of the section, the terrace is composed of layered silty sands and organic matter (Figure 2.6.6); in the lower part of the terrace, an yedoma is exposed. We suppose Holocene age of the terrace. Dating of the filling sediments will allow a more precise timing of these processes.

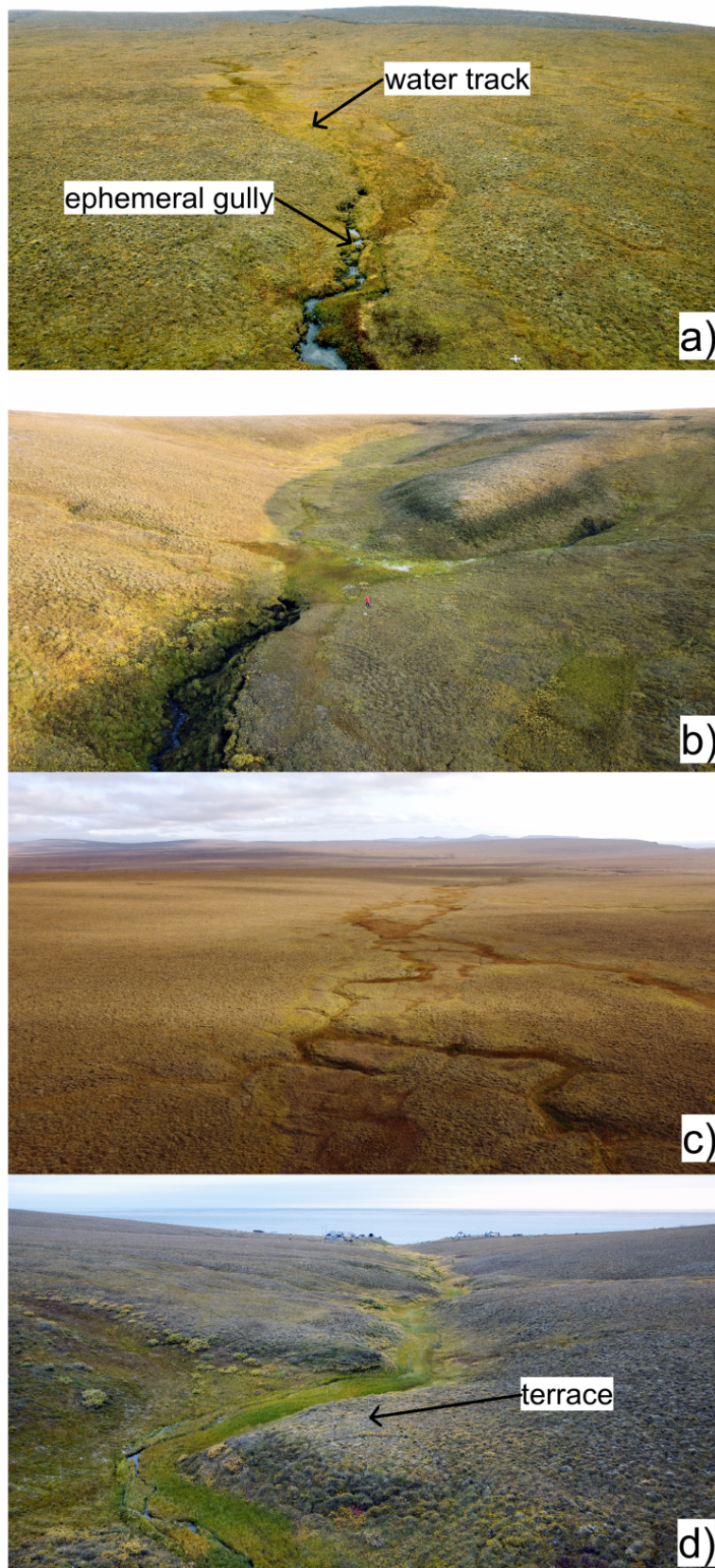


Figure 2.6.7: Thermo-erosion forms of different orders: a) a water track and an ephemeral gully formed in its lower part in 2020, the Crest-Yuryakh Basin; b) a headwater gully of the Meteorologichesky stream, embedded in the valley filling; c) polygonal peat bog in the headwaters of the Crest-Yuryakh River; d) the valley of the Meteorologichesky stream: a modern floodplain in the bottom and a terrace (view down the valley).

Acknowledgments

The reported study was funded by RFBR, projects number 20-05-00840 (A.M. Tarbeeva), 20-35-70027 (L.S. Lebedeva, V.S. Efremov), and contributes to the State Task no. AAAA-A16-116032810084-0, Faculty of Geography MSU.

2.7 New studies of the deep geophysical structure in the southern part of the Lena Delta

Vladimir V. Potapov ^{1,2}, Andrei A. Kartoziia ^{1,2,3,@}, Anna A. Zaplavnova ^{1,2,*}, Petr A. Dergach ^{1,2}

¹ A.A. Trofimuk Institute of Petroleum Geology and Geophysics, Siberian Branch of the Russian Academy of Sciences, Novosibirsk, Russian Federation

² Novosibirsk State University, Novosibirsk, Russian Federation

³ V.S. Sobolev Institute of Geology and Mineralogy, Siberian Branch of the Russian Academy of Sciences, Novosibirsk, Russian Federation

* not in field

@ Corresponding author: andrei.kartoziia@igm.nsc.ru

Fieldwork period and location:

From August 4th to August 22nd, 2020 in the southern part of the Lena Delta.

Objectives

The main goal of our studies was to make a geoelectrical model for the southern part of the region. And the main points are:

- to indicate the depth of a permafrost base or the boundaries of a melting zone in the channel part of the Lena Delta and on its ridges,
- to study deep structure beneath the southern Lena delta part, get information about buried faults in the channel part.

Fieldwork summary

Magnetotelluric sounding:

The survey was carried out using Canadian MT station MTU-5a from “Phoenix Geophysics Ltd”, with a frequency range from 0.003 to 10000 s. The measurements included four MT field components (Ex, Ey, Hx, Hy). We used a standard MTZ measurement plan (x-shape). An approximate step between points was 2 km.

Preliminary results

The MT profile was made (Figure 2.7.1), including 19 points made in summer 2020 and 7 made in summer 2019. The technique revealed the structure with a base depth at approximately 10 km. The preliminary data processing resulted in a 1D model for each point.

As a result of processing, the section has been divided into layers. The high resistivity level in the upmost layer is typical for permafrost. The base depth for this layer varies from 200 m to 1000 m. Those depth variations could be caused by the Lena River and its channels. Points with low resistivity levels indicate fault zones. Based on these points we split our profile into three zones: 0-6 km from the south-west, 6-28 km, and 28-36 km.

We split the middle part into 5 main layers. The upmost layer is interpreted as permafrost. The other four layers are interpreted as a sedimentary bed with different ages of formation. Variations of those layers caused by the Lena River, its channels, and seismic activity in this region.

The main result of the geophysical studies using the MT technique allows us to split the interior at a depth of 10 km into main layers, indicating huge faults. Also marking the base depth of the permafrost layer is an important result. We plan to use this data in conjunction with other techniques.

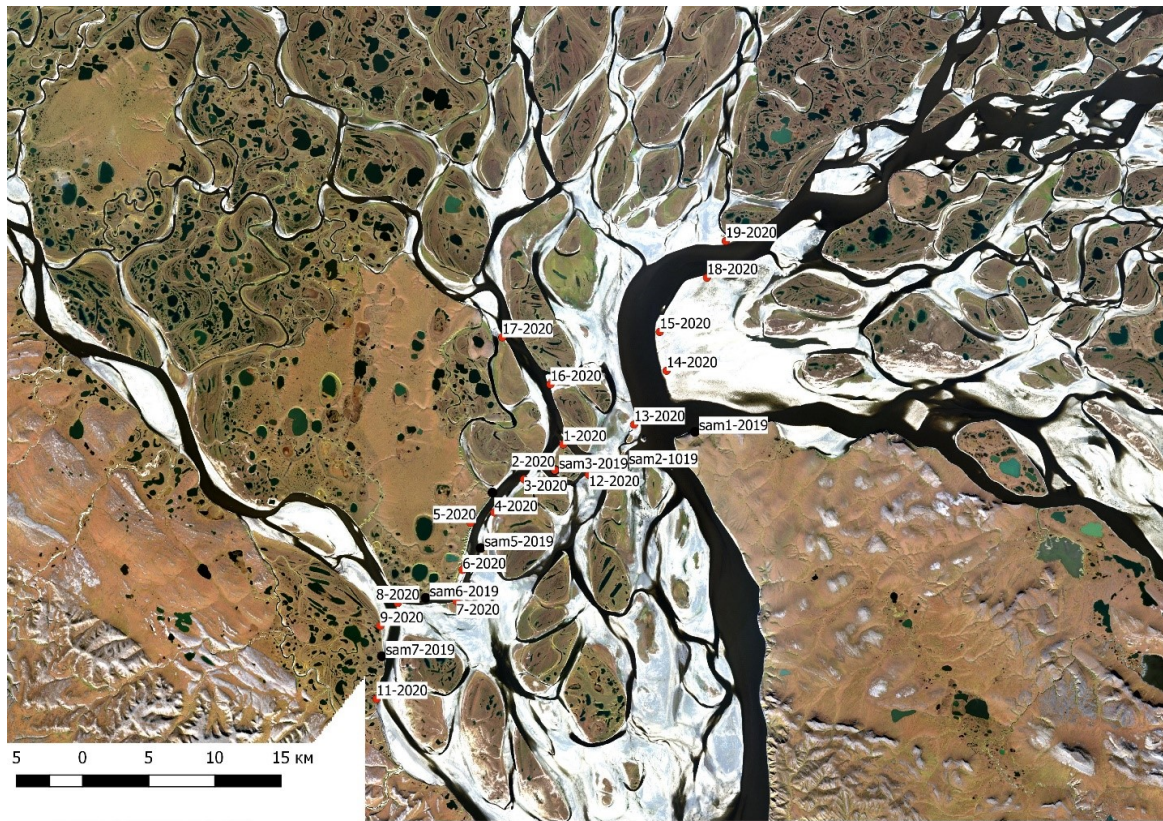


Figure 2.7.1: The MTS measurement points.

2.8 Seismicity of the Laptev Sea Rift

Wolfram H. Geissler ^{1,*,@}, Petr A. Dergach ^{2,3}, Rustam Tuktarov ⁴, Sergey Petrunin ⁴, Stepan A. Gukov ⁴, Andrei Kartoziia ^{2,3,9}, Vladimir Potapov ², Christian Haberland ^{5,*}, Boris V. Baranov ^{6,*}, Sergey V. Shibaev ^{4,*}, Frank Krüger ^{7,*}, Sergey Pravkin ^{8,*}, Nikolay V. Tsukanov ^{6,*}, Aline Ploetz ^{1,*}, Artyom Krylov ^{6,*}, Daniel Vollmer ^{7,*}

¹ Alfred Wegener Institute Helmholtz Center for Polar and Marine Research, Bremerhaven, Germany

² Trofimuk Institute for Petroleum Geology and Geophysics, Siberian Branch of the Russian Academy of Sciences, Yakutia, Russian Federation

³ Novosibirsk State University, Novosibirsk, Russian Federation

⁴ Yakutsk Branch Federal Research Center Geophysical Survey, Russian Academy of Sciences, Yakutia, Russian Federation

⁵ GFZ German Research Center for Geoscience Helmholtz Center Potsdam, Potsdam, Germany

⁶ Shirshov Institute of Oceanology of the Russian Academy of Sciences, Moscow, Russian Federation

⁷ University of Potsdam, Potsdam, Germany

⁸ Arctic and Antarctic Research Institute, St. Petersburg, Russian Federation

⁹ V.S. Sobolev Institute of Geology and Mineralogy, Siberian Branch of the Russian Academy of Sciences, Russian Federation

* not in field

@ Corresponding author: Wolfram.Geissler@awi.de

Fieldwork period and location:

From August 03rd to August 24th, 2020 in the Lena Delta, and July 20th to August 18th, 2020 around Tiksi, and Buor-Khaya Bay.

Objectives

The main goal of the opening study is to investigate the geodynamic processes of the continental Laptev Sea Rift and their major tectonic zones to better describe the amagmatic rifting and its consequences in an arctic and global context. From the Arctic Ocean the ultra-slow spreading Gakkel ridge is propagating towards the continental slope of the Laptev Sea in North-East Siberia. In comparison to the Gakkel Ridge, which separates the North American plate from the Eurasian plate, the Laptev Sea region shows diffuse seismic activities. A few larger earthquakes located south-east to the Gakkel Ridge are suggested to define the further plate boundary (Fujita et al. 2009).

From the Laptev Sea shelf south to the coastal regions of the continent, focal depths increase from 10 to 25 km (Jemsek et al. 1986; Franke et al. 2000; Fujita et al. 2009). Data from local short-term studies in the 80ies showed that there is abundant local seismicity (Kovachev et al. 1994; Avetisov 1999).

According to Sloan et al. 2011, the westernmost limit of seismicity is related to the thick lithosphere of the Siberian shield, which indicates some structural control on the recent tectonic activity. Franke et al. 2000 defined with nine teleseismic events the North-American-Eurasian pole rotation west to the Cherskiy mountains. Furthermore, they assume a separate microplate, based on the concentration of crustal extensions and seismicity to east and west of the Laptev Sea, respectively (Franke et al. 2000). Additionally, focal mechanisms indicate changes between compressional and extensional tectonic phases over short distances. This might be a consequence of the fact that the pole of rotation is close to our study area, probably to the south of Lena delta (Gaina et al. 2002). It is up to now not known if especially the southern Laptev Sea Rift is still in an extensional mode, or if compression already started and how the old continental lithosphere is eroded by the rifting process. This includes verifying the position of the rotation pole between the Eurasian and North-American plates and to prove or disprove, if an independent Laptev Sea microplate exists. Therefore, we are monitoring local earthquakes in the Laptev Sea and Lena Delta to fulfill the following objectives:

1. Location of microseismicity and its relationship with active faults. We want to identify seismologically active fault zones. In a first step, we deployed instruments in earthquake areas, which are already identified by the global seismological network, though with low spatial resolution. We also intend to identify active deep-reaching fault zones, that may also be pathways for methane degassing, e.g., in the western Buor-Khaya Bay.
2. Focal mechanisms. What is the present geodynamic setting, where is extension and where is compression in the Laptev Sea and in the Lena Delta region, where is the exact pole of rotation? What is the relation of the recent seismicity to pre-existing crustal and lithosphere structures (e.g., western Verkhojansk Fold and- Thrust Belt, Olenek Fault-Zone or South Anyui Suture)?
3. Lithosphere structure. It is interesting to note that despite the Cenozoic continental rifting in the Laptev Sea little volcanism is known. Thus, we like to compare the deep crustal and upper mantle structure with other continental rift systems (e.g. Afar) to enhance our understanding of the driving forces.

The focus region for the 2019-2020 measurement campaign is the western Buor Khaya Gulf and the surroundings of Tiksi, to get more precise locations of local seismicity and potentially permafrost-related earthquakes. With the new data, we want to estimate focal depths and focal mechanisms/source kinematics for that area. Parallel measurements of Russian colleagues with ocean bottom seismometers in the central and northern Laptev Sea that started in 2018 are continued.

While measuring seismicity in the last years, it became obvious that seismicity in wintertime (October-March) is dominated by numerous events that cannot be related to tectonic processes, but most probably to freezing of the ground and ice-wedge growth. S-P delay times suggest that the events could be detected and located within distances of more than 10 km. So far interstation distance only allows locations within the TIKSI array, but not yet in the Lena Delta.

Fieldwork summary

2019/2020 we continued our seismological observations in the SW Lena Delta close to the Research Station Samoylov Island and in the western Buor Khaya Bay area close to Tiksi (see Geissler et al. 2017; Ploetz et al. 2019; Geissler et al. 2020), see Figure 2.8.1 and Tables A.2.4, A.2.5, and A.2.6. These observations are carried out within the framework of the Russian-German project SIOLA (Geissler et al. 2018). Also 2019, colleagues from Novosibirsk joined forces to study the seismicity in the vicinity of the Research Station Samoylov Island with first pilot installations (see Table A.2.7).

Due to the Covid-19 pandemic, the fieldwork could not be carried out as planned. But luckily, our partners in Tiksi, Yakutsk and Novosibirsk could organize the recovery of all stations. Besides the stations from IPGG Novosibirsk no new stations were installed due to uncertainties caused by the pandemic and further funding.

In the first half of August, our work was concentrated in the region around Tiksi and the western Buor Khaya Bay (see Table A.2.5). With the exception of one station on Muostakh Island, which was dismantled by the support of a small boat, all stations were dismantled using all-terrain vehicles of Arctic Geocentr Tiksi and Hydrobase Tiksi. All work could be done as planned, however, in the early season high water level of rivers did not allow to reach stations along the coast of Buor Khaya Bay.

Furthermore, all 13 stations of the 2-km-aperture seismological array, our backbone installation for monitoring the regional seismic with the SW Laptev Sea Rift System (see Table A.2.6) were dismantled within one day. This array was located about 10 km east of Tiksi.

All stations in the array and in the Buor Khaya network are equipped with MARK 3C 1s passive sensors, CUBE data acquisition systems and two 80 Ah batteries buried as deep as possible in the partially frozen ground. This configuration with minimum power consumption at low temperatures has proven to be very successful over the last years. After a first test in 2018/2019, several CUBE recorders with a larger storage capacity (64 GB instead of 32 GB) had been deployed to allow a full year recording instead of about nine months previously. Some of the stations were additionally equipped with temperature sensors, that allow to control the functionality of the station set up at low temperatures. Data quality checks are not yet completed, however, most of the recorders seem to have worked without problems. However, stations that were not installed on rocky ground but on partially frozen sedimentary deposits experienced again inclination of the sensors by the freezing and

thawing of the ground (Geissler et al. 2020). If the sensors get inclined too much, that causes a dramatic shift of the eigenfrequencies and the damping factor of the components and makes data analysis more complicated. In worse cases, individual components cannot be used for analysis anymore, which is especially not good for teleseismic methods to study the deep structure of the region.



Figure 2.8.1: Map of the study area showing first locations (red dots) using the previous seismological network (period August-April 2016, Ploetz et al., in prep.). Green and yellow balloons, existing stations of the Lena Delta/Samoylov and Buor Khaya Bay networks; pink balloons, small network/array on Samoylov Island; blue balloons, Tiksi array. Novosibirsk test stations SML01-03 are located nearby LD011, LD033, and LD042.

The data quality control is still underway. Therefore, we cannot yet provide details.

The SW Lena Delta is situated on the southern part of the Olenyok (or Olenek) fault zone, one of the most active fault zones of the Laptev Sea Rift System. However, it is not yet understood, if this part of the rift system is actually still in an extensional mode. Also, local compression is inferred, e.g., by Imaeva et al. 2018. 2019/2020 seven stations were in operation to study these tectonic earthquakes in detail. Furthermore, three stations had been installed on Samoylov Island in 2019. During the analysis of the datasets from 2016/27 and 2017/18 it became clear, that during the wintertime, there is a tremendous increase in seismic activity by very local events. Most probably, these events are related to freezing processes within the permafrost (ice-wedge growth). With the previous configuration of the networks, however, it was not yet possible to locate the source of these events, that are strong enough to mask local earthquakes in the recordings. Even, if Samoylov Island is a noisy place due to the power generator, we decided to install three stations on the island. The stations on Samoylov Island were located at the rim of inclined and therefore dry polygons within sandy fluvial deposits. The three stations were about 1 km apart and should allow to locate permafrost-related seismic activity, even if the sample rate is only 100 Hz. The sites were placed around active permafrost polygons. The three stations will also allow to get better estimated of the source depth of local tectonic earthquakes.

With the support of the Research Station Samoylov Island and their boat *URAL*, the team from Novosibirsk dismantled all stations of the regional network and on Samoylov Island (see Table A.2.4). All these stations were also equipped with MARK 3C 1s passive sensors and CUBE data acquisition systems and two 80 Ah batteries buried as deep as possible in the partially frozen ground.

Our colleagues from Novosibirsk maintained three stations and installed one additional station for testing purpose. The stations were installed within a radius of 25 kilometers from Samoylov Island: one (1) in a 20-m deep borehole with permafrost and others within rocks (see Table A.2.7). Site (1) is located within permafrost on the floor of an emptied thermokarst lake on Kurungnakh Island. Sites (2), (3) and (4) are very close to our previous stations LD010, LD011 and LD033.

The Novosibirsk stations are equipped with GS ONE LF (5 Hz) geophones and SCOUT-3.1 digitizers (see Figure 2.8.2 and tables 2.8-1 and 2.8-2). For power supply, manganese batteries “Baken-BC1” are used. The capacity of a single battery is 350 Ah, and the voltage is 2.6 V. This year we increased the number of batteries from six to eight per one station. This should provide power to the stations for 10 to 12 months.

The first quality checks of last year’s data show that the records frequency range can be extended from the geophone natural frequency up to 1 Hz (Dergach et al. 2019). An example of the comparison of the processed geophone signal with the record of station LD033, which was located in 150 meters distance, is documented in Figure 2.8.3. The amplitude spectra of the corresponding signals are shown in Figure 2.8.4.

Table 2.8-1: Digitizer “SCOUT-3.1” main technical parameters

No.	Parameter	Value
1	ADC resolution	24 bit
2	Number of channels	3
3	Amplifier gain	36 dB
4	Sampling frequency	125 Hz
5	Internal memory	32 Gb industrial SD-card
6	Storage temperature	-40°C to +85°C
7	Operating temperature	-40°C to +70°C

Table 2.8-2: Digitizer “SCOUT-3.1” main technical parameters

No.	Parameter	Value
1	Natural frequency	5 Hz
2	Sensitivity	100.4 V/m/s
3	Damping factor	0.45
4	Coil resistance	2450 Ω
5	Spurious frequency	160 Hz
6	Operating temperatures	-40°C to +80°C
7	Tilt angle when coil hit end stop	30° for vertical, 8° for horizontal



Figure 2.8.2: Photos from Novosibirsk stations. Top: Digitizer “SCOUT-3.1” (32 Gb) and Power source Batteries “BAKEN BC-1” (6 items, 300 Ah). Bottom left: Geophone “GS-ONE LF” (5 Hz, 100 V/m/s). Bottom right: within-rock station at the same place where was LD010 before.

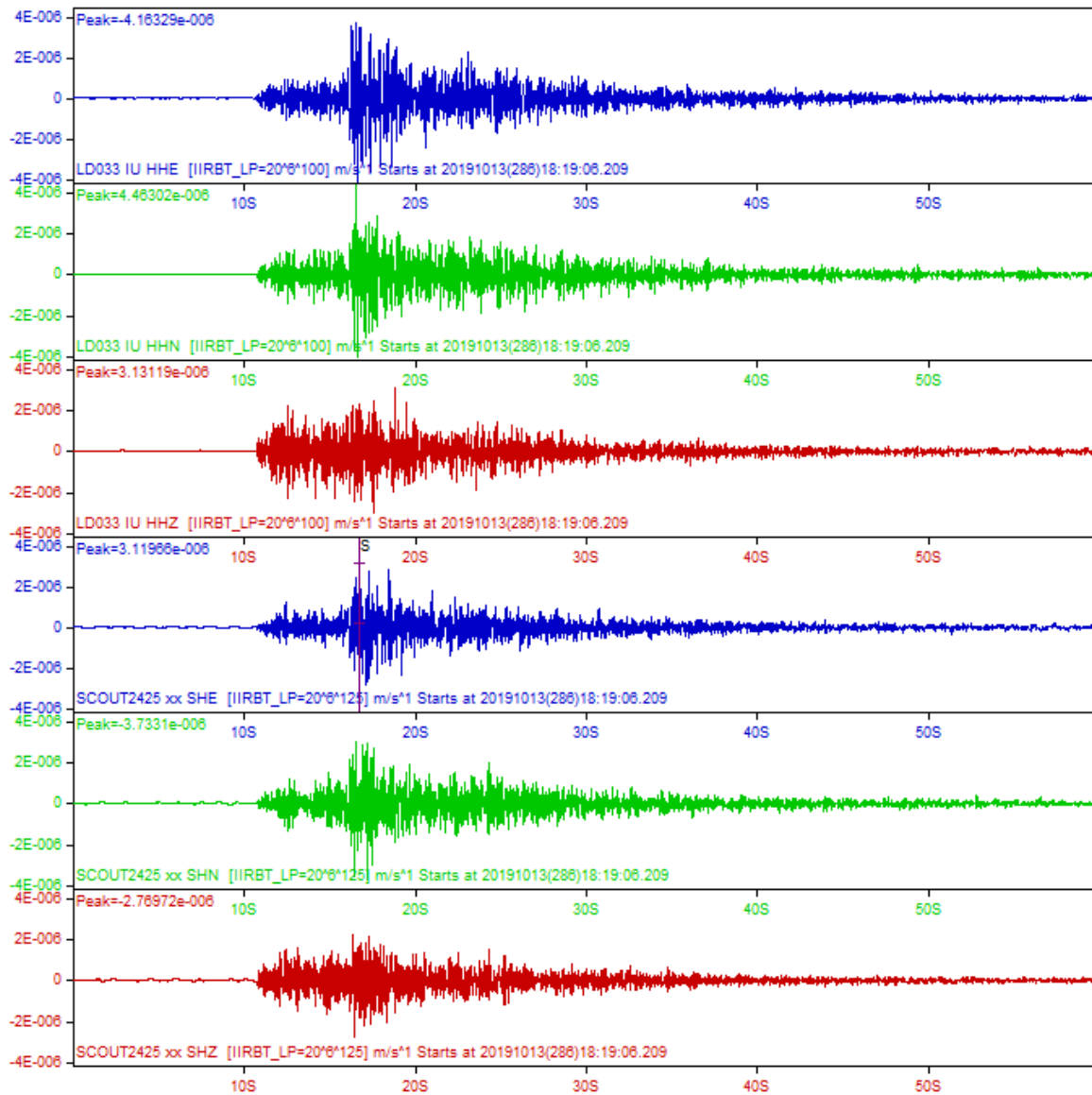


Figure 2.8.3: The comparison of MARK (LD033) and extended to 1 Hz geophone (SCOUT2425) signals by example recording of weak local earthquake.

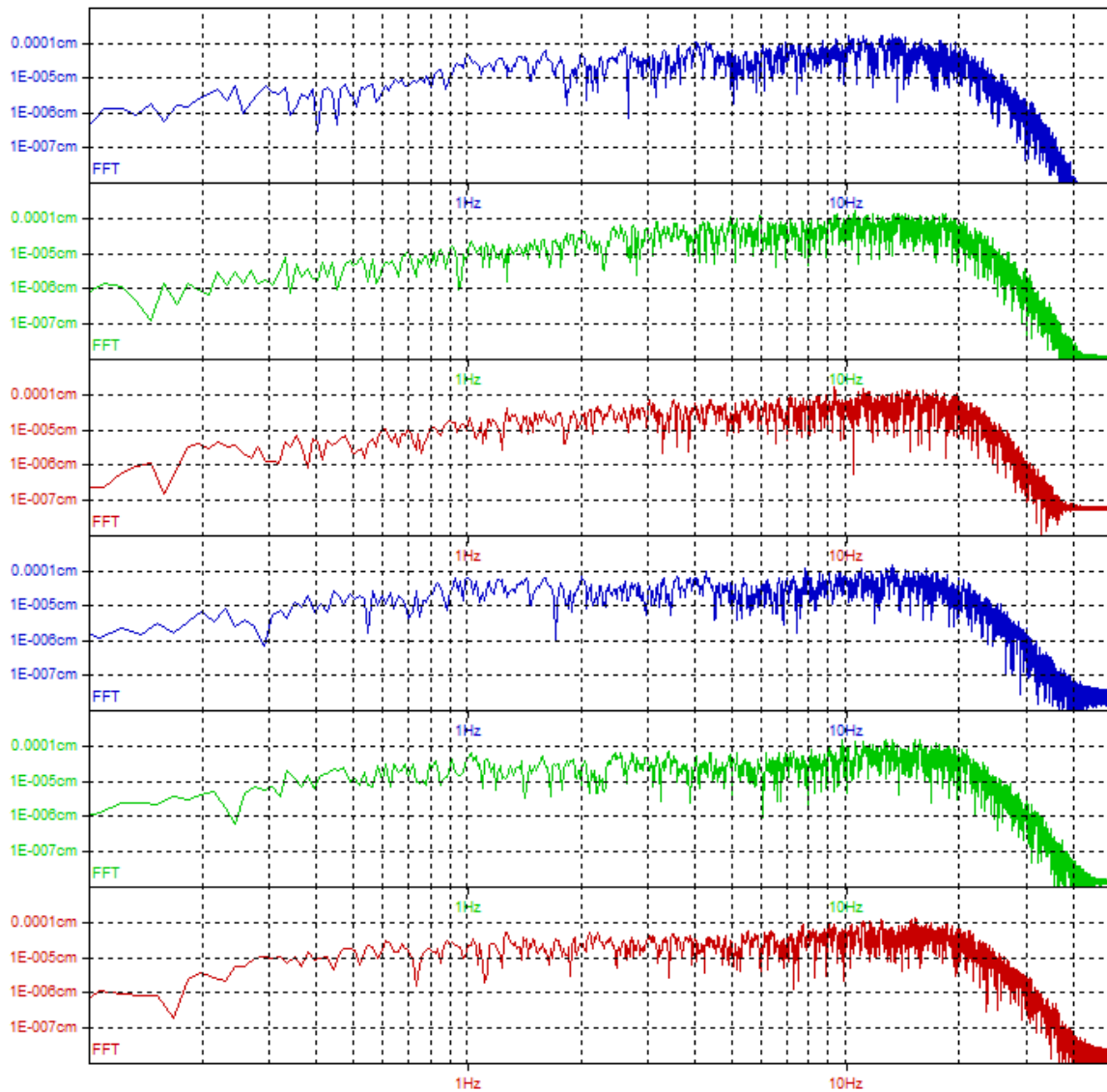


Figure 2.8.4: *The spectra of corresponding signals that are shown at Figure 2.8.3.*

Acknowledgements

We are grateful to our Russian colleagues who worked in the field under the special conditions of the pandemic. Instruments were provided by Geophysical Instrument Pool Potsdam (GIPP). We thank all people of the Research Station Samoylov Island and the Lena Delta Nature Reserve (Ust-Lensky Zapovednik) for their support of our activities in the Lena Delta.

Bibliography

- Antonova, S., H. Sudhaus, T. Strozzi, S. Zwieback, A. Kääb, B. Heim, M. Langer, N. Bornemann, and J. Boike (2018): Thaw Subsidence of a Yedoma Landscape in Northern Siberia, Measured In Situ and Estimated from TerraSAR-X Interferometry. In: *Remote Sensing* 10.4. ISSN: 2072-4292. DOI: 10.3390/rs10040494. URL: <https://www.mdpi.com/2072-4292/10/4/494>.
- Avetisov, G. P. (July 1999): Geodynamics of the zone of continental continuation of Mid-Arctic earthquakes belt (Laptev Sea). In: *Physics of the Earth and Planetary Interiors* 114.1-2, pp. 59–70. DOI: 10.1016/s0031-9201(99)00046-1.
- Boike, J., J. Nitzbon, K. Anders, M. Grigoriev, D. Bolshiyarov, M. Langer, S. Lange, N. Bornemann, A. Morgenstern, P. Schreiber, C. Wille, S. Chadburn, I. Gouttevin, E. Burke, and L. Kutzbach (Feb. 2019): A 16-year record (2002–2017) of permafrost, active-layer, and meteorological conditions at the Samoylov Island Arctic permafrost research site, Lena River delta, northern Siberia: an opportunity to validate remote-sensing data and land surface, snow, and permafrost models. In: *Earth System Science Data* 11.1, pp. 261–299. DOI: 10.5194/essd-11-261-2019.
- Bolshiyarov, D. Yu., A. S. Makarov, V. V. Shnaider, and G. Shtof (2013): Origin and Development of the Lena River Delta. In: *Arkt. Antarkt. Nauchno-Issled. Inst., St. Petersburg*.
- Bowden, W. B., M. N. Gooseff, A. Balsler, A. Green, B. J. Peterson, and J. Bradford (June 2008): Sediment and nutrient delivery from thermokarst features in the foothills of the North Slope, Alaska: Potential impacts on headwater stream ecosystems. In: *Journal of Geophysical Research: Biogeosciences* 113.G2, n/a–n/a. DOI: 10.1029/2007jg000470.
- Cailleux, A. (1942): Les actions éoliennes périglaciaires en Europe. In: *Mémoires de la Société géologique de France* 41. (in French), pp. 1–176.
- Camill, Philip (Jan. 2005): Permafrost Thaw Accelerates in Boreal Peatlands During Late-20th Century Climate Warming. In: *Climatic Change* 68.1-2, pp. 135–152. DOI: 10.1007/s10584-005-4785-y.
- Craig, H. (May 1961): Isotopic Variations in Meteoric Waters. In: *Science* 133.3465, pp. 1702–1703. DOI: 10.1126/science.133.3465.1702.
- Dergach, P. A., Ts. A. Tubanov, V. I. Yushin, and A. A. Duchkov (June 2019): Features of Software Implementation of Low-Frequency Deconvolution Algorithms. In: *Seismic Instruments* 55.3, pp. 345–352. DOI: 10.3103/s0747923919030046.
- Ershov, E., ed. (1982): *Thermal Erosion in Dispersed Sediments*. (in Russian), 194 pp.
- Everdingen, R. van, ed. (1998 (revised 2005)): *Multi-language glossary of permafrost and related ground-ice terms*. The Arctic Institute of North America. The University of Calgary.
- Fortier, D., M. Allard, and Y. Shur (July 2007): Observation of rapid drainage system development by thermal erosion of ice wedges on Bylot Island, Canadian Arctic Archipelago. In: *Permafrost and Periglacial Processes* 18, pp. 229–243. DOI: 10.1002/ppp.595.
- Franke, D., F. Krüger, and K. Klinge (2000): Tectonics of the Laptev Sea - Moma 'Rift' Region: investigation with Seismologic Broadband Data. In: *Journal of Seismology* 4.2, pp. 99–116. DOI: 10.1023/a:1009866032111.
- Freeman, C., C. D. Evans, D. T. Monteith, B. Reynolds, and N. Fenner (Aug. 2001): Export of organic carbon from peat soils. In: *Nature* 412.6849, pp. 785–785. DOI: 10.1038/35090628.
- Frey, Karen E. (2005): Amplified carbon release from vast West Siberian peatlands by 2100. In: *Geophysical Research Letters* 32.9. DOI: 10.1029/2004gl022025.
- Fujita, K., B. M. Koz'min, K. G. Mackey, S. A. Riegel, M. S. McLean, and V. S. Imaev (Sept. 2009): Seismotectonics of the Chersky Seismic Belt, eastern Sakha Republic (Yakutia) and Magadan District, Russia. In: *Stephan Mueller Special Publication Series* 4, pp. 117–145. DOI: 10.5194/smsps-4-117-2009.

- Gaina, C., W. R. Roest, and R. D. Müller (Apr. 2002): Late Cretaceous–Cenozoic deformation of northeast Asia. In: *Earth and Planetary Science Letters* 197.3-4, pp. 273–286. DOI: 10.1016/s0012-821x(02)00499-5.
- Geissler, W. H., P. A. Dergach, F. Krueger, S. Gukov, C. Haberland, N. V. Tsukanov, D. Peresypkin, M. Zeckra, S. Petrunin, L. Y. Eponeshnikova, S. Shibaev, B. Baranov, A. Ploetz, A. Krylow, R. Tuktarov, and D. Vollmer (Jan. 2020): “Seismicity of the Laptev Sea Rift”. In: *Russian-German Cooperation: Expeditions to Siberia in 2019*. Ed. by M. Fuchs, D. Bolshiyarov, M. Grigoriev, A. Morgenstern, L. Pestryakova, L. Tsibizov, and A. Dill. Vol. 749. Bremerhaven: Alfred Wegener Institute Helmholtz Center for Polar and Marine Research, pp. 122–130. DOI: 10.48433/BzPM_0749_2021.
- Geissler, W. H., S. Shibaev, C. Haberland, S. Petrunin, F. Krueger, D. Presypkin, D. Vollmer, S. Gukov, R. Tuktarov, and B. Baranov (2017): “Seismicity of the Laptev Sea Rift”. en. In: *Russian-German Cooperation: Expeditions to Siberia in 2016*. Ed. by P. P. Overduin, F. Blender, D. Y. Bolshiyarov, M. N. Grigoriev, A. Morgenstern, and H. Meyer. Vol. 709. Alfred Wegener Institute Helmholtz Center for Polar and Marine Research, pp. 103–107. DOI: 10.2312/BZPM_0709_2017.
- Godin, E. and D. Fortier (July 2010): “Geomorphology of thermo-erosion gullies – case study from Bylot Island, Nunavut, Canada”. en. In: *Proceedings of GeoCalgary 2010 : the 63. Canadian geotechnical conference and 6. Canadian permafrost conference*. Ed. by C. Kwok, B. Moorman, R. Armstrong, and J. Henderson, pp. 1540–1547. DOI: 10.13140/2.1.4498.9120.
- Grigoriev, M. N. (1993): Cryomorphogenesis in the Lena Delta. In: Permafrost Institute Press, Yakutsk.
- Grosse, G., L. Schirrmeyer, C. Siegert, V. Kunitsky, E. Slogoda, A. Andreev, and A. Dereviagin (Jan. 2007): Geological and geomorphological evolution of a sedimentary periglacial landscape in Northeast Siberia during the Late Quaternary. In: *Geomorphology* 86, pp. 25–51. DOI: 10.1016/j.geomorph.2006.08.005.
- Holmes, Robert Max, James W. McClelland, Bruce J. Peterson, Suzanne E. Tank, Ekaterina Bulygina, Timothy I. Eglinton, Viacheslav V. Gordeev, Tatiana Y. Gurtovaya, Peter A. Raymond, Daniel J. Repeta, Robin Staples, Robert G. Striegl, Alexander V. Zhulidov, and Sergey A. Zimov (Mar. 2011): Seasonal and Annual Fluxes of Nutrients and Organic Matter from Large Rivers to the Arctic Ocean and Surrounding Seas. In: *Estuaries and Coasts* 35.2, pp. 369–382. DOI: 10.1007/s12237-011-9386-6.
- Imaeva, L. P., V. S. Imaev, and B. M. Koz'min (Nov. 2018): Seismotectonic Activation of Modern Structures of the Siberian Craton. In: *Geotectonics* 52.6, pp. 618–633. DOI: 10.1134/s0016852118060031.
- Jemsek, J. P., E. A. Bergman, J. L. Nabelek, and S. C. Solomon (1986): Focal depths and mechanisms of large earthquakes on the Arctic Mid-Ocean Ridge System. In: *Journal of Geophysical Research* 91.B14, p. 13993. DOI: 10.1029/jb091ib14p13993.
- Juhls, Bennet, Anne Morgenstern, Antonina Chetverova, Antje Eulenburg, Jens A Hölemann, Vasily Povazhnyi, and Pier Paul Overduin (2020a): Lena River surface water monitoring near the Samoylov Island Research Station. en. DOI: 10.1594/PANGAEA.913197.
- Juhls, Bennet, Colin A. Stedmon, Anne Morgenstern, Hanno Meyer, Jens Hölemann, Birgit Heim, Vasily Povazhnyi, and Pier P. Overduin (May 2020b): Identifying Drivers of Seasonality in Lena River Biogeochemistry and Dissolved Organic Matter Fluxes. In: *Frontiers in Environmental Science* 8. DOI: 10.3389/fenvs.2020.00053.
- Kovachev, S. A., I. P. Kuzin, and S. L. Soloviev (1994): Short-term study of microseismicity in the Guba Buorkhaya, Laptev Sea, using ocean bottom seismographs. In: *IZVESTIYA PHYSICS OF THE SOLID EARTH C/C OF FIZIKA ZEMLI-ROSSIISKAIA AKADEMIYA NAUK* 30, pp. 647–658. DOI: 1069-3513/95/300708-0007818.00/1.
- Kurchatova, A. N. and V. V. Rogov (2014): New methods and approaches to study of the granulometric and morphological composition of cryogenic soils. In: *Engineering survey* 6, pp. 58–63.
- Morgenstern, A., P. P. Overduin, F. Günther, S. Stettner, J. Ramage, L. Schirrmeyer, M. N. Grigoriev, and G. Grosse (Oct. 2020): Thermo-erosional valleys in Siberian ice-rich permafrost. In: *Permafrost and Periglacial Processes*. DOI: 10.1002/ppp.2087.
- Mycielska-Dowgiałto, E. and B. Woronko (1998): Analiza obtoczenia i zmatowienia powierzchni ziarn kwarcowych frakcji piaszczystej i jej wartość interpretacyjna. In: *Przegląd Geologiczny* 46. (in Polish with English summary), pp. 1275–1281.

- Panin, A., E. Yeremenko, and I. Kovda (Apr. 2015b): LATE PLEISTOCENE CYCLE OF EROSION DISSECTION AND INFILLING OF THE DRAINAGE NETWORK ON THE NORTH-EASTERN STAVROPOL'YE (PAPER I. THE NETWORK OF HOLLOWES). In: *Geomorphology RAS*. (in Russian), p. 77. DOI: 10.15356/0435-4281-2011-1-77-87.
- Perreault, N., E. Lévesque, D. Fortier, D. Gratton, and L. Lamarque (Mar. 2017): Remote sensing evaluation of High Arctic wetland depletion following permafrost disturbance by thermo-erosion gully processes. In: *Arctic Science* 3. DOI: 10.1139/AS-2016-0047.
- Ploetz, A., B. Baranov, T. Fromm, W. Geissler, S. Gukov, C. Haberland, F. Krüger, A. Krylov, D. Peresypkin, S. Petrunin, S. Shibaev, R. Tuktarov, N. Tsukanov, and D. Vollmer (2019): "Seismicity of the Laptev Sea Rift". In: *Russian-German Cooperation: Expeditions to Siberia in 2018*. Ed. by S. Kruse, D. Bolshiyakov, M. Grigoriev, A. Morgenstern, L. Pestryakova, L. Tsibizov, and A. Udke. Vol. 734. Alfred Wegener Institute Helmholtz Center for Polar and Marine Research, pp. 97–101.
- Schirmer, L., V. Kunitsky, G. Grosse, S. Wetterich, H. Meyer, G. Schwamborn, O. Babiy, A. Derevyagin, and C. Siegert (Aug. 2011): Sedimentary characteristics and origin of the Late Pleistocene Ice Complex on north-east Siberian Arctic coastal lowlands and islands – A review. In: *Quaternary International* 241.1-2, pp. 3–25. DOI: 10.1016/j.quaint.2010.04.004.
- Schwamborn, G., V. Rachold, and M. N. Grigoriev (2002): Late Quaternary Sedimentation History of the Lena Delta. In: *Quaternary International* 89, pp. 119–134.
- Sloan, R. A., J. A. Jackson, D. McKenzie, and K. Priestley (Feb. 2011): Earthquake depth distributions in central Asia, and their relations with lithosphere thickness, shortening and extension. In: *Geophysical Journal International* 185.1, pp. 1–29. DOI: 10.1111/j.1365-246x.2010.04882.x.
- Stedmon, C.A., R.M.W. Amon, A.J. Rinehart, and S.A. Walker (Mar. 2011): The supply and characteristics of colored dissolved organic matter (CDOM) in the Arctic Ocean: Pan Arctic trends and differences. In: *Marine Chemistry* 124.1-4, pp. 108–118. DOI: 10.1016/j.marchem.2010.12.007.
- Tarbeeva, A., L. Lebedeva, V. Efremov, V. Shamov, and O. Makarieva (2020): Water tracks in the lower Lena River basin. In: *E3S Web of Conferences* 163. Ed. by O. Makarieva and D. Post, p. 04007. DOI: 10.1051/e3sconf/202016304007.
- Thibodeau, Benoit, Dorothea Bauch, Heidemarie Kassens, and Leonid A. Timokhov (Oct. 2014): Interannual variations in river water content and distribution over the Laptev Sea between 2007 and 2011: The Arctic Dipole connection. In: *Geophysical Research Letters* 41.20, pp. 7237–7244. DOI: 10.1002/2014gl061814.
- Trask, Parker D. (1932): *Origin and Environment of Source Sediments of Petroleum*. By D. Trask Parker, assisted by Harold E. Hammar and C. C. Wu. Gulf Publishing Co., Houston, Texas, 323 pp., 1932. In: *Journal of the Marine Biological Association of the United Kingdom* 19.1, pp. 445–445. DOI: 10.1017/S0025315400055946.
- Wentworth, Chester K. (1922): A Scale of Grade and Class Terms for Clastic Sediments. In: *The Journal of Geology* 30.5, pp. 377–392. ISSN: 00221376, 15375269. URL: <http://www.jstor.org/stable/30063207>.
- Wetterich, Sebastian, Svetlana Kuzmina, Andrei A. Andreev, Frank Kienast, Hanno Meyer, Lutz Schirmer, Tatyana Kuznetsova, and Melanie Sierralta (Aug. 2008): Palaeoenvironmental dynamics inferred from late Quaternary permafrost deposits on Kurungnakh Island, Lena Delta, Northeast Siberia, Russia. In: *Quaternary Science Reviews* 27.15-16, pp. 1523–1540. DOI: 10.1016/j.quascirev.2008.04.007.

Chapter 3

Expeditions to Central Siberia

Edited by Boris K. Biskaborn

3.1 Lake sediment core retrieval and vegetation analysis at Lake Khamra, Central Siberia: Expedition Khamra 2020

Boris K. Biskaborn ^{1,@}, Ulrike Herzschuh ^{1,2}, Luidmila A. Pestryakova ³, Evgenii S. Zakharov ^{3,4}, Jan Kahl ¹, Stefano Meucci ¹, Aleksey Pestryakov ³, Stefan Kruse ^{1,*}, Ramesh Glückler ^{1,*}, Birgit Heim ^{1,*}, Lena Ushnitzkaya ^{3,*}

¹ Alfred Wegener Institute Helmholtz Centre for Polar and Marine Research, Potsdam, Germany

² University of Potsdam, Potsdam, Germany

³ North-Eastern Federal University of Yakutsk, Yakutsk, Russian Federation

⁴ Institute for Biological Problems of Cryolithozone Siberian Branch of RAS, Yakutsk, Russian Federation

* not in field

@ Corresponding author: Boris.Biskaborn@awi.de

Fieldwork period and location:

From March 01st to March 20th, 2020 travel Yakutsk-Lensk-Khamra-Lensk-Yakutsk, and from March 09th to March 18th, 2020 fieldwork at Lake Khamra based in a wooden hut near south-eastern shore and in the lake ice camp.

Objectives

The fastest warming of the Arctic in Russia (Biskaborn et al. 2019b) and the high spatial variability of environmental features over time (Biskaborn et al. 2012; Biskaborn et al. 2019a; Herzschuh et al. 2013), but the very sparse coverage of paleolimnological data in eastern Russia at the same time (Kaufman et al. 2020) shows the high value of lake sediment cores in this region. Our main research focus within the research group “Polar Terrestrial Environmental Systems” at AWI Potsdam is based on paleoenvironmental reconstructions and understanding relationships between climate change, vegetation migrations, biodiversity shifts, and lake trajectories in extreme cold and continental settings of the Siberia. To gain information on these key-interactions our research depends on archives of environmental changes including proxies documenting climate, vegetation, ecosystem composition and sedimentology. Therefore, we plan and execute expeditions together with our Russian partners, i.e. the Northeastern Federal University Yakutsk (NEFU).

Short cores, sediment surface samples, hydrological measurement, as well as vegetation analyses including fire scar samples and unmanned aerial vehicle (UAV)-based photogrammetry were collected during a previous expedition in 2018 (Morgenstern et al. 2019). The new expedition in 2020 was conceived as a follow-up expedition to build on these preliminary results.

Wildfires shape the boreal forests dynamics of Siberia and may increase in intensity and affecting more areas in global warming. Recent fire reconstruction based on sedimentary proxy analyses of Lake Khamra provided evidence for changing fire regimes during the last millenia (Glückler et al. 2020). However, ground truth is exceptionally scarce of the vast forested areas but is necessary for paleoproxy understanding and calibration to reconstruct fire-vegetation interaction on long-time scales and also for satellite upscaling. However, fire scars are in its nature local evidence for fires and provide knowledge on a small scale so that they need to be collected in a larger area to be able to distinguish local fires from lightning and those that spread and thus provide a deeper understanding of the fire history in this area.

Monitoring of the vast remote boreal forests in Siberia is challenging. Often small crowns of the mixed-species forests restrict a species detection of available satellite data (e.g. Sentinel-2, Landsat). UAV-based photogrammetry and orthoimage generation of local (<1 ha) products can help in creation of ground proof for establishing relationships to upscale with Sentinel-2 to larger landscapes. Acquisitions from winter would greatly enhance the possibility of species classification for these mixed-summergreen/evergreen boreal forests.

This expedition Khamra 2020 was planned and conducted as part of the scientific programme of AWI in POF IV Topic 5. Our objectives were as follow:

1. Retrieve long sediment cores from the center of the lake for bioindicator-based palaeoenvironmental reconstruction.
2. Retrieve long sediment cores from the shallower part to track shifts of the waterplant belt.
3. Retrieve short cores and sediment surface samples in the eastern part of the lake for high-resolution reconstructions of the recent lake and catchment history.
4. Collect water depths measurements to complete the bathymetrical survey started in 2018.
5. Collect fire scar samples from the north and east of the lake to reconstruct the data of fires.
6. Apply UAV for acquisition of winter forests to reconstruct of different densities by structure from motion 3D point clouds and from this orthoimages and canopy height models.

Methods and fieldwork summary

Work on the lake and core retrieval

We chartered a MMI-8 helicopter to reach the lake from Lensk together with the drilling system, other material that was too heavy for the helicopter was send by Vezdekhod from Lensk. The helicopter dropped half of the team together with the heavy drilling equipment at the coordinates previously defined as best drilling location in the lake center and the rest of the team near the south-east shore so that they can reach the hut. We had help from Ivan Sokolov and his son Andrey Sokolov transporting people from the hut to the ice camp until the Vezdekhod arrived with a delay about one week. From then on drivers supported us by dragging the tripod system across the lake. Additionally we reached single spots for short coring, surface sample retrieval and water depth measurements wearing snow boots.

We used Jiffy ice augers to drill holes in the ice cover. To recovered water and sediment surface samples we used an UWITEC water sampler and a sediment grabber. We used an UWITEC gravity corer to retrieve short cores. We applied the UWITEC (tripod) piston coring system from the ice cover to retrieve long sediment cores (Figure 3.1.1). Water depths measurements were performed through ice-holes using a calibrated rope. We used an oven in a tent (Figure 3.1.1) to heat up water to unfreeze the equipment before and during each drilling action and protect retrieved cores from freezing until transport and temporary storage in the hut.

Fire scar sampling for fire ground truthing

Trees with fire scars were searched and felled. From these tree discs were cut, if possible at the uppermost location of the scar following the sampling instructions of Arno et al. 1977. Coordinates of the trees were recorded with a handheld GPS device.

UAV data for species recognition

The UAV DJI Phantom4 equipped with a RGB camera was used. Flight planning was done on site with the Pix4D capture app for 150 m long and 20 m wide transects at a flight altitude of 50 m and a 2D flight pattern with 90% overlap of images. Additionally, a MAPIR Survey3-wide RGB camera was attached to the drone shooting an image every 1 s with fixed ISO and preadjusted shutter speed for optimal brightness of images. For a detailed protocol and further information we refer to the report by Morgenstern et al. 2019 and the publication by Brieger et al. 2019.



Figure 3.1.1: Ice camp in the center of Lake Khamra and the UWITEC piston coring system for retrieval of long sediment cores.

Preliminary results

Palaeolimnology

Accumulation rates of short sediment cores from Lake Khamra retrieved in 2018 showed high mean values of $0.14 \pm 0.02 \text{ cm y}^{-1}$ in the last Centuries that enabled sampling and analyses of charcoal and fire history in the surrounding area in a 6-year resolution (Glückler et al. 2020). We therefore aimed for long core records to make use of the high sediment accumulation in this lake to gain insight into small-scale Holocene palaeoenvironmental variability.

During expedition it turned out that the lake ice cover demanded special attention because there was a water layer between the thick snow layer and the top of the lake ice cover. We had to remove the snow from the drilling locations and to use a mixture of snow and water to built a stable platform to mount the tripod for coring. Snow cover was very thick, about a meter at most places. The main ice thickness among all drilling locations was 57 cm. Because of early and thick snow and complex hydrological mechanisms related to on-ice water, the ice cover was less thick than expected. Temperatures fell to less than -40°C in some nights and during most days coring was performed at around -20°C . We retrieved two long cores in the center of the lake and one additional long core near the northern shore, where surface samples showed transitions between minerogenic and plant dominated lake mud (Figure 3.1.2; Table A.2.3). We collected additional water depth measurements that enabled us to complete the water depth map.

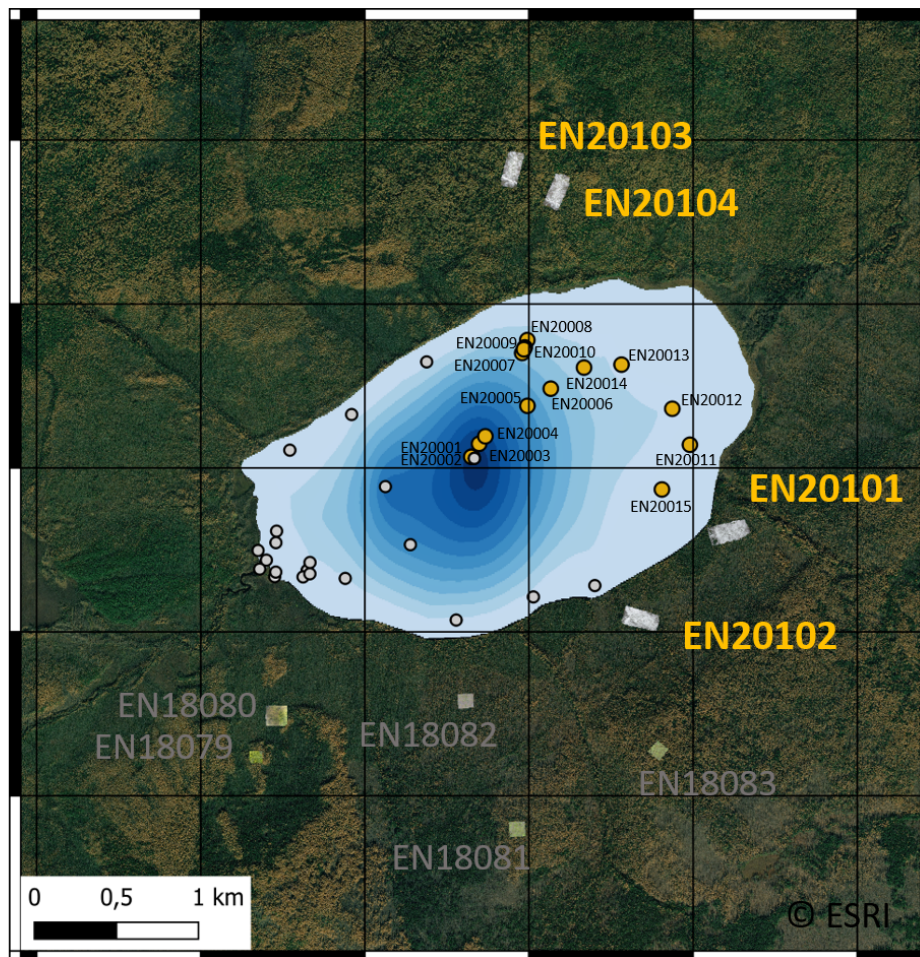


Figure 3.1.2: Overview of sample sites on and around Lake Khamra in expedition 2020 and compared to previous sampling sites from expedition 2018 (Morgenstern et al. 2019).

Fire scar collection and dating

Two pine trees and 12 larch trees were sampled that were identified with apparent scars in winter conditions. They were dried and brought to the lab in Potsdam for scar dating. One to three areas with scars were identified at each of 12 from the 14 discs in total belonging to 11 of the 13 individually sampled trees (Figure 3.1.3). Scar areas were sanded and subsequently scanned and tree rings identified and tried to match with apparent scars. First dating revealed 45 scars among many (N=17) date back to a fire event in year 2006 which can also be seen in satellite data; multiple (N=5) were found for 1996 and some (N=2) around 1965 (Figure 3.1.4). In the current version of this data set, the years of the older scars may not be precise as the tree rings were not cross-correlated with a master chronology yet. This most likely will clarify whether identified scars e.g. around the year 1965, 1996 and 2006 date back to the same fire event or showing multiple events. Furthermore, during ring identification, vacuoles were apparent in multiple tree rings that fall together with fire years.

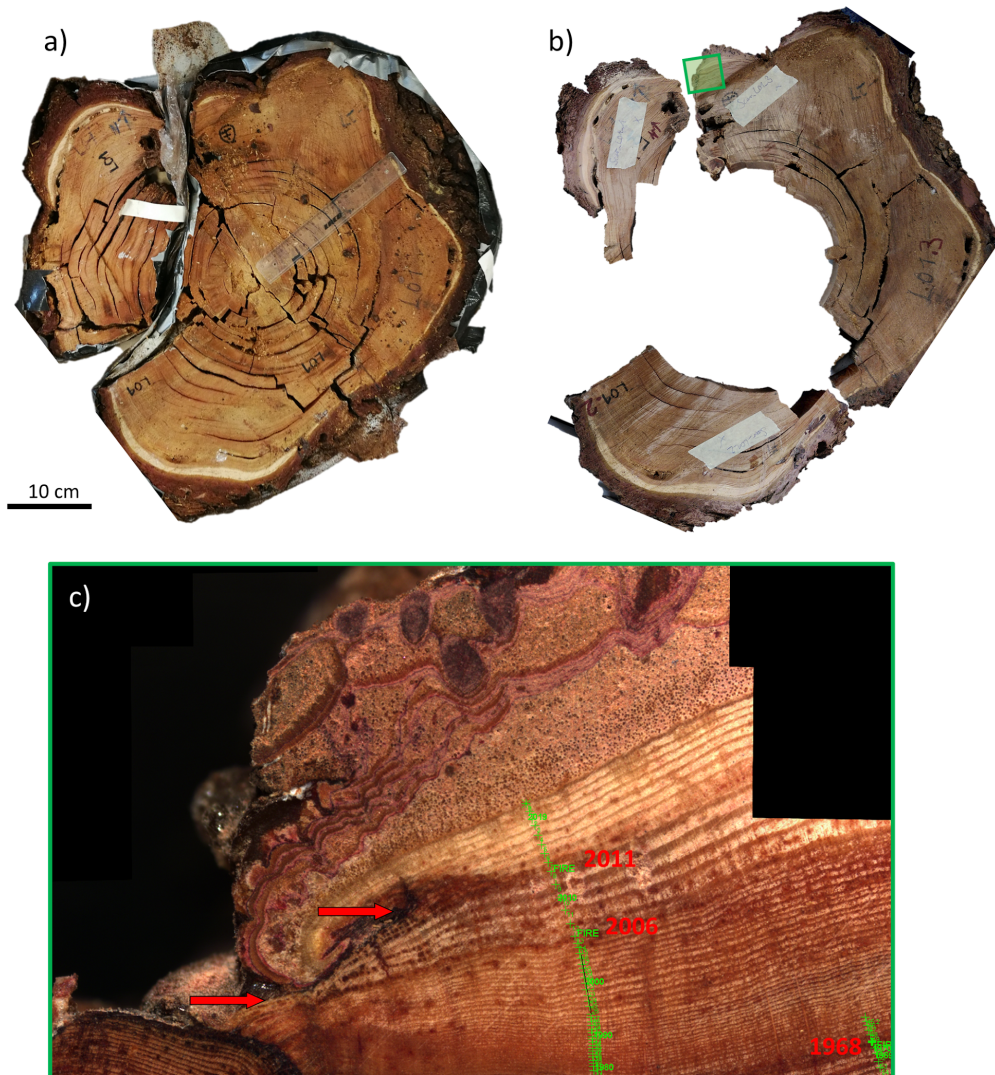


Figure 3.1.3: Example of the processing and dating for fire scars on tree disk L01: a) dried tree disc upon arrival, b) identified and polished fire scar areas (note the missing center that happened during sanding), and c) stitched scan of scar area L01_3 with 3 fire scars highlighted with the red arrows and the tree ring track in green colors in which the ring of the corresponding to the scar is marked as FIRE.

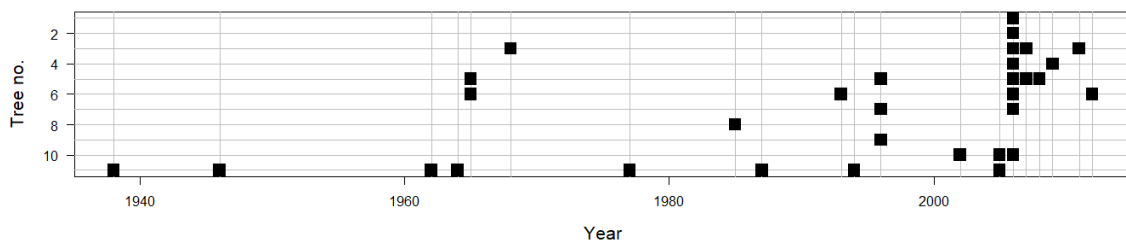


Figure 3.1.4: Preliminary identification of fire scars.

Image acquisition and point cloud reconstruction

At four transects of 20x150 m, flights could be performed (Figure 3.1.2; Table 3.1-1). The weather conditions were good, no wind that could move the objects what would hinder finding good key points. Further, a cloudy sky led to images that are homogeneously exposed. Based on the ca. 140 RGB images per site point clouds and digital elevation models and with these orthoimages were able to be reconstructed (Figure 3.1.5). The ground resolution was ca. 1.8 cm/pix, which is very high. Similar steps were done with the RGN images of which more were taken. Because of more images, the ground resolution was slightly better, but at one site the RGN camera was not used because the battery was too low.

Further, as the crowns were free of fresh snow one has a free view on the needles/branches. This data will allow an identification of evergreen tree individuals and separate them from dead or deciduous trees. With this, this data will help to understand the fraction of summergreen vs. evergreen of these mixed forests close to Lake Khamra, as to be seen in yellow coloring of predominantly larches in fall (compare Figure 3.1.2).

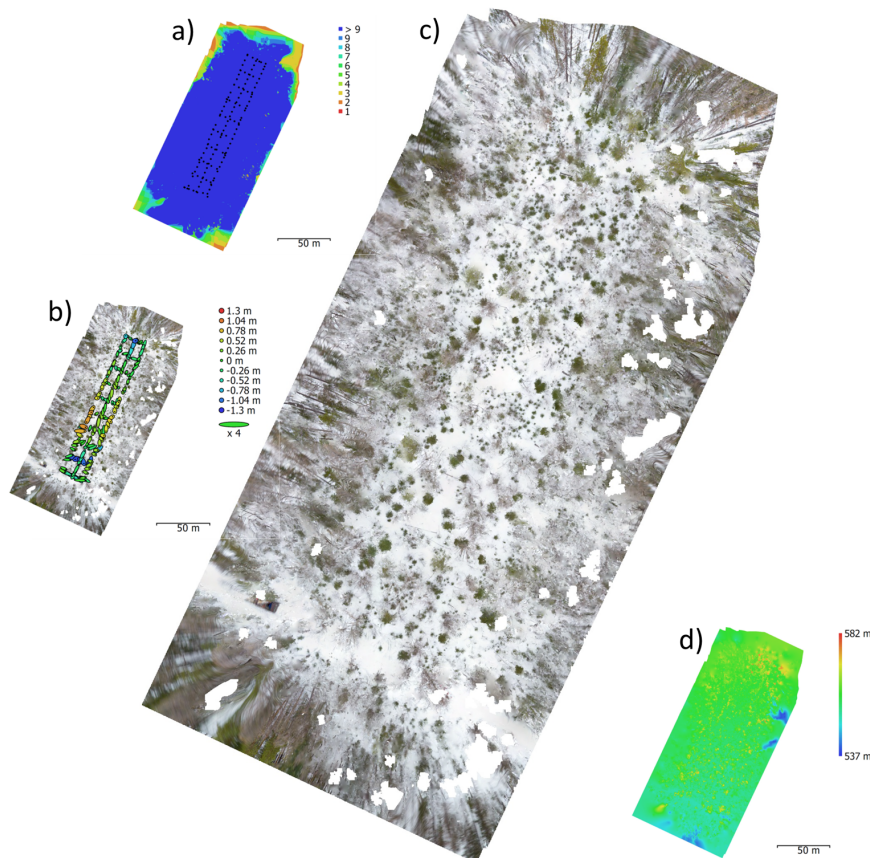


Figure 3.1.5: Example of the processing steps in Agisoft Photoscan: a) camera locations and image overlap, b) error of the camera locations (total x-y-error 1.14 m), c) orthoimage and d) digital elevation model (resolution 1.71 cm/pix).

Table 3.1-1: Image acquisition summary.

Site name	Latitude	Longitude	Number of images RGB/RGN aligned	Flying altitude inferred from images [m]	Ground resolution of orthoimage [cm/pix] RGB/RGN	Coverage area [km ²]
EN20101	N 59.98648°	E 113.01136°	139 of 139/708 of 1491	47.5	1.78/0.437	0.0252
EN20102	N 59.98181°	E 113.00125°	148 of 148/475 of 627	47.9	1.74/1.18	0.0213
EN20103	N 60.00670°	E 112.98887°	140 of 140/499 of 971	47.5	1.72/0.611	0.0197
EN20104	N 60.00537°	E 112.99366°	144 of 144/-	43.5	1.71/-	0.0196/-

3.2 Monitoring a full year-cycle of land surface and snow depth within an alaa and close forests close to Churapcha (Yakutia)

Stefan Kruse ^{1,*,@}, Gennadiy V. Nesterov ⁵, Evgenii S. Zakharov ^{2,3}, Simone M. Stuenzi ^{1,4,*}

¹ Alfred Wegener Institute Helmholtz Centre for Polar and Marine Research, Potsdam Germany

² Institute of Natural Sciences, North-Eastern Federal University of Yakutsk, Yakutsk, Russian Federation

³ Institute for Biological Problems of the Cryolithozone, Siberian Branch of the Russian Academy of Sciences, Yakutsk, Russian Federation

⁴ Humboldt Universität zu Berlin, Geography Department, Berlin, Germany

⁵ State Unitary Enterprise of Housing and Utilities of the Republic of Sakha (Yakutia), Churapchinsky Branch, Churapcha village, Russian Federation

* not in field

@ Corresponding author: Stefan.Kruse@awi.de

Fieldwork period and location:

Setup in the field on April 23rd 2020, monitoring period planned from April 23rd 2020 to April 22nd 2021 with monthly maintenance at the alaa close to Churapcha.

Objectives

The grassland dominated non-forested thermokarst depressions (alaa) in Yakutia are in use since for centuries by Yakuts for animal husbandry and as pastures and hayfields (Crate et al. 2017). Horses freely graze all year round in the forest-alaa landscape and are controlled by horse breeders, and feed and hold in a corral during winter. Due to permafrost-thawing induced ground surface subsidence lakes could develop so that these grasslands cannot be used anymore (Crate et al. 2017). Understanding the permafrost dynamics is therefore crucial to forecast the alaa development under climate change.

For this, a coupled version of a land surface model CryoGrid for permafrost (Westermann et al. 2016, Stuenzi et al. 2020) and the individual-based spatially explicit vegetation model LAVESI for forest dynamics (Kruse et al. 2016) could be applied. However, data for parameterization and validation of this model, knowledge about vegetation phenology and its interaction with snow height and distribution is crucial but very sparse for the permafrost underlain, forested areas in Siberia. Hence, monitoring of these variables need to be established.

Our objectives are therefore to monitor an alaa for a full year April 23rd 2020 to April 22nd 2021 and

- 1. collect sub-daily image data with a time lapse camera capturing in the view the grassland area of the alaa and forest edges to understand vegetation phenology and snow distribution, and**
- 2. collect snow height measurements in different vegetation types within and in the forests surrounding the alaa.**

We choose an alaa that is located 5 km north of the village of Churapcha (Central Yakutia, Lena-Amga interfluvium, basin of the Tatta River, Figure 3.2.1). The village is the regional center of the Churapchinsky region (ulus) of the Republic of Sakha (Yakutia) with a population of 10202 people. The main traditional activities of the population are cattle and horse breeding. During the period of the USSR, this alaa was part of the agricultural land of a large state agricultural enterprise. After the socio-economic restructuring in the country, agricultural land was transferred to new farming enterprises, and the ownership was transferred to private hands and was used for subsidiary farming since the early 2000s. The alaa has the shape of an irregular ellipse 310 m long and 160 m wide (Figure 3.2.1). In the alaa, a swampy area occupies an area in the southeast (180 m x 50 m). The second swampy area in the northwest (60 m x 40 m) becomes waterlogged only in spring or in rainy years. The alaa is used as a pasture for horses and farmland, where the grass is mown every year to create a stock of hay for the winter (Figure 3.2.2). A corral was built for the horses to be kept inside during winter. There are seven horses in the herd inhabiting this territory.

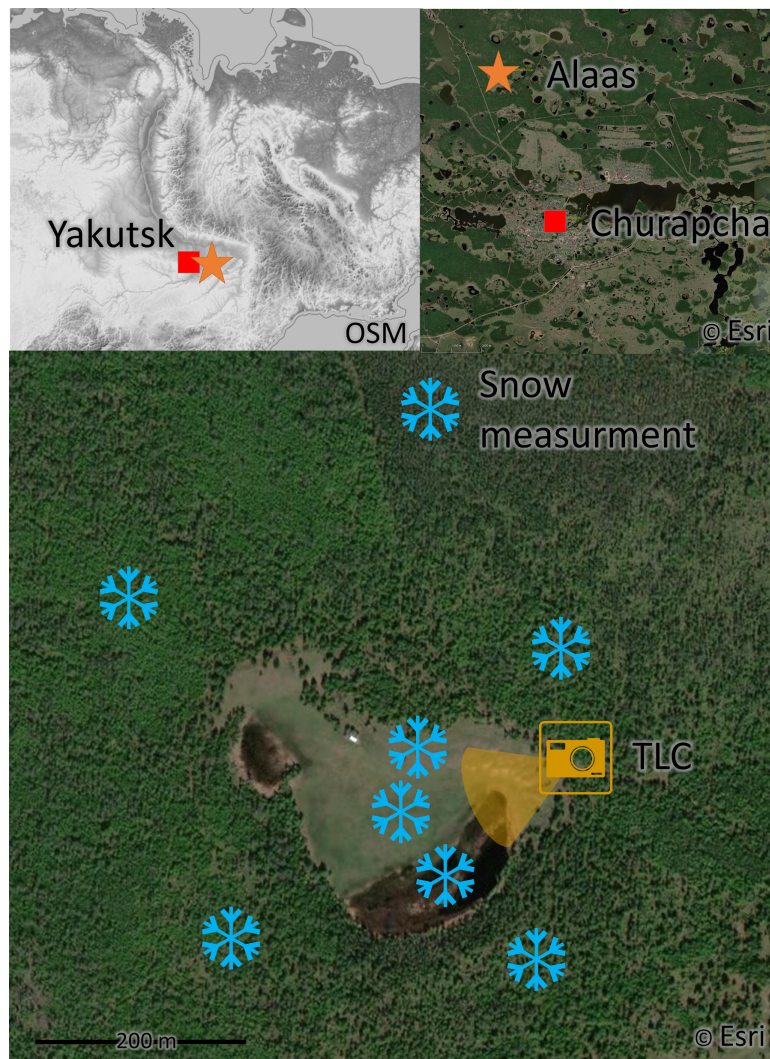


Figure 3.2.1: Overview map showing the location of the alas eastwards of Yakutsk, and the measurement locations in the different land surface cover. Source of high-resolution satellite images: ESRI basemap.



Figure 3.2.2: Hay is produced from the meadow in the alas (a) by using small trucks (c) which is compacted (b) and stored for feeding horses in winter (d-e).

Methods and Fieldwork summary

Image capturing

The time-lapse camera TLC-200 Pro by Brinno® was installed at April 23rd 2020. Batteries should last ~43 days with these settings based on the information provided in the manual; a maintenance (battery change, SD-memory card change) is accordingly planned monthly.

It has a viewing angle of 112°, aperture f/2.0, the size of images is 1280x720 pixels. Settings were: white balance to auto, scene mode to daylight, HDR range to high, exposure to middle, timestamp to on, low light recording to on. Images were taken for testing purposes in 10 min steps (23.04.-02.05.) which was prolonged to 1-hour steps afterwards. The data is stored on a SD-memory card as an AVI-movie file.

Post-processing of the acquired data is done with the tools provided by the software-package *ffmpeg* (<https://ffmpeg.org/>) with the following steps: 1. extracting single frames, 2. manually checking the quality and deleting images, 3. merging all images back to a single video file.

Snow measurements

The first snow measurements were planned on a two-weekly basis for the winter 2020/2021 at multiple positions (Figure 3.2.1, Table A.2.8). The measurement protocol as outlined for each point in Table A.2.8 follows the field guide of the T-Mosaic action group Permafrost Thaw (**Boike2020**, available upon request). We cover the spatial land surface variability across forested and open sites. We achieve representativeness, while still considering accessibility during winter. For the measurements a tape or stick measure will be used and performed on 10 m transects, one measurement per every two meter will be recorded. At each point the stick will be put through the snowpack at a right angle to the snow surface until it reaches the ground, and the snow surface depth will be recorded. Furthermore, images will be made during this process.

In addition to the point measurements, at some key points visible in the time lapse camera view tape ruler or similar will be installed to extract snow height from the images in hourly temporal resolution (Figure 3.2.3).

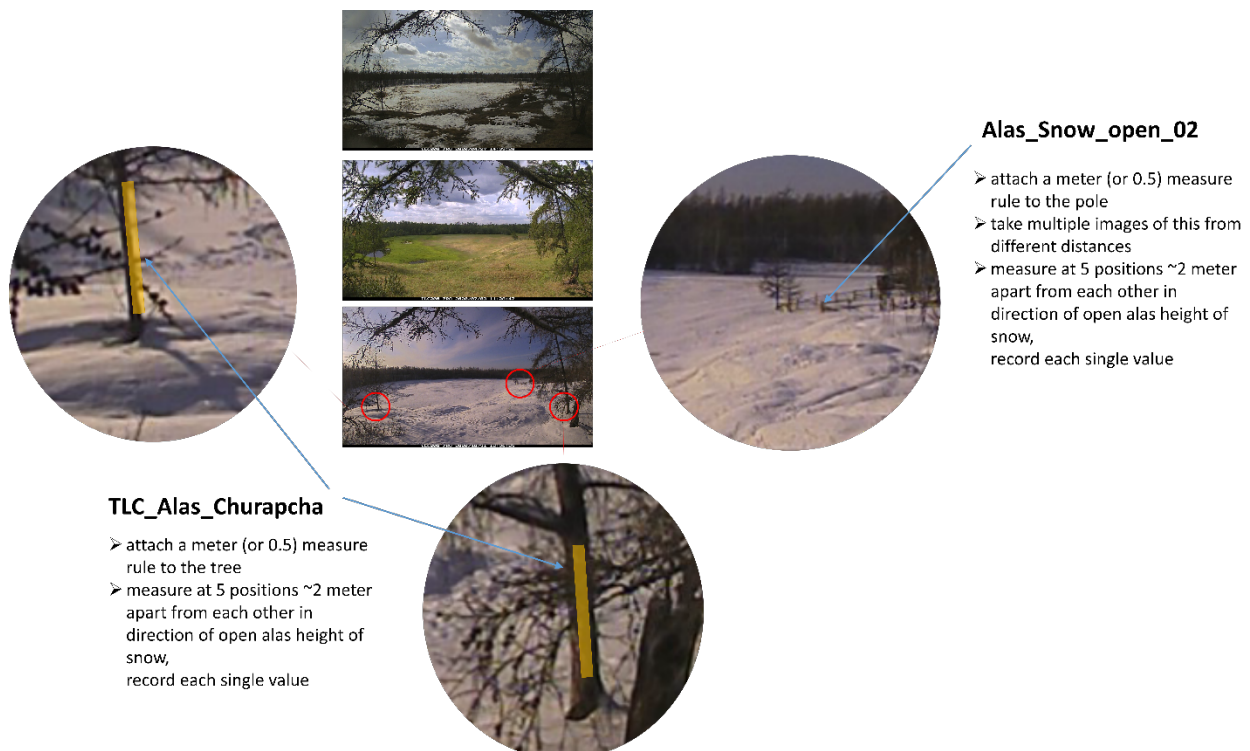


Figure 3.2.3: Scheme for snow measurement instructions.

Preliminary results

Time lapse records

The time lapse camera was fixed to a larch tree stem at ~2 m height at position N 62.04305° and E 132.39172° (Figure 3.2.1). Pointing in the southwest direction. Its view is centered around the center of the alaa (Figure 3.2.4). It has at the borders trees of the forest edge present. In the distance the forest edge of the opposite side of the alaa is visible in the middle and covering ~10% of the image.

Images could be captured in 10-minute resolution within 23.04.-02.05.2020 and from then on in hourly resolution 02.05.-01.11.2020 (Table 3.2-1). Unfortunately, from 27.08. to 20.09. all data is missing as the batteries went low. Haze and rain was visible on some days, and in some images, dew blocked the view on the inside of the weatherproof housing.

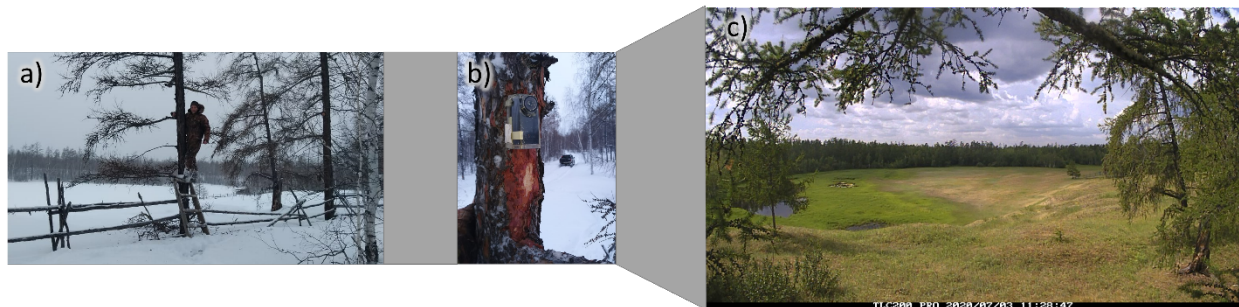


Figure 3.2.4: Attachment on tree (a) and final position close up (b) and field of view of camera in summer (c).

Table 3.2-1: Summary table about available camera data.

No.	Start time	End time	Resolution	Comment
1	2020/04/23 16:59:32	2020/05/02 11:19:32	10-minutely	-
2	2020/05/02 12:31:04	2020/07/03 09:31:04	hourly	- first image with person in field of view deleted - at the end water vapor on lense inside the housing - at the end low battery produced stripes on recorded images
3	2020/07/03 11:28:47	2020/08/26 20:28:47	hourly	- first image with face of person deleted - last 7 images deleted as they were dark and with error due to low battery
4	2020/09/20 19:46:12	2020/10/25 11:46:09	hourly	- first image with hand of a person blocking the view deleted
5	2020/10/25 13:36:24	2020/11/01 09:36:24	hourly	- first frame pointing into wrong a direction deleted

Snow measurements

At the time of this report, the first measurement could already be conducted at December 5th. Snow depths were measured at eight locations and at 5 points at 2 m apart along a line (Table A.2.8). On the open alaa area horse tracks can be observed that are corralled there and thus no disturbance is visible in the forests (Figure 3.2.5). The first measurements revealed 30-40 cm deep snow on this day and no clear difference between them (Figure 3.2.6).

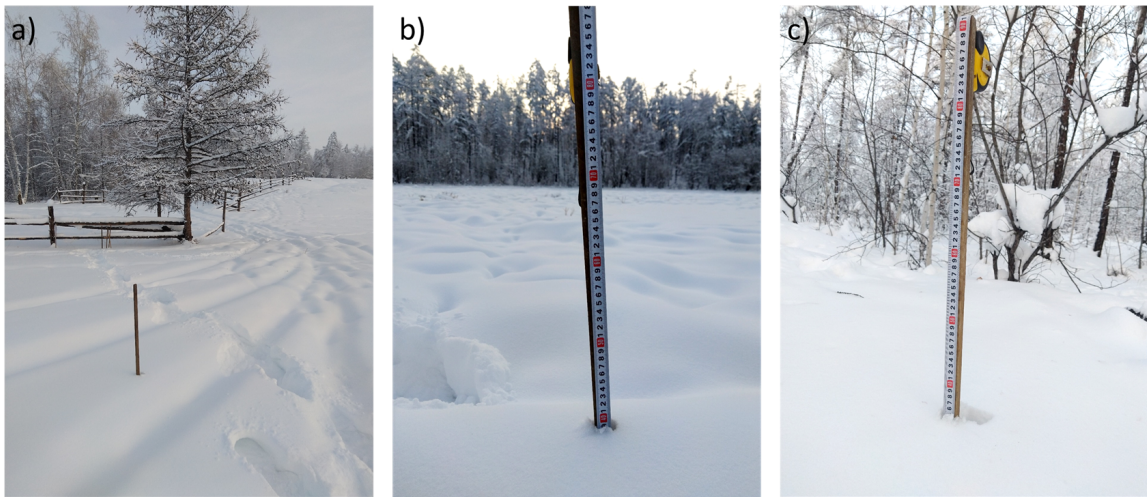


Figure 3.2.5: Example snow depth measurements, at location (a) Alas Snow open 2 (b) Alas Snow open 3 and (c) Alas Snow dense 1.

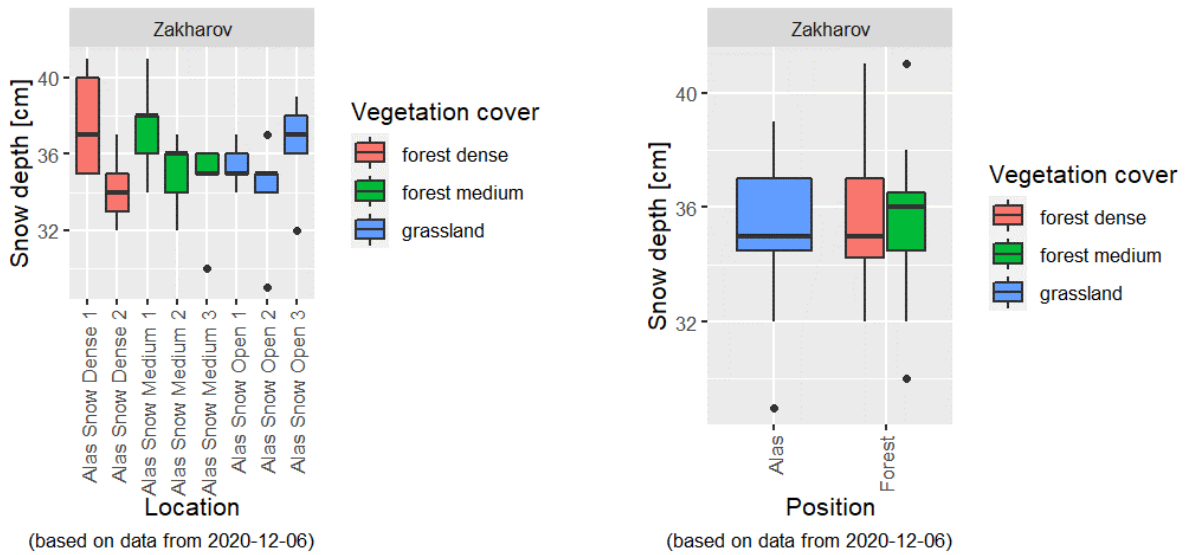


Figure 3.2.6: First snow depth measurements (each N=5) show no difference at the beginning of the winter.

Bibliography

- Arno, S. F. and K. M. Sneek (1977): A method for determining fire history in coniferous forests in the Mountain West. In: Gen. Tech. Rep. INT-GTR-42. Ogden, UT: U.S. Department of Agriculture, Forest Service, Intermountain Forest and Range Experiment Station. 28 p. 042.
- Biskaborn, B. K., U. Herzschuh, D. Bolshiyarov, L. Savelieva, and B. Diekmann (Apr. 2012): Environmental variability in northeastern Siberia during the last ~13,300yr inferred from lake diatoms and sediment–geochemical parameters. In: *Palaeogeography, Palaeoclimatology, Palaeoecology* 329-330, pp. 22–36. DOI: 10.1016/j.palaeo.2012.02.003.
- Biskaborn, B. K., L. Nazarova, L. A. Pestryakova, L. Strykh, K. Funck, H. Meyer, B. Chaplignin, S. Vyse, R. Gorodnichev, E. Zakharov, R. Wang, G. Schwamborn, H. L. Bailey, and B. Diekmann (2019a): Spatial distribution of environmental indicators in surface sediments of Lake Bolshoe Toko, Yakutia, Russia. In: *Biogeosciences* 16.20, pp. 4023–4049. DOI: 10.5194/bg-16-4023-2019.
- Biskaborn, B. K., S. L. Smith, J. Noetzli, H. Matthes, G. Vieira, D. A. Streletskiy, P. Schoeneich, V. E. Romanovsky, A. G. Lewkowicz, A. Abramov, M. Allard, J. Boike, W. L. Cable, H. H. Christiansen, R. Delaloye, B. Diekmann, D. Drozdov, B. Etzelmüller, G. Grosse, M. Guglielmin, T. Ingeman-Nielsen, K. Isaksen, M. Ishikawa, M. Johansson, H. Johannsson, A. Joo, D. Kaverin, A. Kholodov, P. Konstantinov, T. Kröger, C. Lambiel, J.-P. Lanckman, D. Luo, G. Malkova, I. Meiklejohn, N. Moskalenko, M. Oliva, M. Phillips, M. Ramos, A. B. K. Sannel, D. Sergeev, C. Seybold, P. Skryabin, A. Vasiliev, Q. Wu, K. Yoshikawa, M. Zheleznyak, and H. Lantuit (2019b): Permafrost is warming at a global scale. In: *Nature Communications* 10.1. DOI: 10.1038/s41467-018-08240-4.
- Brieger, F., U. Herzschuh, L. A. Pestryakova, B. Bookhagen, E. S. Zakharov, and S. Kruse (2019): High-resolution photogrammetric point clouds from northeast Siberian forest stands. Alfred-Wegener-Institute research expedition "Chukotka 2018". In: Supplement to: Brieger, Frederic; Herzschuh, Ulrike; Pestryakova, Luidmila A; Bookhagen, Bodo; Zakharov, Evgenii S; Kruse, Stefan (2019): Advances in the Derivation of Northeast Siberian Forest Metrics Using High-Resolution UAV-Based Photogrammetric Point Clouds. *Remote Sensing*, 11(12), 1447, <https://doi.org/10.3390/rs11121447>. DOI: 10.1594/PANGAEA.902259. URL: <https://doi.org/10.1594/PANGAEA.902259>.
- Crate, S., M. Ulrich, J. O. Habeck, A. R. Desyatkin, R. V. Desyatkin, A. N. Fedorov, T. Hiyama, Y. Iijima, S. Ksenofontov, C. Mészáros, and H. Takakura (June 2017): Permafrost livelihoods: A transdisciplinary review and analysis of thermokarst-based systems of indigenous land use. In: *Anthropocene* 18, pp. 89–104. DOI: 10.1016/j.ancene.2017.06.001.
- Glückler, R., U. Herzschuh, S. Kruse, A. Andreev, S. A. Vyse, B. Winkler, B. K. Biskaborn, L. Pestryakova, and E. Dietze (2020): Wildfire history of the boreal forest of southwestern Yakutia (Siberia) over the last two millennia documented by a lake-sedimentary charcoal record. In: *Biogeosciences Discussions* 2020, pp. 1–42. DOI: 10.5194/bg-2020-415. URL: <https://bg.copernicus.org/preprints/bg-2020-415/>.
- Herzschuh, U., L. A. Pestryakova, L. A. Savelieva, L. Heinecke, T. Böhmer, B. K. Biskaborn, A. Andreev, A. Ramisch, A. L. C. Shinneman, and H. J. B. Birks (Sept. 2013): Siberian larch forests and the ion content of thaw lakes form a geochemically functional entity. In: *Nature Communications* 4.1. DOI: 10.1038/ncomms3408.
- Kaufman, D. et al. (Apr. 2020): A global database of Holocene paleotemperature records. In: *Scientific Data* 7.1. DOI: 10.1038/s41597-020-0445-3.
- Kruse, Stefan, Mareike Wiczorek, Florian Jeltsch, and Ulrike Herzschuh (Oct. 2016): Treeline dynamics in Siberia under changing climates as inferred from an individual-based model for *Larix*. In: *Ecological Modelling* 338, pp. 101–121. DOI: 10.1016/j.ecolmodel.2016.08.003.
- Morgenstern, A., D. Bolshiyarov, A. Udke, M. N. Grigoriev, L. Pestryakova, S. Kruse, and L. Tsibizov (2019): Russian-German Cooperation: Expeditions to Siberia in 2018. en. In: DOI: 10.2312/BZPM_0734_2019.

- Stuenzi, S. M., J. Boike, W. Cable, U. Herzschuh, S. Kruse, L. Pestryakova, T. Schneider von Deimling, S. Westermann, E. Zakharov, and M. Langer (June 2020): Variability of the Surface Energy Balance in Permafrost Underlain Boreal Forest. In: DOI: [10.5194/bg-2020-201](https://doi.org/10.5194/bg-2020-201).
- Westermann, S., M. Langer, J. Boike, M. Heikenfeld, M. Peter, B. Eitzelmüller, and G. Krinner (Feb. 2016): Simulating the thermal regime and thaw processes of ice-rich permafrost ground with the land-surface model CryoGrid 3. In: *Geoscientific Model Development* 9.2, pp. 523–546. DOI: [10.5194/gmd-9-523-2016](https://doi.org/10.5194/gmd-9-523-2016).

Chapter 4

Appendix

A.1 List of participants

Table A.1.1: List of participants in the Expedition Lena 2020 based on the Research Station Samoylov Island

No.	Name	Institution	Duration
1	Abramova, Ekaterina	LDR	22.07.20-15.09.20
2	Dergach, Petr	IPGG	03.08.20-25.08.20
3	Efremov, Vladimir	MPI	24.08.20-07.09.20
4	Grigoriev, Mikhail	MPI	10.08.20-27.08.20
5	Kartozia, Andrey	IPGG	03.08.20-25.08.20
6	Kut, Anna	MPI	10.08.20-27.08.20
7	Lebedeva, Luidmila	MPI	24.08.20-07.09.20
8	Lupachev, Alexei	ISB-PSN	10.08.20-27.08.20
9	Maximov, Georgii	MPI	10.08.20-27.08.20
10	Potapov, Vladimir	IPGG	03.08.20-25.08.20
11	Tarbeeva, Anna	MSU	24.08.20-07.09.20
12	Tikhonravova, Yana	MPI	10.08.20-27.08.20

Table A.1.2: List of participants in the Expedition Lena 2020 based on the Khabarov meteostation

No.	Name	Institution	Duration
1	Efremov, Vladimir	MPI	24.08.20-07.09.20
2	Lebedeva, Luidmila	MPI	24.08.20-07.09.20
3	Tarbeeva, Anna	MSU	24.08.20-07.09.20

Table A.1.3: List of participants in the Expedition Lena 2020 working in the southern Lena Delta

No.	Name	Institution	Duration
1	Gukov, Stepan	YB GS RAS	01.09.20-15.09.20
2	Petrinin, Sergei	YB GS RAS	01.09.20-15.09.20
3	Tuktarov, Rustam	YB GS RAS	01.09.20-15.09.20

Table A.1.4: List of participants in the Khamra expedition (Yakutia). We kindly acknowledge the help of father and son Sokolov and two drivers.

No.	Name	Institution	Duration
1	Biskaborn, Boris	AWI-P	01.03.20-20.03.20
2	Herzschuh, Ulrike	AWI-P	06.03.20-20.03.20
3	Kahl, Jan	AWI-P	01.03.20-20.03.20
4	Meucci, Stefano	AWI-P	01.03.20-20.03.20
5	Pestryakov, Alexei	NEFU	01.03.20-20.03.20
6	Pestryakova, Ludmila	NEFU	01.03.20-20.03.20
7	Zakharov, Evgenii	NEFU	01.03.20-20.03.20

Table A.1.5: List of participating institutions

Abbr.	Institution
AWI P	Alfred Wegener Institute Helmholtz Centre for Polar and Marine Research, Potsdam, Germany
IPGG	Trofimuk Institute of Petroleum-Gas Geology and Geophysics, Siberian Branch, Russian Academy of Sciences, Novosibirsk, Russian Federation
ISB-PSN	Institute of Physico-Chemical and Biological Problems of Soil Science, Russian Academy of Sciences, Russian Federation
LDR	Lena Delta Reserve, Tiksi, Russian Federation
MPI	Melnikov Permafrost Institute, Siberian Branch, Russian Academy of Sciences, Yakutsk, Russian Federation
MSU	Lomonosov Moscow State University, Moscow, Russian Federation
NEFU	Federal State Autonomous Educational Institution of Higher Education "M.K. Ammosov North-Eastern Federal University", Yakutsk, Russian Federation
PGI	Pacific Geographical Institute Far-Eastern Branch, Russian Academy of Sciences, Vladivostok, Russian Federation
YB GS RAS	Yakutsk Branch of the Geophysical Survey of the Russian Academy of Sciences, Russian Federation

A.2 Supplementary material - Expedition Lena 2020

Table from section 2.2

Table A.2.1: List of samples collected to date (as of August 2020)

ID	Date	Time (Tiksi time)	ID	Date	Time (Tiksi time)
1	2018-04-20	21:00:00	30	2018-08-07	21:00:00
2	2018-04-24	20:30:00	31	2018-08-11	19:00:00
3	2018-04-26	18:00:00	32	2018-08-15	19:00:00
4	2018-04-30	12:00:00	33	2018-08-19	19:00:00
5	2018-05-04	19:00:00	34	2018-08-23	19:00:00
6	2018-05-08	14:00:00	35	2018-08-27	19:00:00
7	2018-05-12	10:30:00	36	2018-09-01	19:00:00
8	2018-05-16	10:00:00	37	2018-09-05	19:00:00
9	2018-05-20	10:00:00	38	2018-09-09	19:00:00
10	2018-05-24	12:00:00	39	2018-09-13	19:00:00
11	2018-05-28	14:00:00	40	2018-09-17	11:00:00
12	2018-06-01	12:00:00	41	2018-09-21	14:00:00
13	2018-06-05	13:00:00	42	2018-09-25	10:00:00
14	2018-06-09	14:00:00	43	2018-09-29	19:00:00
15	2018-06-13	12:00:00	44	2018-10-03	08:00:00
18	2018-06-17	12:00:00	45	2018-10-07	19:00:00
19	2018-06-21	14:00:00	46	2018-10-11	08:00:00
20	2018-06-25	15:00:00	47	2018-10-15	14:00:00
21	2018-06-29	11:00:00	48	2018-10-19	14:00:00
22	2018-07-03	20:00:00	49	2018-10-24	08:00:00
23	2018-07-08	11:30:00	50	2018-10-31	19:00:00
24	2018-07-12	08:30:00	51	2018-11-03	12:00:00
25	2018-07-16	19:00:00	52	2018-11-07	14:00:00
26	2018-07-20	20:00:00	53	2018-11-11	14:00:00
27	2018-07-26	19:00:00	54	2018-11-16	16:00:00
28	2018-07-30	20:05:00	55	2018-11-20	14:00:00
29	2018-08-03	20:00:00	56	2018-11-24	14:00:00
			57	2018-11-28	11:00:00
			58	2018-12-02	13:00:00
			59	2018-12-06	14:00:00
			60	2018-12-09	15:00:00

ID	Date	Time (Tiksi time)	ID	Date	Time (Tiksi time)
61	2018-12-14	15:00:00	95	2019-05-31	14:00:00
62	2018-12-18	13:00:00	96	2019-06-01	10:00:00
63	2018-12-22	13:00:00	97	2019-06-02	10:00:00
64	2018-12-26	15:00:00	98	2019-06-03	16:00:00
65	2019-01-06	14:00:00	99	2019-06-04	15:00:00
66	2019-01-11	14:00:00	100	2019-06-05	10:00:00
67	2019-01-18	15:10:00	101	2019-06-06	10:00:00
68	2019-01-25	14:00:00	102	2019-06-07	14:00:00
69	2019-02-02	16:00:00	103	2019-06-08	10:00:00
70	2019-02-07	14:00:00	104	2019-06-09	16:00:00
71	2019-02-12	14:00:00	105	2019-06-10	14:00:00
72	2019-02-19	15:00:00	106	2019-06-11	16:00:00
73	2019-02-25	16:00:00	107	2019-06-12	08:00:00
74	2019-03-01	16:00:00	108	2019-06-13	21:00:00
75	2019-03-11	14:00:00	109	2019-06-14	19:00:00
76	2019-03-19	14:00:00	110	2019-06-15	14:00:00
77	2019-03-28	17:00:00	111	2019-06-16	10:00:00
78	2019-04-06	13:00:00	112	2019-06-17	12:00:00
79	2019-04-11	15:00:00	113	2019-06-18	09:00:00
80	2019-04-22	12:00:00	114	2019-06-19	18:00:00
81	2019-04-30	15:00:00	115	2019-06-20	22:00:00
82	2019-05-06	12:00:00	116	2019-06-21	18:00:00
83	2019-05-10	14:00:00	117	2019-06-22	10:00:00
84	2019-05-16	14:00:00	118	2019-06-23	14:00:00
85	2019-05-20	14:00:00	119	2019-06-24	13:00:00
86	2019-05-22	10:00:00	120	2019-06-25	12:00:00
87	2019-05-23	14:00:00	121	2019-06-26	08:00:00
88	2019-05-24	13:00:00	122	2019-06-27	18:00:00
89	2019-05-25	11:00:00	123	2019-06-28	13:30:00
90	2019-05-26	15:00:00	124	2019-06-29	10:00:00
91	2019-05-27	18:00:00	125	2019-06-30	11:00:00
92	2019-05-28	17:00:00	126	2019-07-01	14:00:00
93	2019-05-29	18:00:00	127	2019-07-02	11:00:00
94	2019-05-30	13:00:00	128	2019-07-04	14:00:00

ID	Date	Time (Tiksi time)	ID	Date	Time (Tiksi time)
129	2019-07-07	16:30:00	203	2019-09-15	11:00:00
130	2019-07-10	11:00:00	204	2019-09-17	09:00:00
131	2019-07-12	14:30:00	205	2019-09-19	12:00:00
132	2019-07-14	15:20:00	206	2019-09-21	09:00:00
133	2019-07-16	16:30:00	207	2019-09-23	10:00:00
134	2019-07-18	11:00:00	208	2019-09-25	08:00:00
135	2019-07-20	10:00:00	209	2019-09-27	09:00:00
136	2019-07-22	11:30:00	210	2019-09-28	08:00:00
137	2019-07-24	10:00:00	211	2019-09-30	08:00:00
138	2019-07-26	10:30:00	212	2019-10-02	08:00:00
139	2019-07-28	11:00:00	213	2019-10-04	09:00:00
140	2019-07-30	10:10:00	214	2019-10-06	08:00:00
141	2019-08-01	10:30:00	215	2019-10-08	08:00:00
142	2019-08-03	11:20:00	216	2019-10-10	08:00:00
143	2019-08-05	11:20:00	217	2019-10-12	08:00:00
144	2019-08-07	09:20:00	218	2019-10-14	10:00:00
145	2019-08-09	14:40:00	219	2019-10-16	08:00:00
146	2019-08-12	11:00:00	220	2019-10-18	09:00:00
147	2019-08-14	21:30:00	221	2019-10-20	09:00:00
148	2019-08-16	10:30:00	222	2019-10-22	08:00:00
149	2019-08-18	11:00:00	223	2019-10-24	09:00:00
150	2019-08-20	10:30:00	224	2019-10-26	08:00:00
151	2019-08-22	10:40:00	225	2019-10-28	10:00:00
152	2019-08-24	10:40:00	226	2019-10-30	10:00:00
153	2019-08-26	09:00:00	227	2019-11-01	10:00:00
154	2019-08-28	10:30:00	228	2019-11-03	10:00:00
155	2019-08-30	15:30:00	229	2019-11-05	11:00:00
156	2019-09-01	17:00:00	230	2019-11-07	12:00:00
157	2019-09-03	16:00:00	231	2019-11-09	12:00:00
198	2019-09-05	10:00:00	232	2019-11-11	11:00:00
199	2019-09-07	10:00:00	233	2019-11-13	10:00:00
200	2019-09-09	09:00:00	234	2019-11-15	10:00:00
201	2019-09-11	10:00:00	235	2019-11-17	12:00:00
202	2019-09-13	06:00:00	236	2019-11-19	12:00:00

ID	Date	Time (Tiksi time)	ID	Date	Time (Tiksi time)
237	2019-11-21	12:00:00	271	2020-02-15	13:00:00
238	2019-11-23	12:00:00	272	2020-02-19	12:00:00
239	2019-11-25	11:00:00	273	2020-02-23	13:00:00
240	2019-11-27	12:00:00	274	2020-02-27	13:00:00
241	2019-11-29	12:00:00	275	2020-03-01	12:00:00
242	2019-12-01	12:00:00	276	2020-03-05	12:00:00
243	2019-12-03	11:00:00	277	2020-03-09	13:00:00
244	2019-12-05	12:00:00	278	2020-03-13	12:00:00
245	2019-12-07	10:00:00	279	2020-03-17	11:00:00
246	2019-12-09	11:00:00	280	2020-03-21	11:00:00
247	2019-12-11	10:00:00	281	2020-03-25	12:00:00
248	2019-12-13	11:00:00	282	2020-03-29	12:00:00
249	2019-12-15	11:00:00	283	2020-04-04	12:00:00
250	2019-12-17	11:00:00	284	2020-04-11	12:00:00
251	2019-12-19	12:00:00	285	2020-04-18	12:00:00
252	2019-12-21	11:00:00	286	2020-04-25	12:00:00
253	2019-12-23	12:00:00	287	2020-05-02	12:00:00
254	2019-12-25	12:00:00	288	2020-05-09	10:00:00
255	2019-12-27	13:00:00	289	2020-05-10	09:00:00
256	2019-12-29	13:00:00	290	2020-05-11	09:00:00
257	2019-12-31	13:00:00	291	2020-05-12	09:00:00
258	2020-01-02	13:00:00	292	2020-05-13	08:00:00
259	2020-01-04	12:00:00	293	2020-05-14	09:00:00
260	2020-01-06	12:00:00	294	2020-05-15	08:00:00
261	2020-01-08	13:00:00	295	2020-05-16	08:00:00
262	2020-01-11	12:00:00	296	2020-05-17	10:00:00
263	2020-01-14	13:00:00	297	2020-05-18	08:00:00
264	2020-01-18	13:00:00	298	2020-05-19	09:00:00
265	2020-01-22	13:00:00	299	2020-05-20	10:00:00
266	2020-01-26	12:00:00	300	2020-05-21	10:00:00
267	2020-01-30	12:00:00	301	2020-05-22	10:00:00
268	2020-02-03	12:00:00	302	2020-05-23	10:00:00
269	2020-02-07	12:00:00	303	2020-05-24	11:00:00
270	2020-02-11	12:00:00	304	2020-05-25	10:00:00

ID	Date	Time (Tiksi time)	ID	Date	Time (Tiksi time)
305	2020-05-26	09:00:00	340	2020-07-15	09:00:00
306	2020-05-27	10:00:00	341	2020-07-17	15:00:00
307	2020-05-28	09:00:00	342	2020-07-19	11:00:00
308	2020-05-29	09:00:00	343	2020-07-21	17:00:00
309	2020-05-30	09:00:00	344	2020-07-23	20:00:00
310	2020-05-31	09:00:00	345	2020-07-25	09:00:00
311	2020-06-01	09:00:00	346	2020-07-27	09:00:00
312	2020-06-02	09:00:00	347	2020-07-29	09:00:00
313	2020-06-03	09:00:00	348	2020-07-31	09:00:00
314	2020-06-04	09:00:00	349	2020-08-01	09:00:00
315	2020-06-05	09:00:00	350	2020-08-04	09:00:00
316	2020-06-06	09:00:00	351	2020-08-06	09:00:00
317	2020-06-07	09:00:00	352	2020-08-08	09:00:00
318	2020-06-08	09:00:00	353	2020-08-10	09:00:00
319	2020-06-09	12:00:00	354	2020-08-12	09:00:00
320	2020-06-10	09:00:00	355	2020-08-14	09:00:00
321	2020-06-11	09:00:00	356	2020-08-16	09:00:00
322	2020-06-12	09:00:00	357	2020-08-18	09:00:00
323	2020-06-13	09:00:00	358	2020-08-20	09:00:00
324	2020-06-14	09:00:00	359	2020-08-22	08:00:00
325	2020-06-15	09:00:00	360	2020-08-24	09:00:00
326	2020-06-17	09:00:00	361	2020-08-26	09:00:00
327	2020-06-19	09:00:00			
328	2020-06-21	09:00:00			
329	2020-06-23	09:00:00			
330	2020-06-25	09:00:00			
331	2020-06-27	09:00:00			
332	2020-06-29	09:00:00			
333	2020-07-01	09:00:00			
334	2020-07-03	09:00:00			
335	2020-07-05	09:00:00			
336	2020-07-07	09:00:00			
337	2020-07-09	09:00:00			
338	2020-07-11	09:00:00			
339	2020-07-13	09:00:00			

Table from section 2.4.

Table A.2.2: The results of surveying the position of the permafrost table under channels in the delta of the Lena

# Gps	Coordinates		Distance [m]	Water depth [m]	Depth to permafrost thickness [m]	Thaw thickness [m]
	Latitude [°]	Longitude [°]				
Profile 1. South-East coast of Samoylov Island						
1023	N 72.36531	E 126.5192	0	0	1.04	1.04
1024	N 72.36535	E 126.5190	8.4	0	1.03	1.03
1025	N 72.36541	E 126.5187	20.8	0	0.87	0.87
1026	N 72.36548	E 126.5184	32.9	0	0.93	0.93
1027	N 72.36556	E 126.5180	48.9	0	0.75	0.75
1028	N 72.36560	E 126.5179	56.6	0.23	1.33	1.1
1029	N 72.36562	E 126.5177	61.1	0.55	1.54	0.99
1030	N 72.36564	E 126.5173	75.4	1.02	2.09	1.07
1032	N 72.36567	E 126.5172	79.3	1.32	2.36	1.04
1031	N 72.36567	E 126.5172	81	1.34	2.39	1.05
1033	N 72.36567	E 126.5170	87.4	1.85	2.99	1.14
1034	N 72.36563	E 126.5168	96.1	2.35	3.81	1.46
1035	N 72.36559	E 126.5165	107	3.52	5.09	1.57
1036	N 72.36553	E 126.5162	117.3	4.15	-	-
Profile 2. East cape of Samoylov Island; across Olenekskaya channel						
1037	72.37404	126.5254	0	0.2	0.92	0.92
1038	72.37403	126.5256	8	0.2	0.86	0.86
1039	72.37400	126.5259	17.6	0	0.94	0.94
1040	72.37401	126.5261	24.7	0.2	1.19	0.99
1041	72.37402	126.5263	30.9	0.43	1.25	0.82
1042	72.37401	126.5269	50.9	0.79	1.49	0.7
1043	72.37393	126.5273	67	1.09	1.63	0.54
1044	72.37391	126.5276	77.6	1.33	2.04	0.71
1045	72.37374	126.5279	99.6	1.14	1.83	0.69
1046	72.37369	126.5285	118.6	1	1.87	0.87
1047	72.37358	126.5286	132.6	0.92	2	1.08
1048	72.37362	126.5292	154	0.77	2.16	1.39
1049	72.37362	126.5299	174.9	0.93	1.94	1.01
1050	72.37364	126.5309	210.5	0.83	2.06	1.23
1051	72.37319	126.5318	268.9	1.72	3.11	1.39

# Gps	Coordinates		Distance [m]	Water depth [m]	Depth to permafrost thickness [m]	Thaw thickness [m]
	Latitude [°]	Longitude [°]				
1061	72.37291	126.5316	301.2	3	4.08	1.08
1052	72.37271	126.5322	333.5			
1062	72.37251	126.5323	355.8	5.5		
1065	72.37064	126.5339	571.7	4.5		
1066	72.37067	126.5354	619.7	3.32		
1059	72.37067	126.5363	650.5	0.85	2.28	1.43
1058	72.37065	126.5360	658.6	0.67	2.26	1.59
1057	72.37061	126.5362	663.9	0.34	2.34	2
1056	72.37052	126.5364	678	0.38	2.22	1.84
1055	72.37043	126.5369	696.4	0	1.79	1.79
1054	72.37023	126.5376	730.4	0.1	1.44	1.44
1053	72.37008	126.5381	752.9	0.1	1.33	1.33
Profile 3. From Samoylovsky isl till Ebe-Kumaga sands						
1067	72.37589	126.5245	0	0.1	1.09	1.09
1068	72.37598	126.5249	16.6	0	1.13	1.13
1069	72.37602	126.5251	25.6	0.55	1.35	0.8
1070	72.37685	126.5256	79	1.69	2.92	1.23
1071	72.37615	126.5267	105.5	1.56	2.68	1.12
1072	72.37652	126.5276	131.9	0.79	1.95	1.16
1073	72.37644	126.5283	152.8	0.56	1.75	1.19
1074	72.37658	126.5288	178.2	0.31	1.59	1.28
1075	72.37668	126.5294	202.8	0	1.29	1.29
1076	72.37684	126.5305	244.5	0.1	1.21	1.21
Profile 4. Sistyakh-Ary-Uesya channel						
1083	72.29857	126.5095	0	0.1	1.22	1.22
1084	72.29854	126.5104	30.6	0	1.07	1.07
1085	72.29853	126.5104	32	0.41	1.48	1.07
1086	72.29852	126.5106	37.6	0.57	1.58	1.01
1087	72.29834	126.5120	87	0.89	1.53	0.64
1088	72.29834	126.5133	133.5	1.03	1.88	0.85
1089	72.29839	126.5144	171.9	0.56	1.4	0.84
1090	72.29831	126.5149	188.3	0.38	1.15	0.77
1091	72.29833	126.5155	211.1	0	0.88	0.88

# Gps	Coordinates		Distance [m]	Water depth [m]	Depth to permafrost thickness [m]	Thaw thickness [m]
	Latitude [°]	Longitude [°]				
Profile 5. Between islands Sasyl-Ary and Sordokh-Ary						
1107	72.32215	126.4703	0	0	1.2	1.2
1106	72.32201	126.4710	29.8	0.46	1.49	1.03
1105	72.32185	126.4716	54.7	0.75	1.74	0.99
1104	72.32145	126.4721	102.7	1.27	2.36	1.09
1103	72.32106	126.4729	153.1	2.1	3.34	1.24
1102	72.32075	126.4740	205.4	3.05	4.18	1.13
1101	72.32023	126.4760	293	5.4		
1099	72.31973	126.4778	376.4	5.15		
1098	72.31894	126.4807	507.6	2.75	5.16	2.41
1097	72.31836	126.4837	629.1	5.2		
1096	72.31778	126.4869	752.9	5.73		
1095	72.31731	126.4893	925.5	3.3	4.69	1.39
1094	72.31694	126.4912	982	2.56	3.68	1.12
1093	72.31657	126.4923	1041.2	2.12	3.29	1.17
1092	72.31650	126.4940	1083.7	0.59	1.97	1.38
1082	72.31626	126.4950	1093.4	0	1.28	1.28
1081	72.31620	126.4952	1112.6	0.23	1.28	1.05
1080	72.31609	126.4956	1132.2	0	1.05	1.05
1079	72.31600	126.4962	1153.1	0.1	1.25	1.25
Profile 6. On unnamed channel which pour in Sistyakh-Ary-Uesya channel						
1109	72.27708	126.6171	0	0.1	1.36	1.36
1108	72.27682	126.6174	31.5	0	2.12	2.12
1110	72.27666	126.6178	53	0.36	2.17	1.81
1111	72.27654	126.6182	71.5	0.35	2.34	1.99
1112	72.27637	126.6189	103.9	0.44	2.54	2.1
1113	72.27615	126.6196	137.8	0.58	3.18	2.6
1114	72.27578	126.6207	193.5	1.9	4.35	2.45
1115	72.27566	126.6222	243.3	4.12	5.23	1.11
1116	72.27536	126.6233	293.6	3.4		
1117	72.27514	126.6245	341.6	3.97		
1118	72.27451	126.6256	420.9	2.9	4	1.1
1120	72.27459	126.6263	445.7	2.85	2.87	0.02
1119	72.27447	126.6264	460.2	1.4	1.4	

# Gps	Coordinates		Distance [m]	Water depth [m]	Depth to permafrost thickness [m]	Thaw thickness [m]
	Latitude [°]	Longitude [°]				
Profile 7. Chai-Tumus site, small channel which pour in Olenekskaya channel						
024	72.33008	125.7706	182.4	0.28	1.2	0.92
026	72.33004	125.7708	180.8	0.4	1.34	0.94
028	72.33004	125.7706	176.4	0.45	1.28	0.83
029	72.33001	125.7705	173.1	0.48	1.4	0.92
030	72.33	125.7705	171	0.5	1.17	0.67
031	72.33	125.7698	147.5	1.14	1.88	0.74
032	72.32984	125.7694	125	1.22	2.02	0.8
033	72.32979	125.7687	100.9	1.26	1.93	0.67
034	72.32957	125.7682	70.8	0.7	1.22	0.52
035	72.32941	125.7681	52.5	0.41	1.1	0.69
036	72.32937	125.7679	43.5	0.25	0.88	0.63
037	72.32931	125.7676	32.7	0.2	0.6	0.4
038	72.32921	125.7673	16.8	0	0.57	0.57
039	72.32910	125.7669	0	0	0.71	0.71
Profile 8. on drilling profile between Bh 1c-14 and 2c-14						
1125	72.37565	126.4481	0	0.87	1.88	1.01
1126	72.37611	126.4452	113.3	1.35	2.73	1.38
1127	72.37663	126.4430	205.3	1.88	3.38	1.5

Table from section 3.1.

Table A.2.3: Samples retrieved and measurements of water and ice at Lake Khamra during expedition in 2020. GravCor UWITEC Gravity Corer 60 mm; Piston UWITEC Piston Coring System 60 mm; Grabber; Sediment Grabber; Jiffy Jiffy Ice Auger. Coring penetration represents the in-field estimated absolute depth reached by the core chamber.

Sample ID	CE Date of sampling	Latitude [°]	Longitude [°]	Gear	Piston position [cm]	Core length [cm]	Water depth [m]	Ice thickness [cm]	Coring penetration [cm]
EN20001-1	10.03.2020	59.9910	112.9835	Water sampler	NA	NA	20.6	65	NA
EN20001-2	11.03.2020	59.9910	112.9835	GravCor	NA	30	20.6	65	30
EN20001-3	11.03.2020	59.9910	112.9835	Piston	-50	234	20.6	65	250
EN20001-4	11.03.2020	59.9910	112.9835	Piston	200	267	20.6	65	500
EN20001-5	11.03.2020	59.9910	112.9835	Piston	450	299	20.6	65	750
EN20001-6	12.03.2020	59.9910	112.9835	Piston	700	286	20.6	65	1000
EN20001-7	12.03.2020	59.9910	112.9835	Piston	950	182	20.6	65	1140
EN20002-1	13.03.2020	59.9910	112.9834	GravCor	NA	30	20.6	65	36
EN20002-2	13.03.2020	59.9910	112.9834	Piston	-50	259	20.6	65	250
EN20002-3	13.03.2020	59.9910	112.9834	Piston	200	287	20.6	65	500
EN20002-4	14.03.2020	59.9910	112.9834	Piston	450	300	20.6	65	750
EN20002-5	14.03.2020	59.9910	112.9834	Piston	700	287	20.6	65	1000
EN20002-6	14.03.2020	59.9910	112.9834	Piston	950	188	20.6	65	1150
EN20003	14.03.2020	59.9917	112.9843	Grabber	NA	1	17	0.4	NA
EN20004	14.03.2020	59.9921	112.9850	Grabber	NA	1	13	0.6	NA

Sample ID	CE Date of sampling	Latitude [°]	Longitude [°]	Gear	Piston position [cm]	Core length [cm]	Water depth [m]	Ice thickness [cm]	Coring penetration [cm]
EN20005	14.03.2020	59.9937	112.9897	Grabber	NA	1	6.5	0.6	NA
EN20006	14.03.2020	59.9946	112.9923	Jiffy	NA	-	4.5	0.1	NA
EN20007	14.03.2020	59.9966	112.9893	Grabber	NA	1	3.5	0.6	NA
EN20008	14.03.2020	59.9973	112.9899	Grabber	NA	1	2.5	1.2	-
EN20009-1	15.03.2020	59.9969	112.9896	Grabber	NA	1	3.04	85	NA
EN20009-2	15.03.2020	59.9969	112.9896	GravCor	NA	10	3.04	85	10
EN20009-3	15.03.2020	59.9969	112.9896	GravCor	-10	173	3.04	85	190
EN20009-4	15.03.2020	59.9969	112.9896	GravCor	140	279	3.04	85	440
EN20010-1	15.03.2020	59.9968	112.9895	Grabber	NA	1	3.3	85	NA
EN20011	16.03.2020	59.9913	113.0073	GravCor	NA	1	2	70	NA
EN20012	16.03.2020	59.9933	113.0055	GravCor	NA	1	2.15	65	NA
EN20013	16.03.2020	59.9958	113.0001	GravCor	NA	38	3	76	38
EN20014	16.03.2020	59.9957	112.9960	GravCor	NA	5	3.75	85	NA
EN20015	17.03.2020	59.9889	113.0041	Jiffy	NA	NA	2.8	68	NA

Table from section 2.8.

Table A.2.4: Station list Lena Delta and Samoylov Island

Name	Locality	Latitude	Longitude	Elevation [m]	s/n seismometer	s/n recorder	Date of Recovery	Days of recording
LD010	Chai Tumus	N 72.3261°	E 125.7601°	34	1877	DC-771 T-Log02	08.08. 2020	283
LD011	Amerika Khaya	N 72.4762°	E 126.2749°	73	1170	DC-776	10.08. 2020	283
LD015	GeoCamp	N 72.1173°	E 126.9817°	54	1331a	DC-772	17.08. 2020	283
LD018	White Mountains	N 71.9293°	E 127.3126°	23	1348a	DC-867	17.08. 2020	283
LD019	Norden-shield	N 72.0750°	E 128.3248°	35	1342a	DC-765	21.08. 2020	285
LD033	Stolb/ Sokol-Cliff	N 72.4031°	E 126.7969°	57	1178	DC-764	17.08. 2020	61
LD042	Kurungnakh Island	N 72.2874°	E 126.1886°	30	1190	DC-766	07.08. 2020	283
SAM01	Samoylov	N 72.3888°	E 126.4876°	?	1335	DC-774	04.08. 2020	283
SAM02	Samoylov	N 72.3814°	E 126.5106°	?	1831	DC-770	04.08. 2020	283
SAM03	Samoylov	N 72.3782°	E 126.4800°	?	1336	DC-773	05.08. 2020	283

Table A.2.5: Station list Buor Khaya Bay

Name	Locality	Latitude	Longitude	Elevation [m]	s/n seismometer	s/n recorder	Date of Recovery	Days of recording
BK03B	Buor Khaya Bay 3B	N 70.8488°	E 130.8800°	?	3049	DC-453	05.08. 2020	?
BK004	Buor Khaya Bay 4	N 71.0630°	E 130.1619°	16	3048	DC-778	07.08. 2020	?
BK005	Buor Khaya Bay 5	N 71.4015°	E 129.4080°	13	1887	DC-458	08.08. 2020	?
BK06B	Buor Khaya Bay 6B	N 71.8116°	E 129.3314°	?	1006	DC-860	29.07. 2020	?
BK07B	Buor Khaya Bay 7B	N 71.5778°	E 130.0038°	?	1009	DC-455	20.07. 2020	?
BK009	Sogo	N 71.5636°	E 128.9566°	?	3040	DC-769 T-Log03	15.08. 2020	?
BK010	Poljarka	N 71.5865°	E 128.9201°	22	3039	DC-862	18.08. 2020	?
BK012	Lake S of Tiksi	N 71.4175°	E 128.7237°	164	3044	DC-452 T-Log06	26.07. 2020	?
TIX00	Tiksi (TIXI)	N 71.6342°	E 128.8669°	40	1886	DC-456	18.08. 2020	?

Table A.2.6: Station list Tiksi array

Name	Locality	Latitude [°N]	Longitude [°E]	Elevation [m]	s\n seismo-meter	s\n recorder	Date of Maintenance	Days of recording
TIK01	central station	71.57404	129.07278	135	3051	DC-777 T-Log04	17.08. 2020	?
TIK02	inner circle	71.57619	129.06778	139	1889	DC-451	17.08. 2020	?
TIK03	inner circle	71.57623	129.07838	131	1895	DC-613	17.08. 2020	?
TIK04	inner circle	71.57397	129.08076	136	2828	DC-457 T-Log05	17.08. 2020	?
TIK05	inner circle	71.57166	129.07796	140	2829	DC-616	17.08. 2020	?
TIK06	inner circle	71.57156	129.06871	121	2860	DC-454	17.08. 2020	?
TIK07	inner circle	71.57433	129.06503	119	4191	DC-617	17.08. 2020	?
TIK08	outer circle	71.58415	129.06926	85	4192	DC-614	17.08. 2020	?
TIK09	outer circle	71.57856	129.09906	98	2830	DC-863	17.08. 2020	?
TIK10	outer circle	71.56872	129.09734	120	1015	DC-668	17.08. 2020	?
TIK11	outer circle	71.56288	129.07483	146	2895	DC-861	17.08. 2020	?
TIK12	outer circle	71.57182	129.04309	50	1007	DC-775	17.08. 2020	?
TIK13	outer circle	71.58188	129.04929	109	3052	DC-610	17.08. 2020	?

Table A.2.7: Station list Lena Delta and Samoylov Island

Name	Locality	Latitude	Longitude	Elevation [m]	Date of Maintenance/ Deployment*/ Recovery†
SML01	Kurungnakh Island	N 72.2903°	E 125.1844°	18	15.08.2020
SML02	America-Haya mountain	N 72.4762°	E 126.2749°	73	10.08.2020
SML03	Stolb/Sokol - Cliff	N 72.4023°	E 126.7939°	101	17.08.2020
SML04	Tchai Tumus	N 72.3226°	E 125.7568°	34	20.08.2020

Table from section 3.2.

Table A.2.8: Planned snow measurements, location and instructions.

Name of location	Position [N/E]	Instruction	Comment
Alas_Snow_open_01	62.04272° 132.38847°	- measure at 5-10 positions ca. 1 m apart from each other in line height of snow, record each single value - 1 Snow pit image	open, center may be compacted/disturbed by horses
Alas_Snow_open_02	62.04314° 132.38886°	- attach a 1 m (or 0.5 m) measure rule to the pole - take multiple images of this from different distances - measure at 5-10 positions ca. 1 m apart from each other in line in direction of open alas height of snow, record each single value	open, pole may be compacted/disturbed by horses
Alas_Snow_open_03	62.04208° 132.38939°	- measure at 5-10 positions ca. 1 m apart from each other in line height of snow, record each single value	open, water may be compacted/disturbed by horses
Alas_Snow_medium_01	62.04358° 132.39292°	- attach a meter (or 0.5) measure rule to a tree stem - take multiple images of this from different distances - measure at 5-10 positions ca. 1 m apart from each other in line height of snow, record each single value	forested
Alas_Snow_medium_03	62.04136° 132.39072°	- attach a meter (or 0.5) measure rule to a tree stem - take multiple images of this from different distances - measure at 5-10 positions ca. 1 m apart from each other in line height of snow, record each single value - 1 Snow pit image	forested
Alas_Snow_medium_02	62.04175° 132.38636°	- attach a meter (or 0.5) measure rule to a tree stem - take multiple images of this from different distances - measure at 5-10 positions ca. 1 m apart from each other in line height of snow, record each single value	forested

Name of location	Position [N/E]	Instruction	Comment
Alas_Snow_dense_02	62.04453° 132.38933°	<ul style="list-style-type: none"> - attach a meter (or 0.5) measure rule to a tree stem - take multiple images of this from different distances - measure at 5-10 positions ca. 1 m apart from each other in line height of snow, record each single value - 1 Snow pit image 	forested
Alas_Snow_dense_01	62.04453° 132.38933°	<ul style="list-style-type: none"> - attach a meter (or 0.5) measure rule to a tree stem - take multiple images of this from different distances - measure at 5-10 positions ca. 1 m apart from each other in line height of snow, record each single value 	forested

Die **Berichte zur Polar- und Meeresforschung** (ISSN 1866-3192) werden beginnend mit dem Band 569 (2008) als Open-Access-Publikation herausgegeben. Ein Verzeichnis aller Bände einschließlich der Druckausgaben (ISSN 1618-3193, Band 377-568, von 2000 bis 2008) sowie der früheren **Berichte zur Polarforschung** (ISSN 0176-5027, Band 1-376, von 1981 bis 2000) befindet sich im electronic Publication Information Center (**ePIC**) des Alfred-Wegener-Instituts, Helmholtz-Zentrum für Polar- und Meeresforschung (AWI); see <https://epic.awi.de>. Durch Auswahl "Reports on Polar- and Marine Research" (via "browse"/"type") wird eine Liste der Publikationen, sortiert nach Bandnummer, innerhalb der absteigenden chronologischen Reihenfolge der Jahrgänge mit Verweis auf das jeweilige pdf-Symbol zum Herunterladen angezeigt.

The **Reports on Polar and Marine Research** (ISSN 1866-3192) are available as open access publications since 2008. A table of all volumes including the printed issues (ISSN 1618-3193, Vol. 377-568, from 2000 until 2008), as well as the earlier **Reports on Polar Research** (ISSN 0176-5027, Vol. 1-376, from 1981 until 2000) is provided by the electronic Publication Information Center (**ePIC**) of the Alfred Wegener Institute, Helmholtz Centre for Polar and Marine Research (AWI); see URL <https://epic.awi.de>. To generate a list of all Reports, use the URL <http://epic.awi.de> and select "browse"/ "type" to browse "Reports on Polar and Marine Research". A chronological list in declining order will be presented, and pdf-icons displayed for downloading.

Zuletzt erschienene Ausgaben:

756 (2021) Russian-German Cooperation: Expeditions to Siberia in 2020, edited by Boris K. Biskaborn, Dmitry Yu. Bolshiyarov, Mikhail N. Grigoriev, Anne Morgenstern, Luidmila A. Pestryakova, Leonid V. Tsibizov, and Antonia Dill

755 (2021) The Expedition PS124 of the Research Vessel POLARSTERN to the southern Weddell Sea in 2021, edited by Hartmut H. Hellmer and Moritz Holtappels with contributions of the participants

754 (2021) MOSAiC Expedition: Airborne Surveys with Research Aircraft POLAR 5 and POLAR 6 in 2020, edited by Andreas Herber, Sebastian Becker, Hans Jakob Belter, Jörg Brauchle, André Ehrlich, Marcus Klingebiel, Thomas Krumpen, Christof Lüpkes, Mario Mech, Manuel Moser, and Manfred Wendisch

753 (2021) The Expedition PS123 of the Research Vessel POLARSTERN to NEUMAYER STATION III in 2020/2021, edited by Tim Heitland with contributions of the participants

752 (2021) Expeditions to Fennoscandia in 2020, edited by Matthias Fuchs, Lona van Delden, Nele Lehmann, and Torben Windirsch

751 (2021) The MOSES Sternfahrt Expeditions of the Research Vessels ALBIS, LITTORINA, LUDWIG PRANDTL, MYA II and UTHÖRN to the Elbe River, Elbe Estuary and German Bight in 2020, edited by Ingeborg Bussmann, Norbert Anselm, Holger Brix, Philipp Fischer, Götz Flöser, Felix Geissler, Norbert Kamjunke

750 (2021) International Online Symposium: Focus Siberian Permafrost – Terrestrial Cryosphere and Climate Change, editorial board: Pfeiffer EM, Vybornova O, Kutzbach L, Fedorova I, Knoblauch C, Tsibizov L & Beer C

749 (2021) Russian-German Cooperation: Expeditions to Siberia in 2019, edited by Matthias Fuchs, Dmitry Bolshiyarov, Mikhail Grigoriev, Anne Morgenstern, Luidmila Pestryakova, Leonid Tsibizov, and Antonia Dill

748 (2020) Das Alfred-Wegener-Institut in der Geschichte der Polarforschung: Einführung und Chronik, 2., erweiterte und überarbeitete Auflage, von Christian R. Salewski, Reinhard A. Krause, Elias Angele

Recently published issues:



ALFRED-WEGENER-INSTITUT
HELMHOLTZ-ZENTRUM FÜR POLAR-
UND MEERESFORSCHUNG

BREMERHAVEN

Am Handelshafen 12
27570 Bremerhaven
Telefon 0471 4831-0
Telefax 0471 4831-1149
www.awi.de

HELMHOLTZ